WORKSHOP WMFE

Automated Circuit Design using Electromagnetic Simulators

Monday, May 15, 1995
Orlando, Florida

1995 IEEE MTT-S INTERNATIONAL MICROWAVE SYMPOSIUM
Orlando, Florida
May 14-19, 1995

MTT-S WORKSHOP

WMFE: Automated Circuit Design Using Electromagnetic Simulators

Date: Monday, May 15, 1995

Time: 8:00 am - 5:00 pm

Location: Convention Center, Room 20 F

Sponsors: MTT-1 Computer-Aided Design
MTT-15 Microwave Field Theory

Organizers & Chairmen: John W. Bandler, Optimization Systems Associates Inc., Canada
Roberto Sorrentino, Università degli studi di Perugia, Italy

Speakers: Fritz Arndt, Technische Universität Bremen, Germany
Shao Hua Chen, Optimization Systems Associates Inc., Canada
Wolfgang J.R. Hoefer, University of Victoria, Canada
Nitin Jain, M/A-COM
Rolf H. Jansen, University of Aachen, Germany
Tony M. Pavio, Motorola
Robert A. Pucel, RCP Consultants
Roberto Sorrentino, Università degli studi di Perugia, Italy
Dan G. Swanson, Jr., Watkins-Johnson

Recent advances in microwave CAD technology, the availability of powerful workstations and massively parallel systems, indicate the feasibility of interfacing electromagnetic (EM) simulators into optimization systems or CAD frameworks for direct application of powerful optimizers. With the increasing availability of fast, robust, commercial EM simulators it is tempting to include them both in performance-driven and yield-driven circuit optimization, to combine the advantages of yield-driven design with the accuracy of electromagnetic simulation for first-pass success.

Thus, the push is to go beyond traditional uses of EM simulators for validation, for generation of equivalent circuits or look-up tables. It is to integrate EM simulations directly into the linear/nonlinear circuit design process in a manner transparent to the designer. The EM simulators, whether stand-alone or incorporated into CAD frameworks, may not realize their full potential to the designer unless they are driven by optimization routines to automatically adjust some designable parameters.

This workshop will address the evolution of the state of this novel art. Expectations of using EM simulators as effective tools in an automated design environment have been raised, based on the considerable and excellent work currently in progress.

WMFE: Automated Circuit Design Using Electromagnetic Simulators

Date:	Monday, May 15, 1995
Time:	8:00 am - 5:00 pm
Location:	Convention Center, Room 20 F

<u>Tentative Workshop Schedule</u>

8:00 am	John Bandler Welcome: Introductions
8:05 am	Robert A. Pucel
8:30 am	Dan G. Swanson, Jr.
9:10 am	Shao Hua Chen
9:50 am	Discussion Period
10:00 am	Coffee
10:30 am	Tony M. Pavio
11:10 am	Nitin Jain
11:40 am	Discussion Period
12:00 am	Lunch
1:00 pm	Wolfgang J.R. Hoefer
1:40 pm	Roberto Sorrentino
2:20 pm	Speakers from the floor
3:00 pm	Coffee
3:30 pm	Rolf Jansen
4:00 pm	Fritz Arndt
4:40 pm	Closing Discussion
5:00 pm	End

RCP Consultants

Expectations of a MMIC CAD System for the Next Century

R. A. Pucel
RCP Consultants
Needham, MA 02192

Workshop on Automated Circuit Design Using Electromagnetic Simulators

1995 IEEE MTT-S International Microwave Symposium
Orlando , Florida

May 15, 1995

1

RCP Consultants

Four Coming Developments of Importance to MMIC CAD for the Next Century

- 10-fold increase in speed of workstations/PC's by the year 2000 (using 1993 as the reference)
- Emergence of multi- (parallel) processor WS's and PC's
- Development of circuit layout optimization techniques based on EM simulation
- Feasibility of real-time 2D-numerical simulation of active devices in CAD simulators

2

RCP Consultants

Realized and Projected Speed Increase of Workstations and PCs into the Next Century

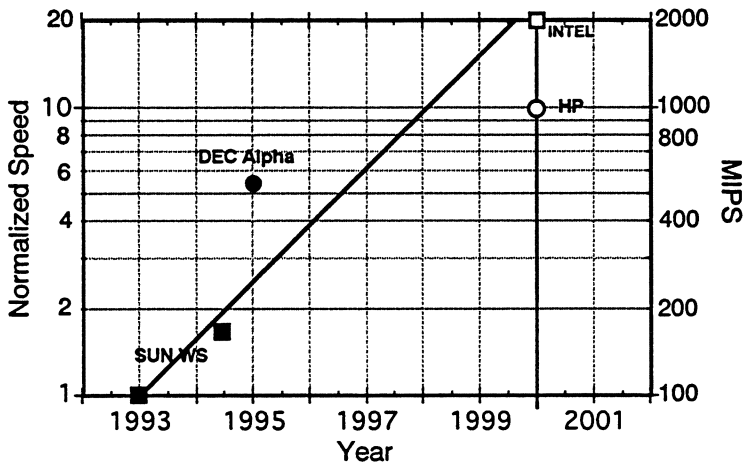

RCP Consultants

Realized and Projected Increase in Pentium Clock Speed with Time

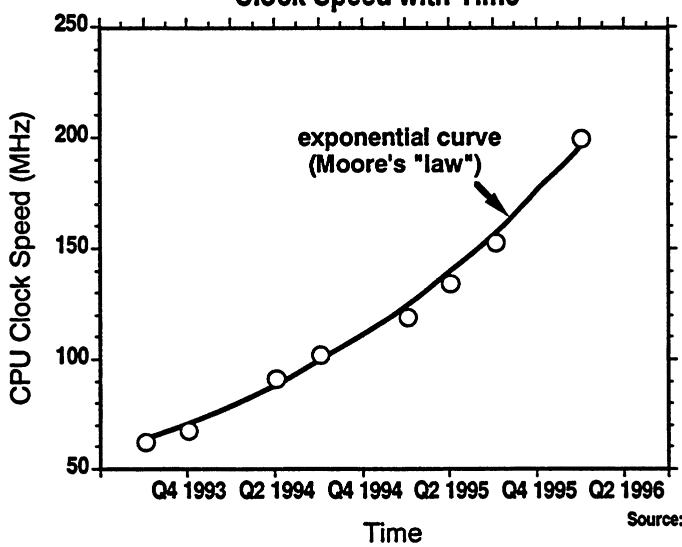

Source: InfoCorp.

RCP Consultants

Trends in System Performance of Massively-Parallel Supercomputers

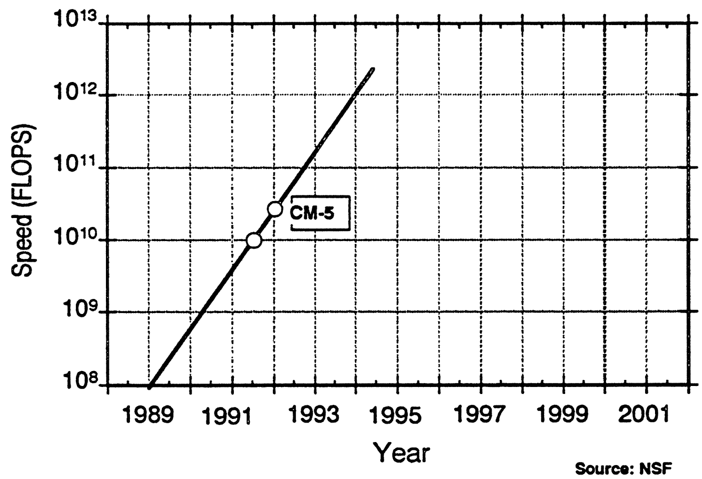

Source: NSF

RCP Consultants

Some Expectations of Active (LS) Device Models

- (1) Physics-based accuracy, (2) predictive, (3) geometric scalability
- Platform independent (transportable)
- Handle 2D geometry and 2D physical mechanisms
- Handle time-dependent phenomena (pulses, transit time effects)
- Seamless coupling to process simulators (parameters and statistics)
- Good correlation with SS models
- Thermal modeling (self-heating, environment)

R Consultants P

Types of Large-signal Device Models

- ◆ Curve-fitting functions
  - fast, no predictive properties, little scalability
- ◆ "Physics-based" (1D) models
  - slower, modest accuracy, some predictive properties and scalability
- ◆ Numerical models (2D, 3D, time-dependent)
  - highest accuracy, predictive properties, scalable, platform independent, *but too slow at present*

R Consultants P

An FET Model Rating Matrix

Model	analytic?	Fast execution?	Physical basis?	Predictive?	Handle 2D geometry?	Handle 2D physics?	Use with proc. simulator?	Useful for yield opt.?	Time dependency?	Potential accuracy?	Scalability?	Include temp. effects?
Curve fitting	+	+	-	-	-	-	-	-	0	-	-	0
1D "Physics-Based"	0	0	0	0	-	-	+	+	+	0	+	0
2D Numerical	-	-	+	+	+	+	+	+	+	+	+	+

+: positive feature

-: negative feature

0: "weak" feature

Some expectations of Passive Device Models

- Physics-based accuracy
- Compatibility with all circuit simulators and *platform independent*
- Extension to *true* 2D and 3D geometries and field distributions
- Inclusion of effects of finite volume of enclosure (packaging, shielding, etc.)
- Accurate treatment of dielectric and conductor losses
- Extension to larger element groups (coupling to adjacent elements)
- Fast execution (analytic or look-up tables)

What is required to realize outlined expectations for active and passive devices?

- *Numerical* simulation of devices
- Increased computer speeds and disk storage capabilities
- Use of computational techniques such as parallel processing in conjunction with partitioning techniques for active and passive components
- Real-time circuit optimization based on numerical simulators (EM and device)

RCP Consultants

Some Simple Cases of Parallel Processing Applied to *Conventional* Circuit Simulators

Two examples:

- Analysis cycle —1 CPU assigned to each frequency
- Optimization cycle — 1 CPU assigned to each optimized element

---

RCP Consultants

Parallel Processing of a Conventional CAD Simulator by Multiple Workstations

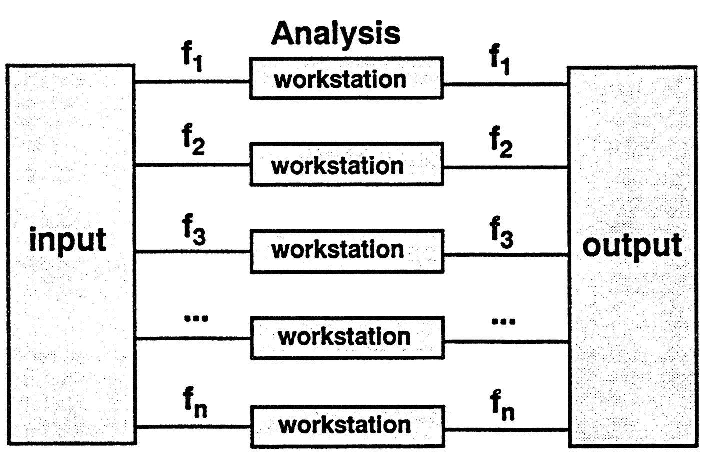

RCP Consultants

Example of Parallel Processing in Conventional CAD Simulators by a Multiprocessor Computer or WS

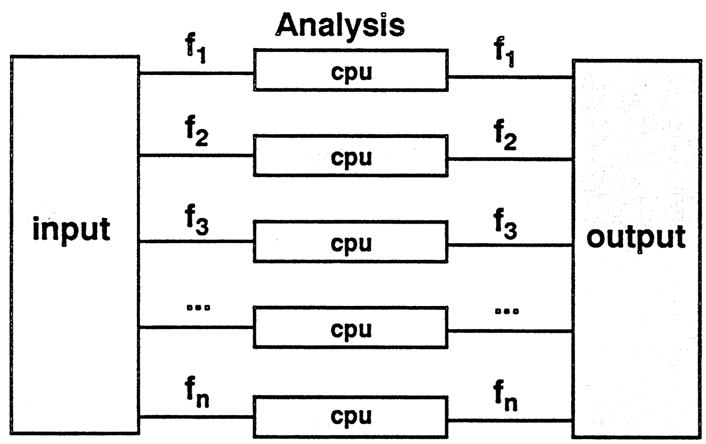

RCP Consultants

Example of Optimization in Conventional CAD Simulators by Parallel Processing

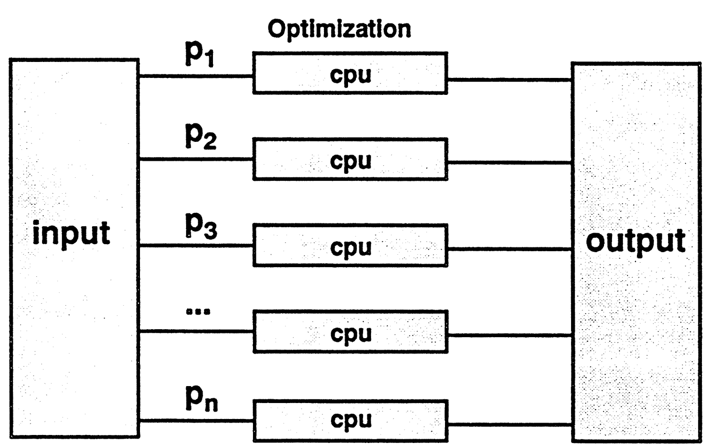

p: parameter being optimized

RCP Consultants

Parallel Processing Applied to Device Partitioning
— A Step in the Right Direction

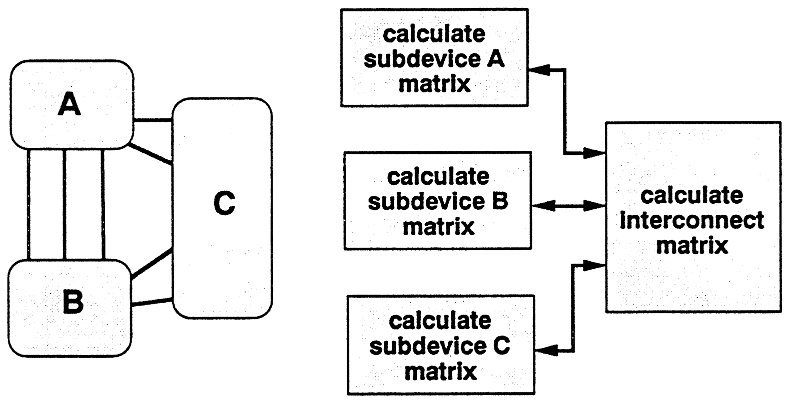

Partitioned Device

Processor Assignments

RCP Consultants

Parallel Processing Applied to Circuit Partitioning
— A Step in the Right Direction

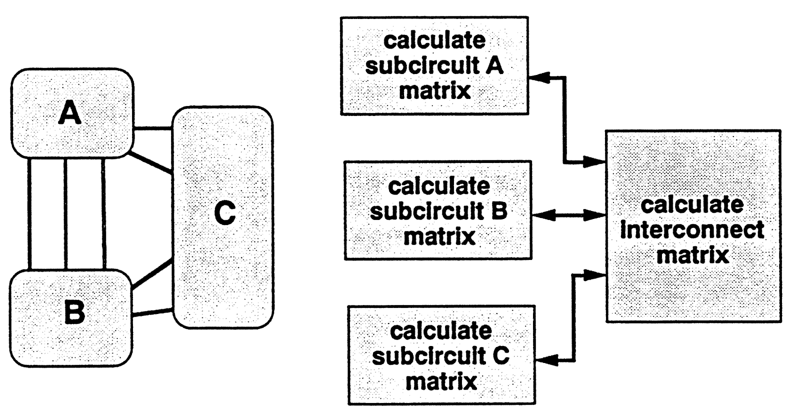

Partitioned Circuit

Processor Assignments

RCP Consultants

Visions of A Possible Approach to Circuit Simulation at the Highest Level of Parallelism

one circuit element ◄── one processor

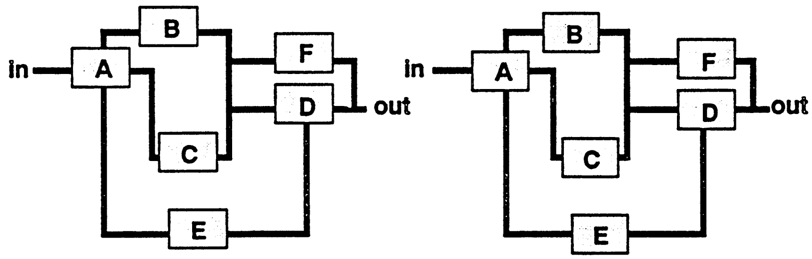

Each block is a circuit element | **Each block is a processor**

Interconnections denote *signal* flow | **Interconnections denote *data* flow**

RCP Consultants

A Proposed Design Methodology for the Next Century

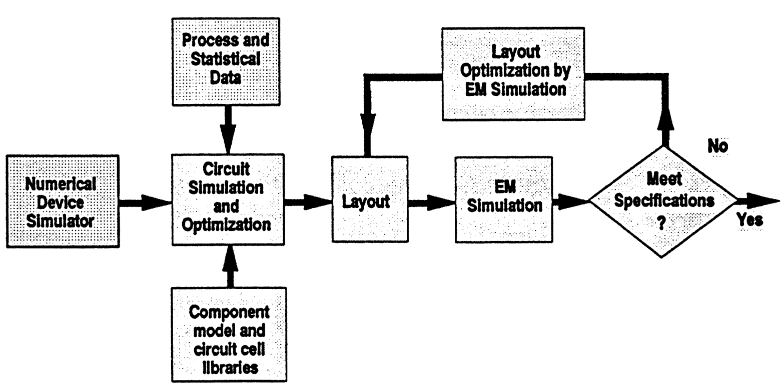

RCP Consultants

Predictions

- By end of the century 1000 MIP CPU's in multiprocessor workstations will become available in the laboratory
- Parallel computation with fast CPUs will make numerical simulation of active and passive components a viable approach in the next generation CAD
- Within a decade, numerical device and circuit simulation could become interactive CAD tools and make first-pass success a routine design procedure.

RCP Consultants

Expectations of a MMIC CAD System for the Next Century

- Verifiable active and passive component models to 100 GHz
- Models of electro-optic devices and quasi-optic techniques
- Numerical simulation techniques (active and passive components)
- Routine use of tolerance statistics and yield optimization
- Extension of EM simulation techniques to *entire* MMICs
- Automatic layout optimization by EM simulation technique (first pass design)
- Exploitation of parallel computation techniques
- First-pass design will be a routine procedure

Optimizing Microstrip Filters Using Electromagnetics

Mr. Daniel G. Swanson, Jr.
Staff Scientist

dswanson@netcom.com

Watkins-Johnson Company
3333 Hillview Avenue
Palo Alto, CA 94304

Outline

- The Optimization Process
- Pseudo Lumped Bandpass Filter
- Elliptic Lowpass Filter
- Conclusion

All analysis times are for a 50 MHz SPARC 10 with 64 MB RAM.

The Optimization Process

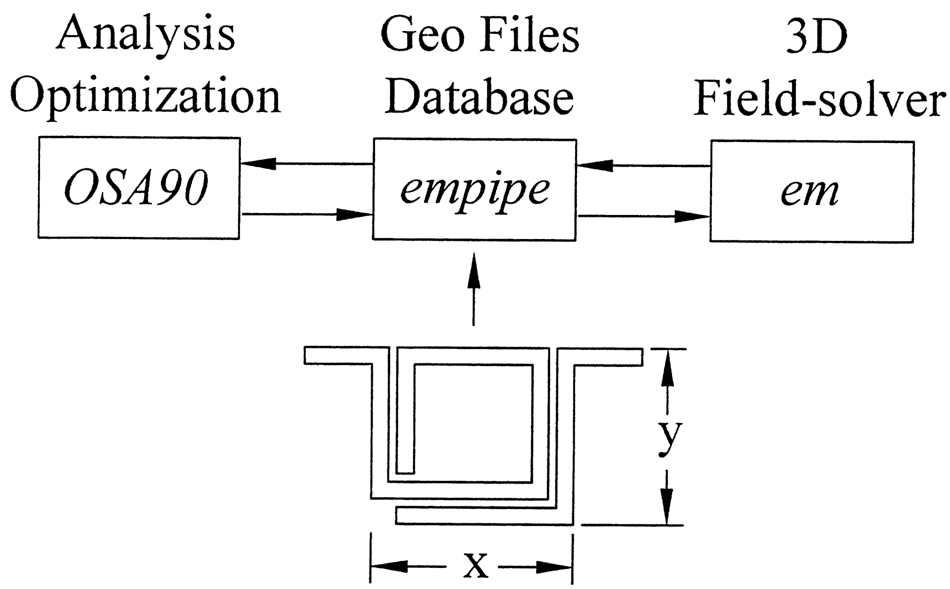

3.72 GHz Bandpass Filter

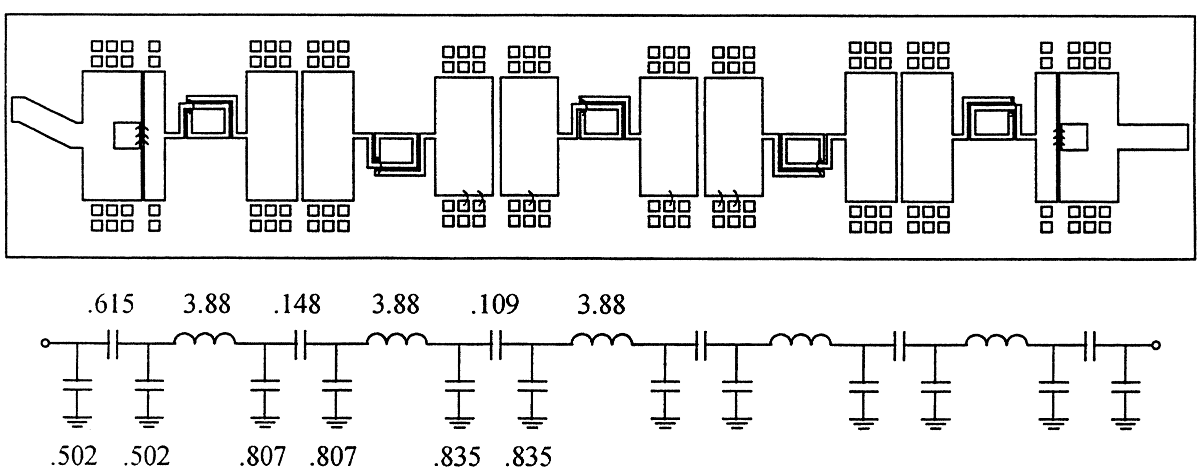

Units are pf and nH.

PINET Analytical Models

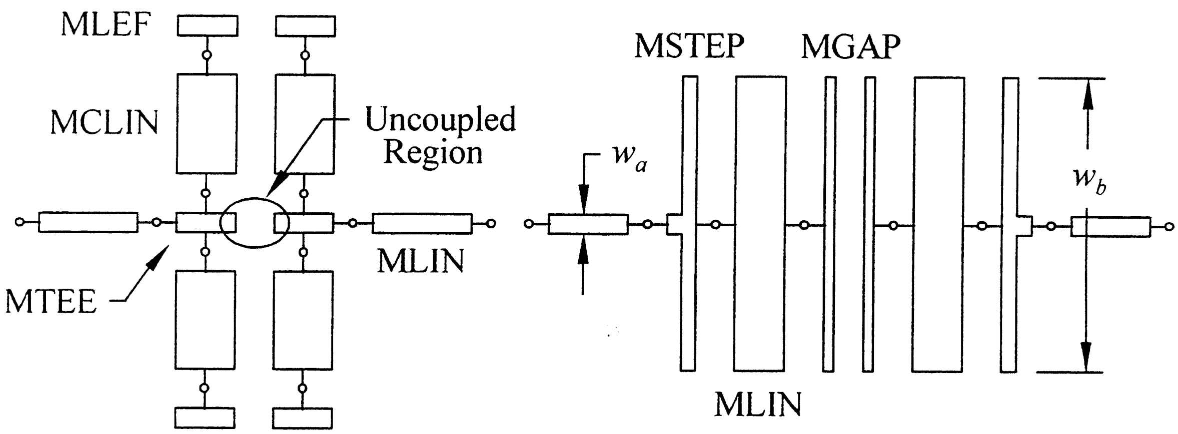

- Odd Mode Impedance
- Step: $w_a << w_b$
- Gap: $w_b >> h$
- Line: $w_b >> h$

Pi-network Visualization

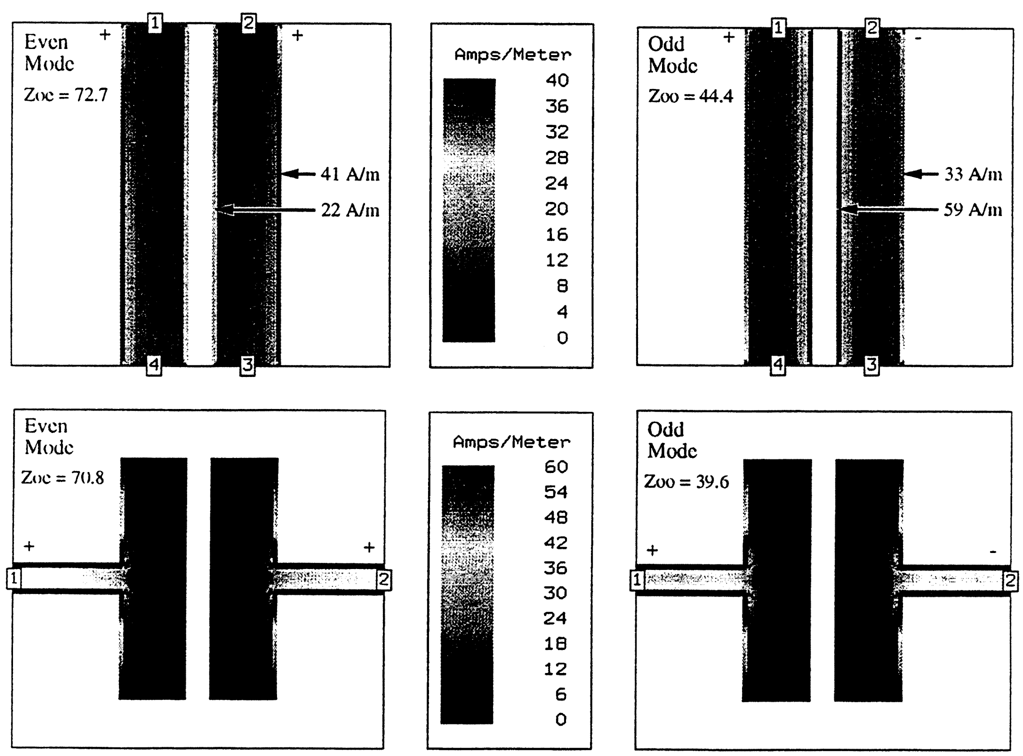

Circuit Theory Model of the Filter

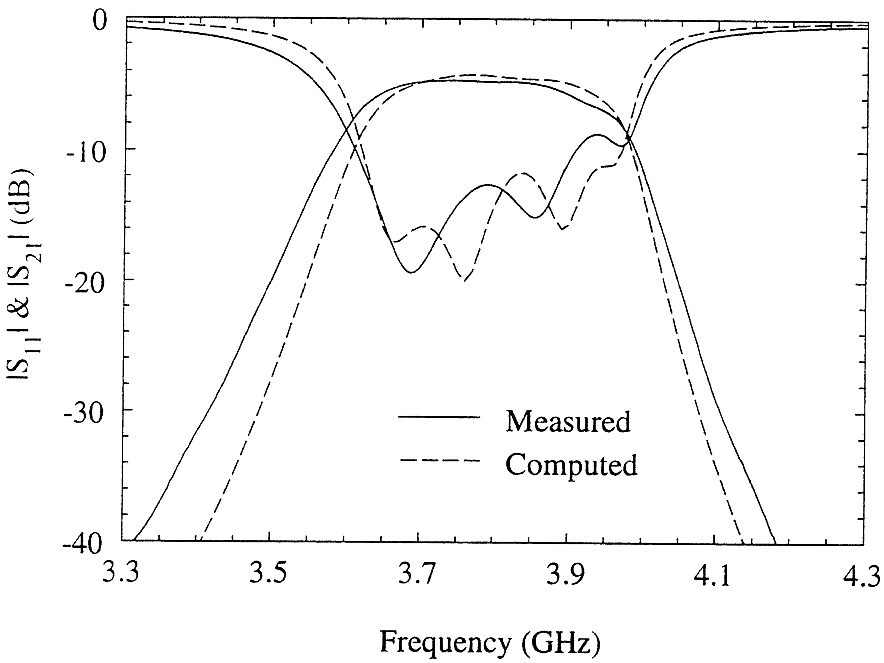

Meshing the PINETs

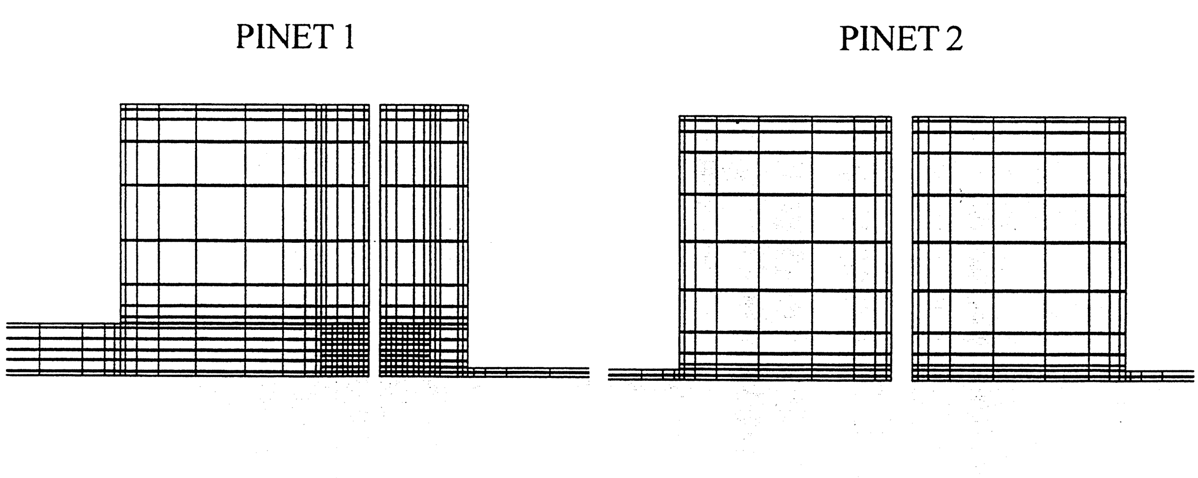

cell size = 1mil
subsections = 1213
6 min : 48 sec per freq

cell size = 1 mil
subsections = 454
2 min : 18 sec per freq

Meshing the Spiral Inductor

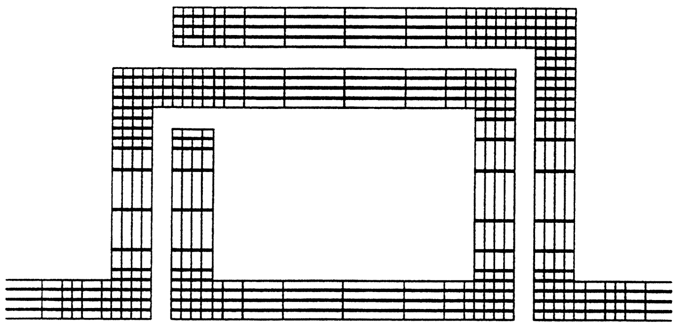

- ✓ Resolution in corners
- ✓ Cross-over region
- ✓ Convergence ?

width = 4 mils
gap = 2 mils

cell size = 1 mil
subsections = 976
4 min : 14 sec per freq

3.72 GHz Filter Results

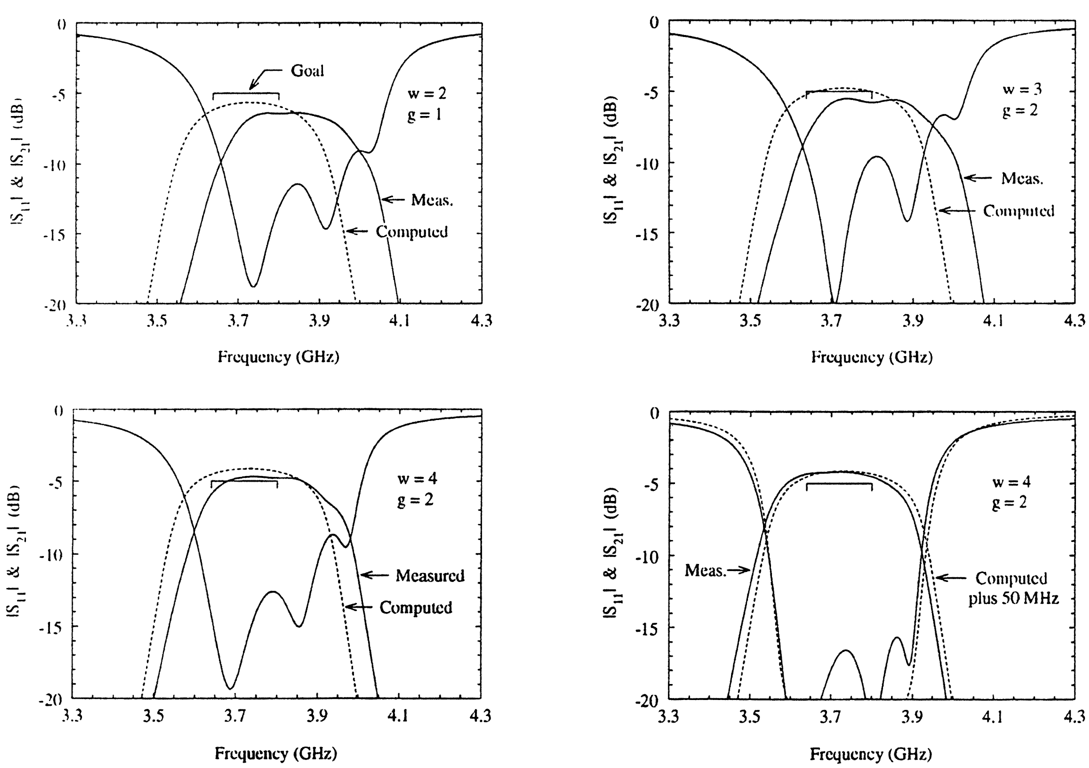

Analytical vs. Field-Solver Solutions

Analytical Solution

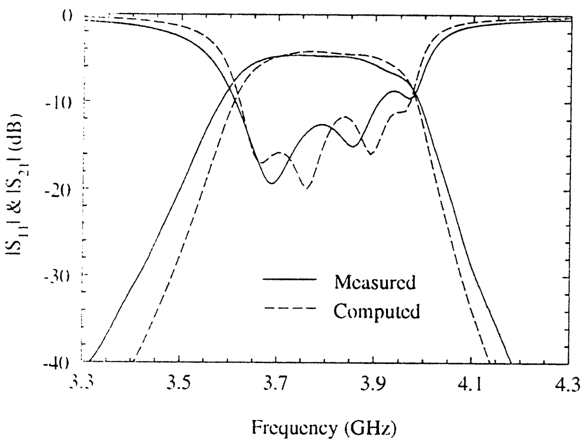

Field-Solver Solution

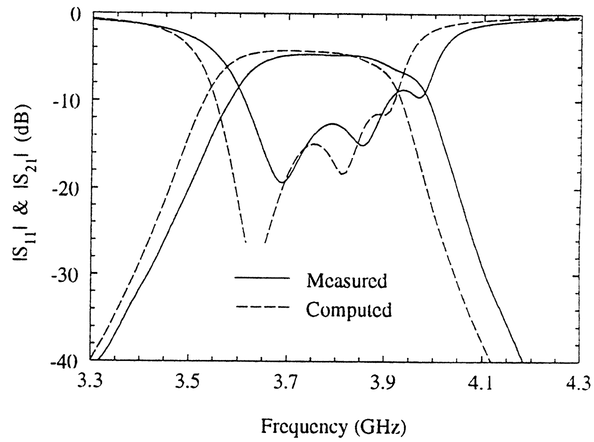

✓About 25 MHz bandwidth error.
✓Center frequency error?

✓About 50 MHZ center freq. error.
✓Very little bandwidth error.

Forcing Error Below 1%

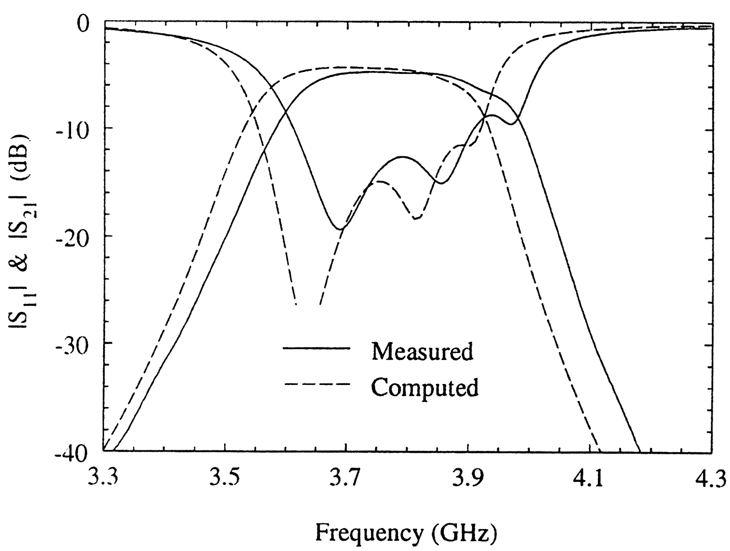

- ✓ Manufacturing Tolerances
- ✓ Substrate Parameters
- ✓ Parasitic Couplings
- ✓ Compensating Blunders

Bandpass Filter Summary

- ❑ Analytical filter model has about 15% bandwidth error.
- ❑ Field-solver filter model has about 1% center frequency error.
- ❑ User must watch for convergence on structures like spiral inductors.
- ❑ Validation of 1% errors for a large circuit is difficult.
- ❑ Direct driven em optimization based on interpolation works well for this type of problem.

19.3 GHz Elliptic Lowpass Filter

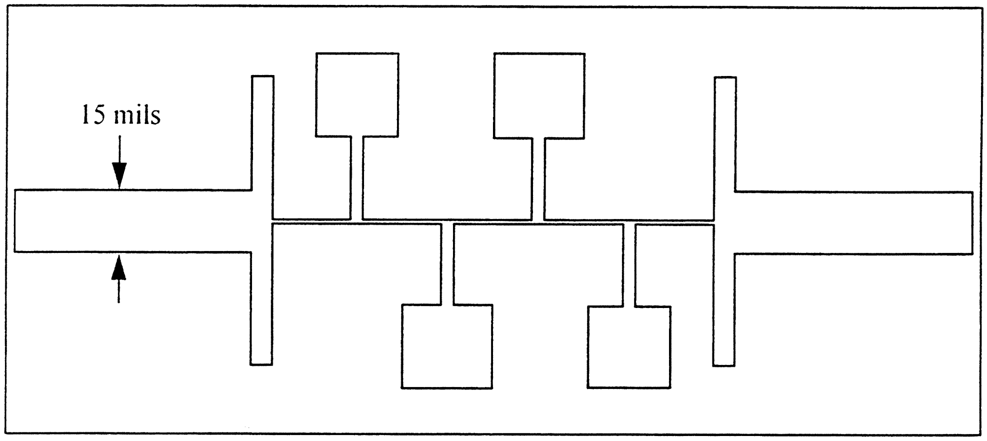

h = 15 mils, ε_r = 9.8

Measured vs. Circuit Theory

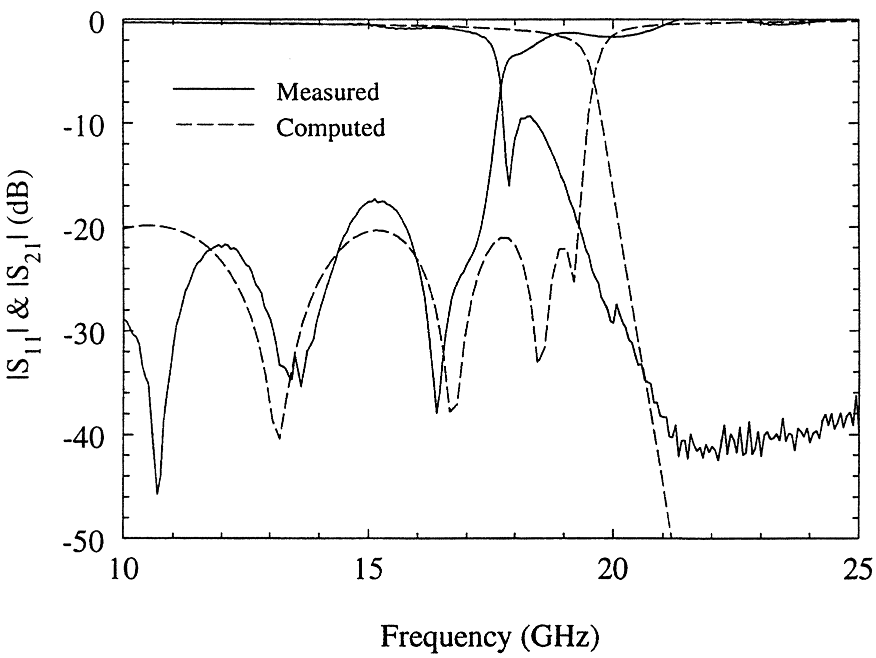

Approximate Couplings Using Circuit Theory

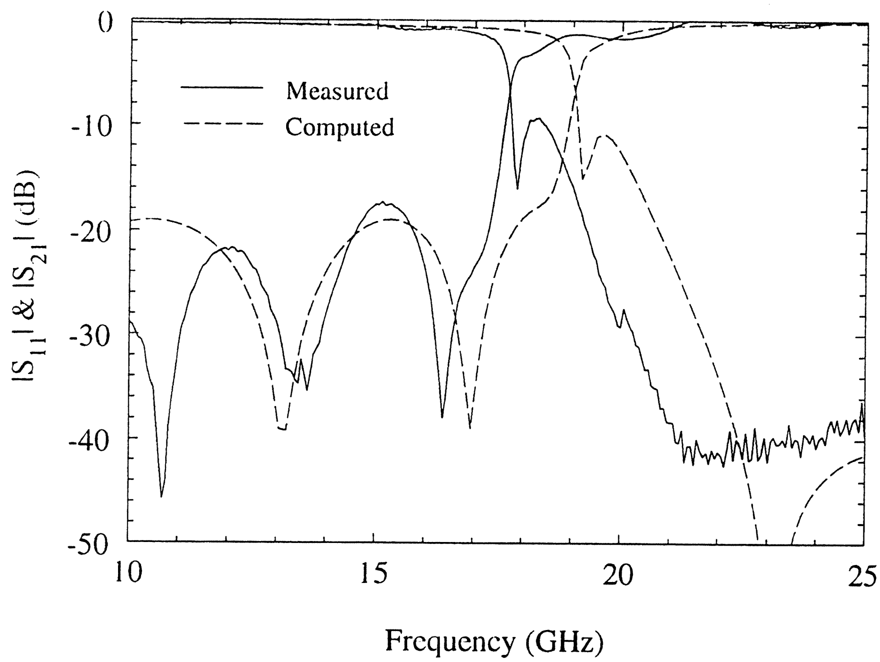

Field-Solver Analysis of the Complete Filter

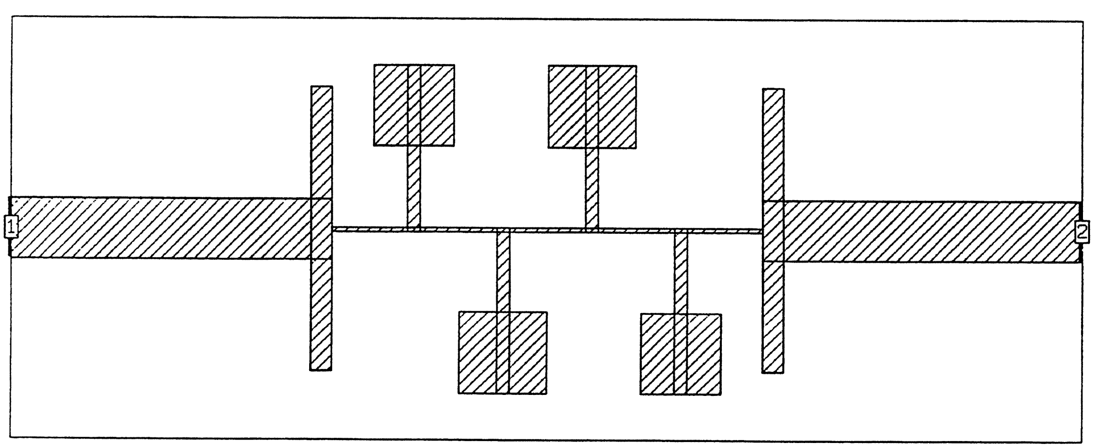

cell size = 0.25 mil
subsections = 2276
96 min : 36 sec per freq

Measured vs. Field-Solver

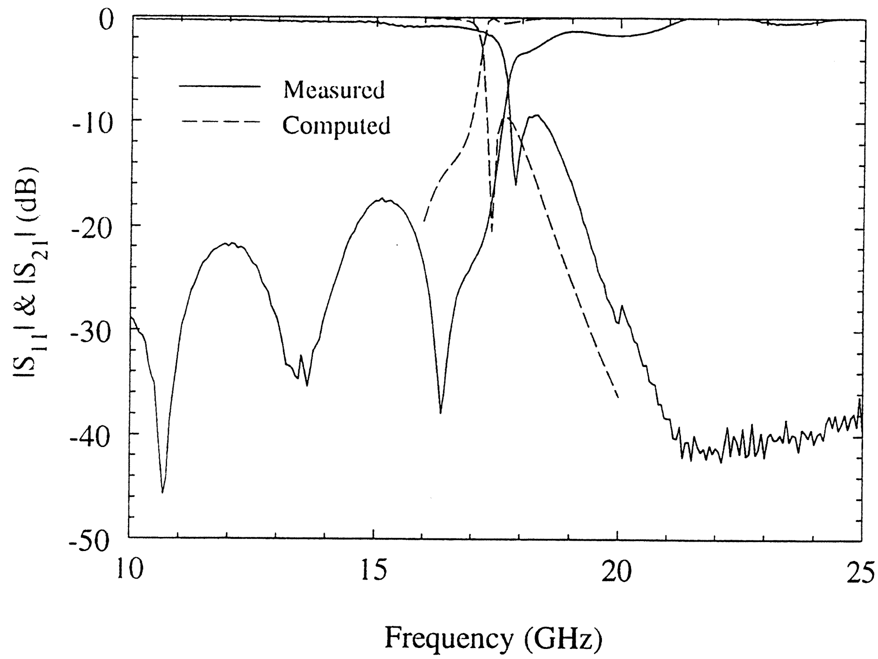

Summary of First Iteration Modeling

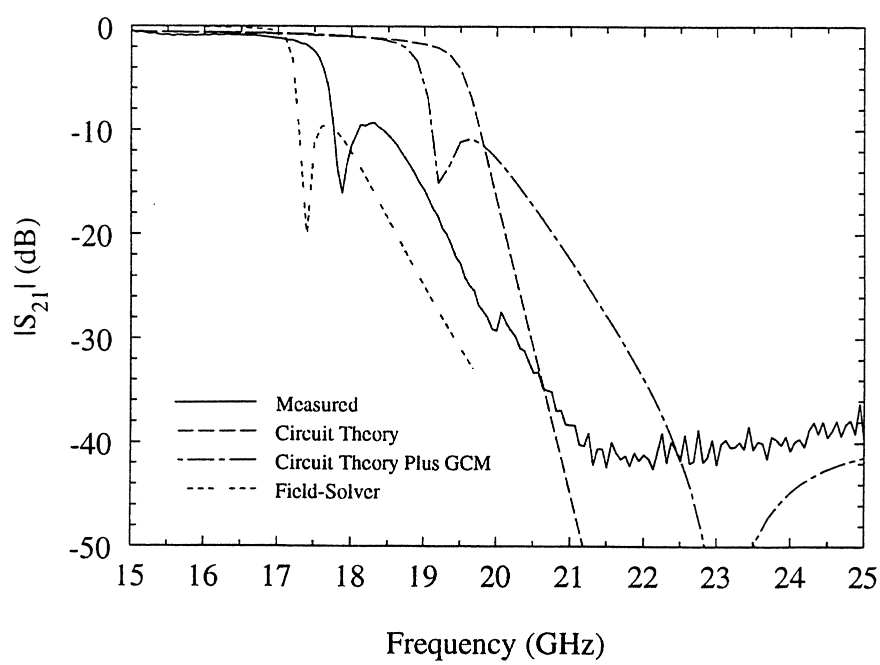

Optimizing the Lowpass Filter

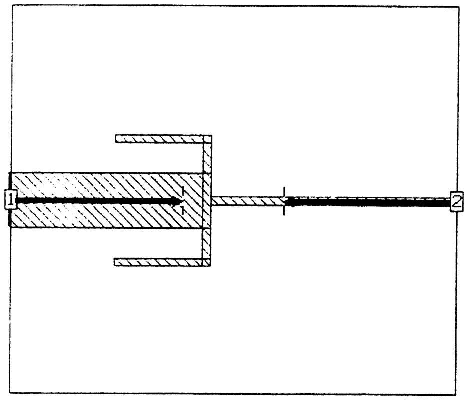

cell size = 1 mil
subsections = 401
1 min : 0 sec per freq

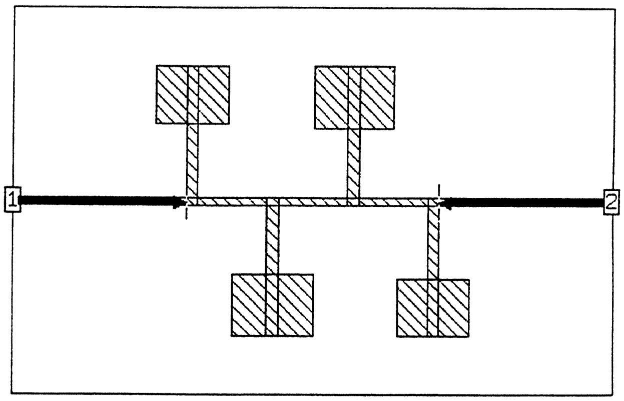

cell size = 0.5 mil
subsections = 955
1 min : 45 sec per freq

Optimizing the Lowpass Filter

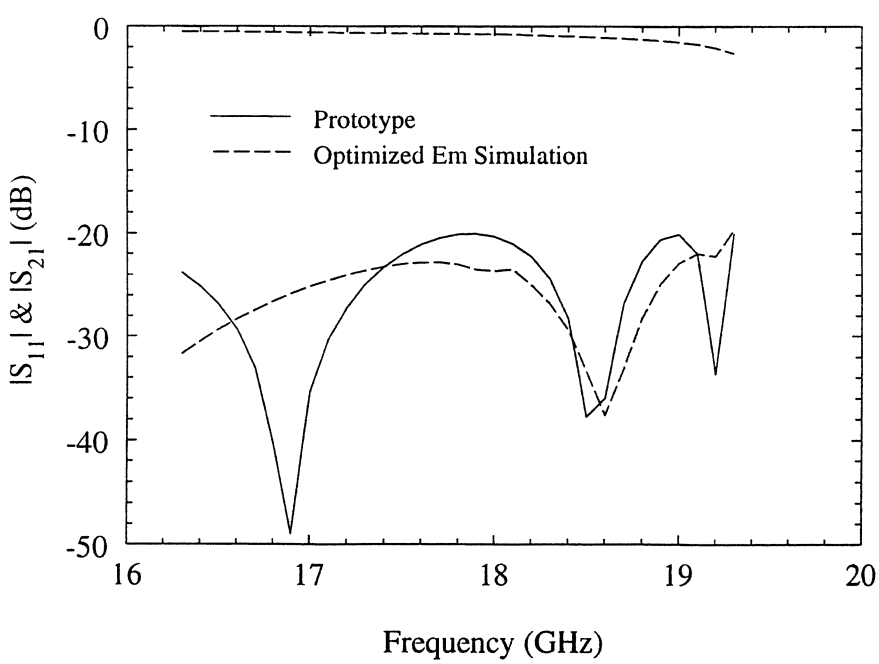

2nd Iteration of Lowpass Filter

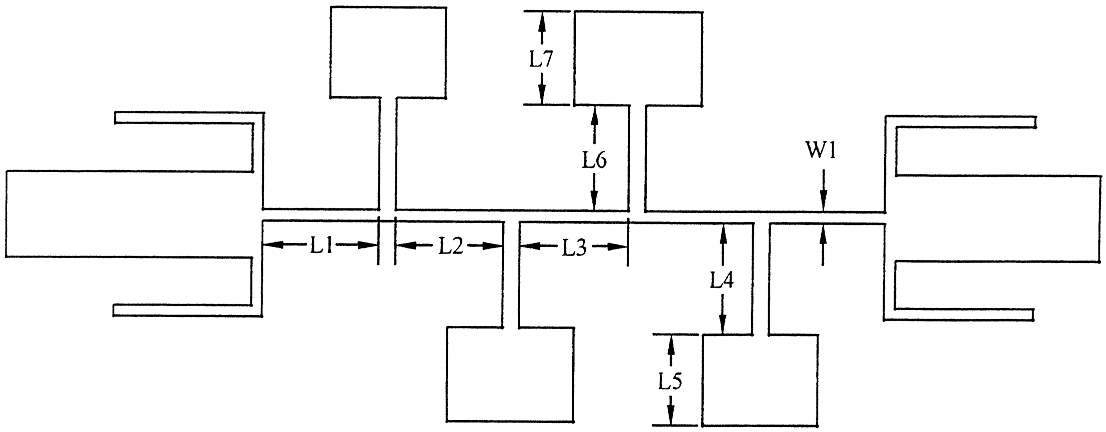

	W1	L1	L2	L3	L4	L5	L6	L7
1st Iter	1.0	18.1	18.3	18.3	19.3	19.1	19.0	19.6
2nd Iter	1.8	19.1	17.8	18.0	18.5	15.0	17.5	15.5

Dimensions are mils.

2nd Iteration Filter Results

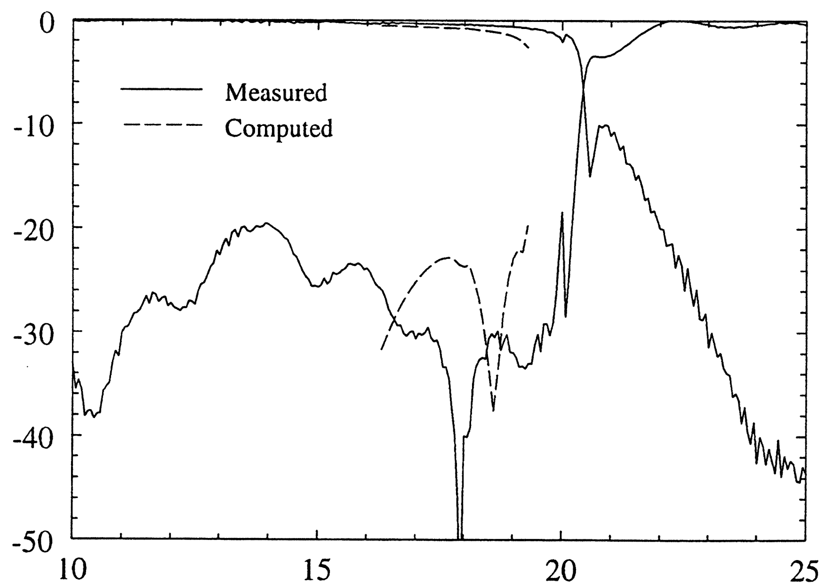

Lowpass Filter Summary

- Field-solver needed to model parasitic couplings.
- Accuracy of high impedance lines is a problem with the field-solver.
- Many poles and many variables in the same network stretches the capabilities of interpolation based em optimization.
- Space-mapping or genetic algorithms may be a better approach for this type of problem.

Conclusions

- Bandpass Filter
  - Few variables per network.
  - No poles in the network.
  - Interpolation based optimization works well.
- Lowpass Filter
  - Many variables per network.
  - Many poles per network.
  - Pushes the limits of this optimization technique.
  - Space-mapping or genetic algorithms might be better.
- Modeling Issues Unrelated to Optimization

AUTOMATED EM OPTIMIZATION OF LINEAR AND NONLINEAR CIRCUITS, WITH GEOMETRY CAPTURE FOR ARBITRARY PLANAR STRUCTURES

S.H. Chen

Optimization Systems Associates Inc.
P.O. Box 8083, Dundas, Ontario
Canada L9H 5E7

presented at

WORKSHOP ON AUTOMATED CIRCUIT DESIGN USING ELECTROMAGNETIC SIMULATORS
1995 IEEE MTT-S Int. Microwave Symposium, Orlando, FL, May 15, 1995

Critical Issues of Automated EM Optimization

interfaces between gradient-based optimizers and discretized EM field solvers: interpolation and database

integration of EM analysis with circuit simulation, including harmonic balance simulation of nonlinear circuits

Geometry Capture™: user-defined optimizable structures of arbitrary geometry

Space Mapping™ optimization: intelligent correlation between engineering models: EM models, empirical models and equivalent circuit models

smoothness and continuity of response interpolation

robustness of optimization algorithms and uniqueness of the solutions

parallel and massively parallel EM analyses

Interface Between Optimizer and EM Solver
(*Bandler et al., 1993*)

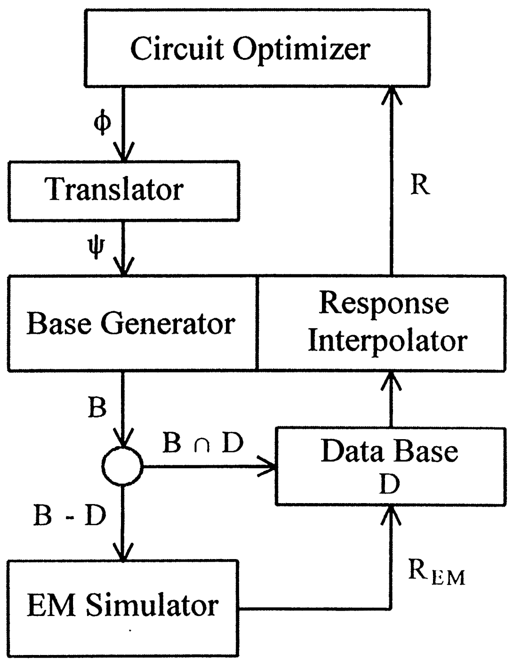

EM Optimization Environment

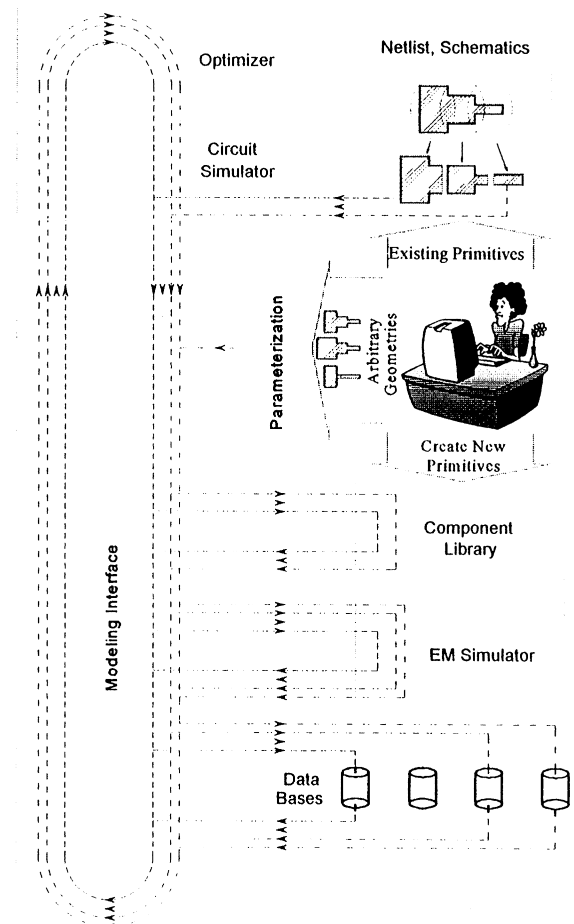

Simulation of Static Structures via Empipe™
(*OSA, 1992*)

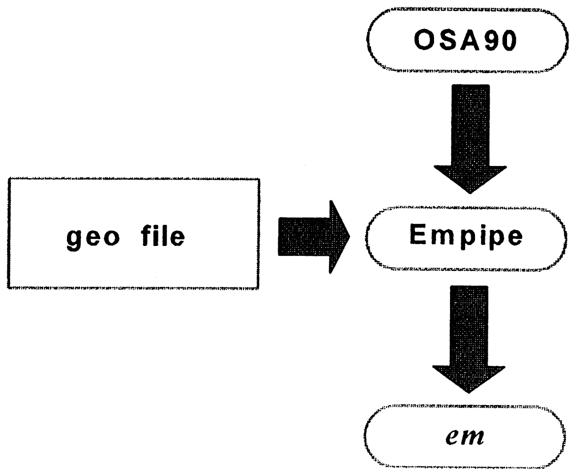

useful for analyzing circuits of mixed EM and empirical models

unsuitable for EM optimization

Empipe™ Optimizable Library Structures
(*OSA, 1992*)

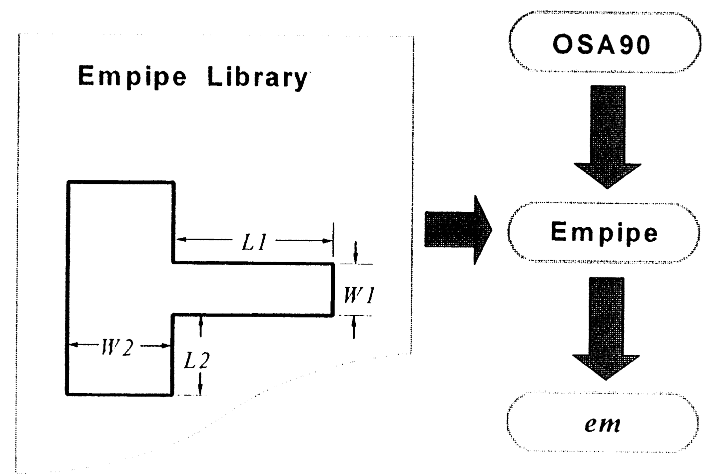

preprogrammed, ready to use

limited selection

complex structure decomposed into elementary structures connected by circuit theory, neglecting couplings between the elements

Empipe™ Library of Microstrip Structures

bend
cross junction
double patch capacitors
interdigital capacitors
line
mitered bend
open stub
overlay double patch capacitors
rectangular structure
spiral inductors
step junction
symmetrical and asymmetrical folded double stubs
symmetrical and asymmetrical gaps
symmetrical and asymmetrical double stubs
T junction

Geometry Capture™
(*OSA, 1994*)

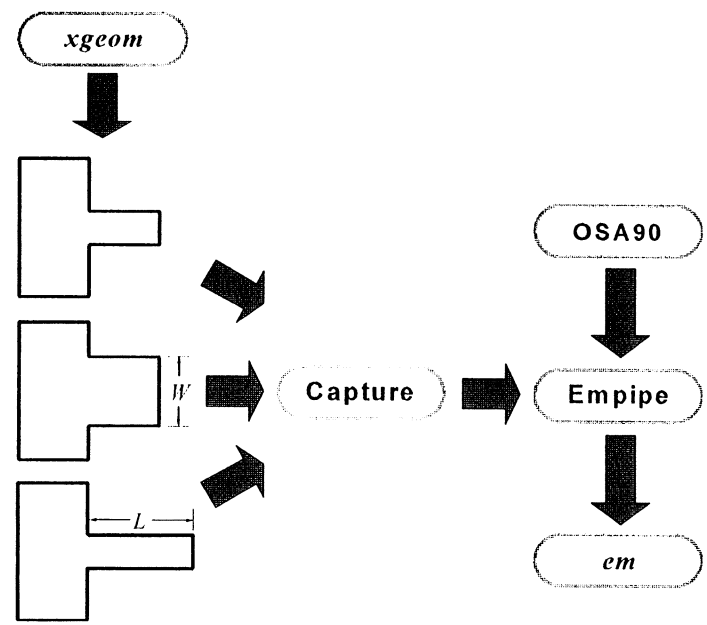

intuitive and totally flexible

graphical description of parameters and constraints

optimization not limited to geometrical dimensions but can also include substrate/metallization parameters

Microstrip Double Folded Stub Filter
(*Rautio, 1992*)

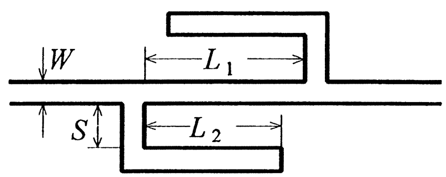

em™ driven by OSA90/hope™ through Empipe™

minimax optimization to move the center frequency of the stop band from 15 GHz to 13 GHz

W fixed at 4.8 mils

L_1, L_2 and S are variables

substrate thickness: 5 mils

relative dielectric constant: 9.9

design specifications

$\lvert S_{21}\rvert > -3$ dB	for $f < 9.5$ GHz and $f > 16.5$ GHz
$\lvert S_{21}\rvert < -30$ dB	for 12 GHz $< f <$ 14 GHz

EM Simulation of the Double Folded Stub Filter

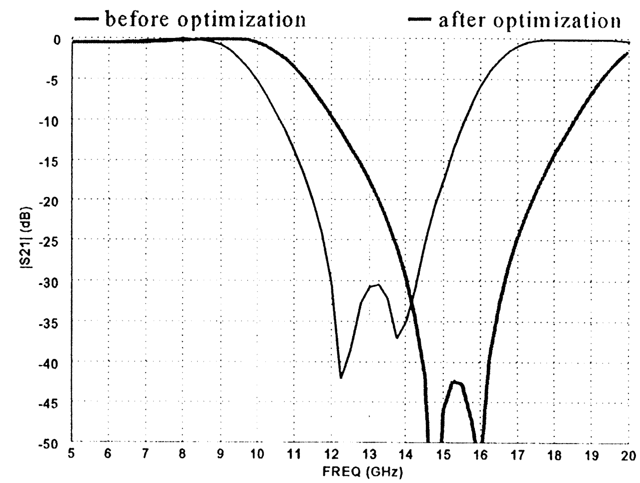

26-40 GHz Interdigital Bandpass Filter
(*Swanson, 1992*)

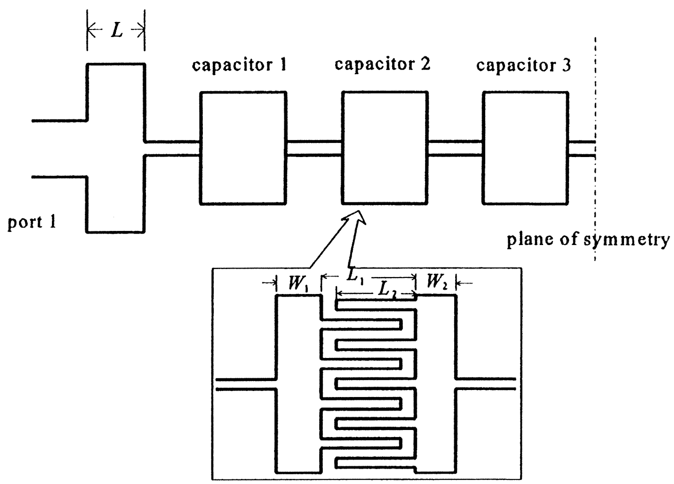

the initial design was obtained by matching a synthesized lumped ladder prototype at the center frequency using ***em***™

when the filter was simulated by ***em***™ in the whole frequency range, significant discrepancies w.r.t. the prototype necessitated manual adjustment and made a satisfactory design very difficult to achieve

EM Optimization of the Interdigital Bandpass Filter

a total of 13 designable parameters including the distance between the patches L_1, the finger length L_2 and two patch widths W_1 and W_2 for each of the three interdigital capacitors, and the length L of the end capacitor

the second half of the circuit, to the right of the plane of symmetry, is assumed identical to the first half, so it contains no additional variables

the transmission lines between the capacitors were fixed at the originally designed values

design specifications

$|S_{11}| < -20$ dB   and $|S_{21}| > -0.04$ dB

for 26 GHz $< f <$ 40 GHz

substrate thickness: 10 mils

dielectric constant: 2.25

Simulation of the Interdigital Bandpass Filter After Optimization

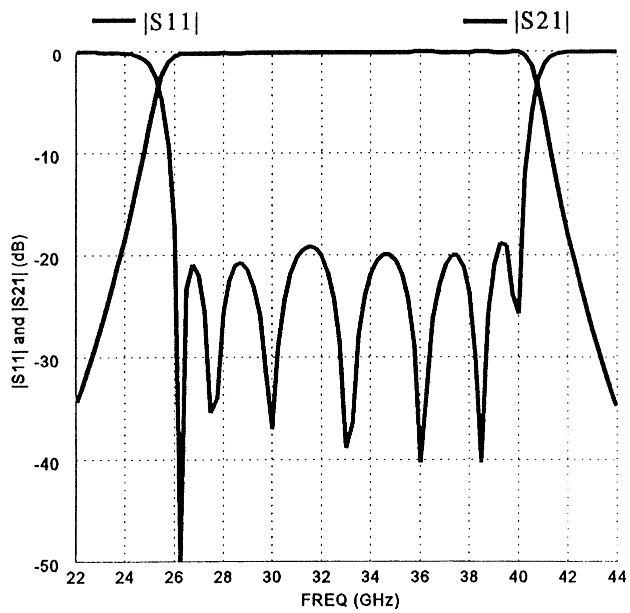

a typical minimax equal-ripple response of the filter was achieved after a series of consecutive optimizations with different subsets of optimization variables and frequency points

the resulting geometrical dimensions were rounded to 0.1 mil resolution

Nonlinear FET Class B Frequency Doubler
(*Microwave Engineering Europe, 1994*)

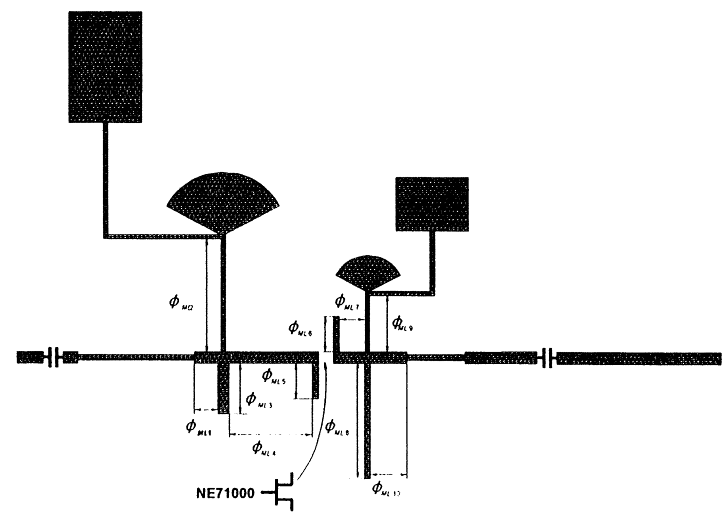

using Geometry Capture™, the linear subcircuit is defined as one optimizable structure with 10 variables

design specifications

conversion gain > 3 dB

spectral purity > 20 dB

at 7 GHz and 10 dBm input power

Conversion Gain Before and After Optimization

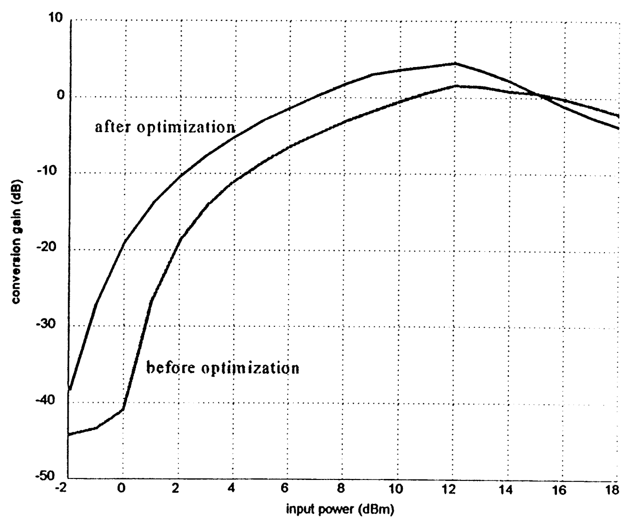

Optimization Systems Associates Inc.

Conversion Gain Before and After Optimization

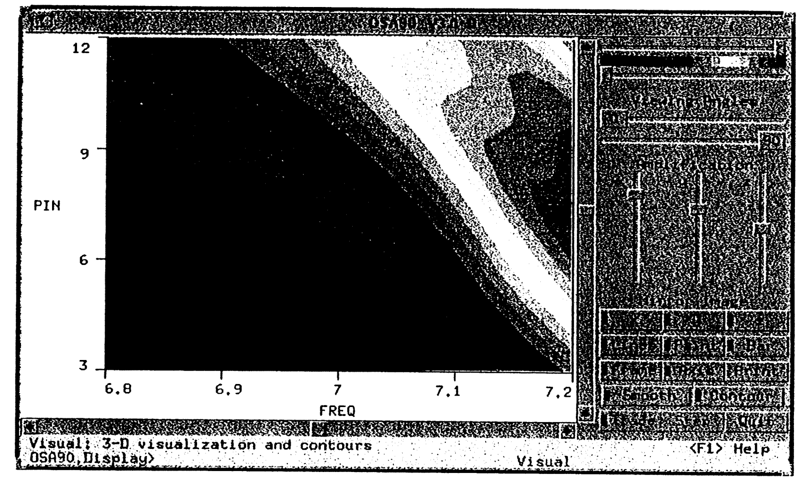

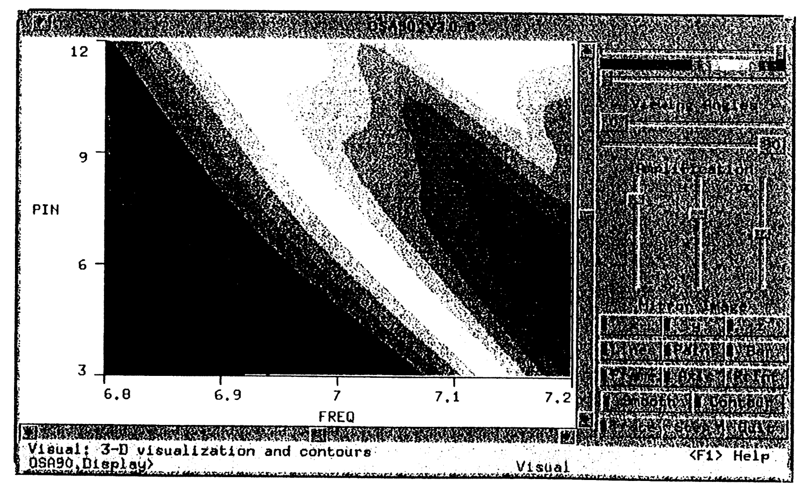

Spectral Purity Before and After Optimization

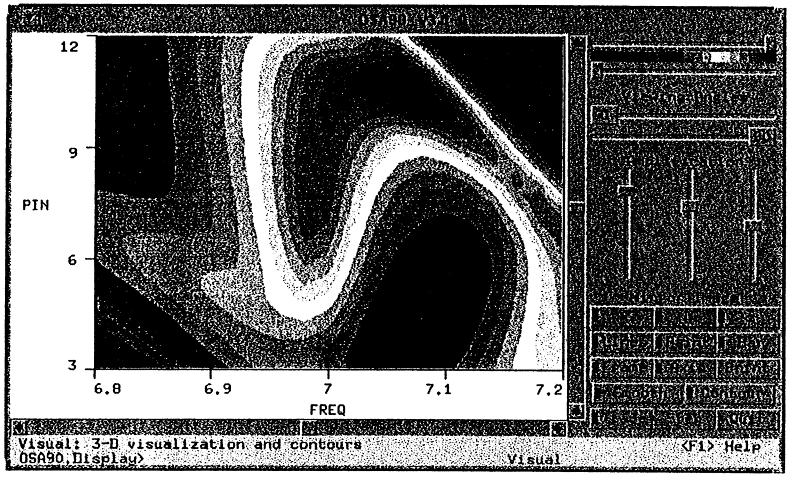

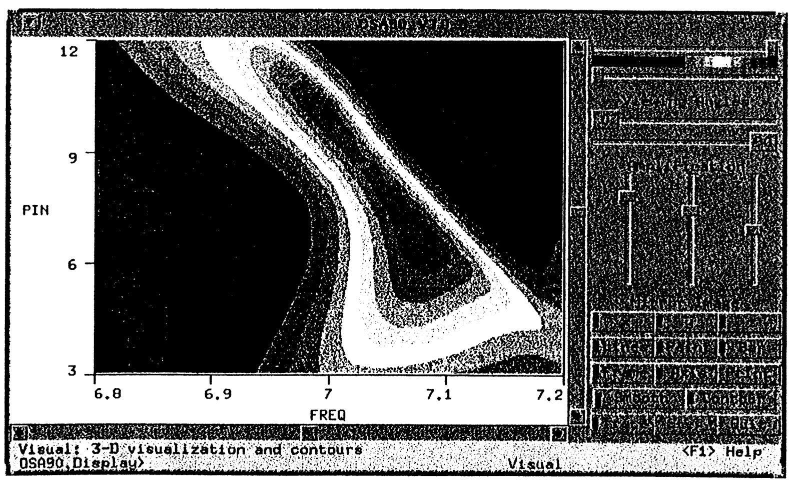

Space Mapping™
(*Bandler et al., 1994*)

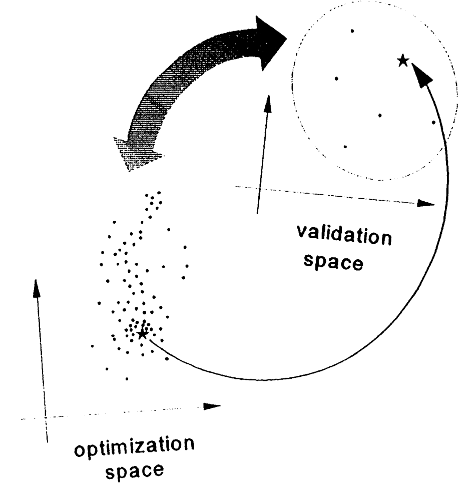

optimization model:	$\boldsymbol{R}_{os}(\boldsymbol{x}_{os})$
EM model:	$\boldsymbol{R}_{em}(\boldsymbol{x}_{em})$
Space Mapping:	$\boldsymbol{x}_{os} = \boldsymbol{P}(\boldsymbol{x}_{em})$
such that	$\boldsymbol{R}_{os}(\boldsymbol{P}(\boldsymbol{x}_{em})) \approx \boldsymbol{R}_{em}(\boldsymbol{x}_{em})$
Space Mapped solution:	$\bar{\boldsymbol{x}}_{em} = \boldsymbol{P}^{-1}(\boldsymbol{x}^{*}_{os})$

Aggressive Space Mapping™
(*Bandler et al., 1995*)

new algorithm aggressively exploits *every* EM simulation

avoids upfront EM analyses at many base points

applies the classical Broyden update to the mapping

quasi-Newton iteration

$$x_{em}^{(j+1)} = x_{em}^{(j)} - B^{(j)^{-1}} (P^{(j)}(x_{em}^{(j)}) - x_{os}^{*})$$

Broyden update:

$$B^{(j+1)} = B^{(j)} + \frac{(P^{(j+1)}(x_{em}^{(j+1)}) - x_{os}^{*})\, h^{(j)^T}}{h^{(j)^T} h^{(j)}}$$

where

$$h^{(j)} = x_{em}^{(j+1)} - x_{em}^{(j)}$$

The HTS Quarter-Wave Parallel Coupled-Line Filter
(*Westinghouse, 1993*)

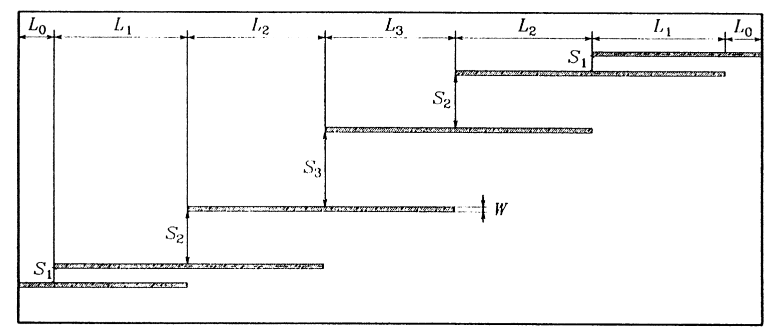

20 mil thick lanthanum aluminate substrate

the dielectric constant is 23.4

the x and y grid sizes for ***em*** simulation are 1.0 and 1.75 mil

100 elapsed minutes are needed for ***em*** analysis at a single frequency on a Sun SPARCstation 10

design specifications

$|S_{21}| < 0.05$ for $f < 3.967$ GHz and $f > 4.099$ GHz

$|S_{21}| > 0.95$ for 4.008 GHz $< f < 4.058$ GHz

Optimization Systems Associates Inc.

Starting Point of EM Optimization: Design Using Empirical Circuit Model

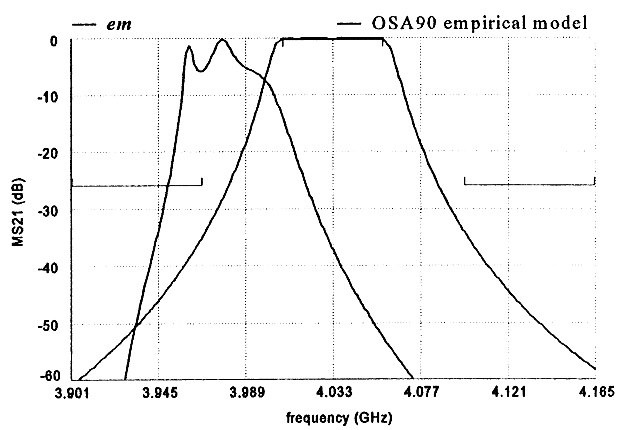

Optimization Systems Associates Inc.

Solution by Aggressive Space Mapping: 4 Iterations Only

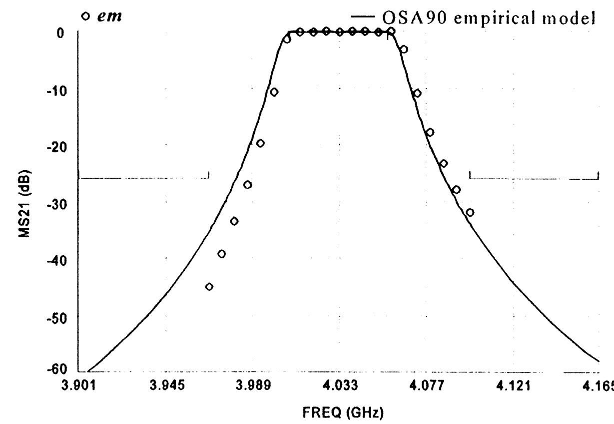

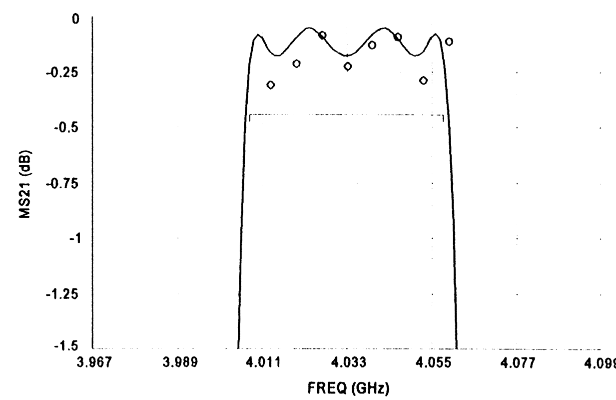

Solution Uniqueness Tested by Random Starting Points

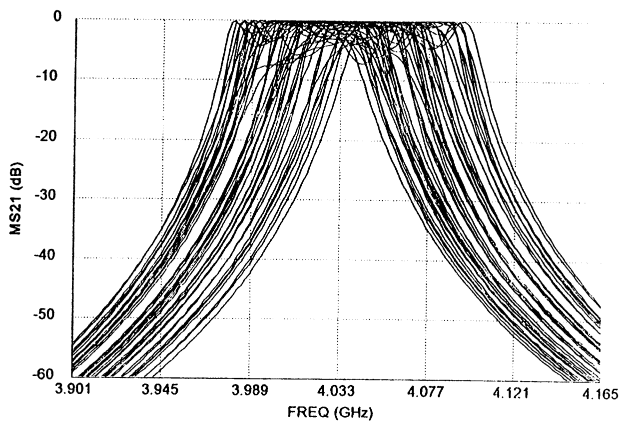

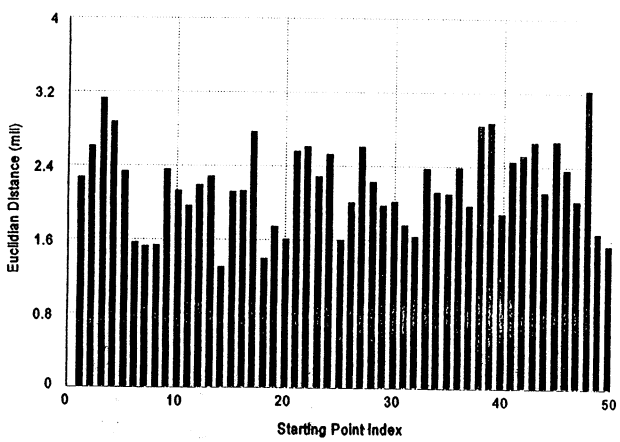

Solutions from the Random Starting Points

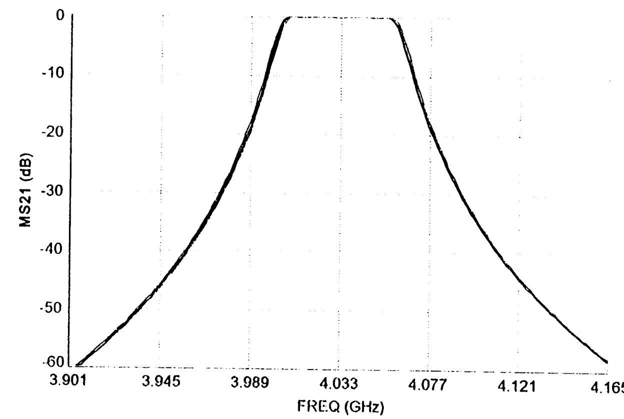

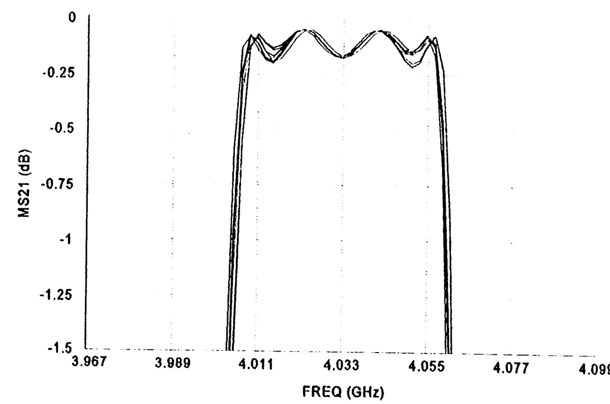

Two Distinct Solutions with Similar Responses

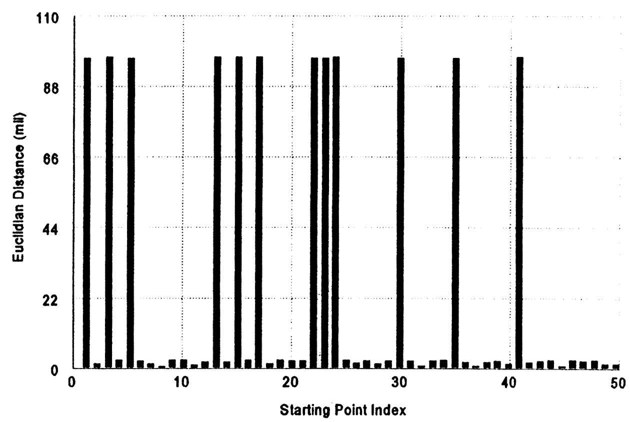

Truncation to the Nearest On-Grid Point

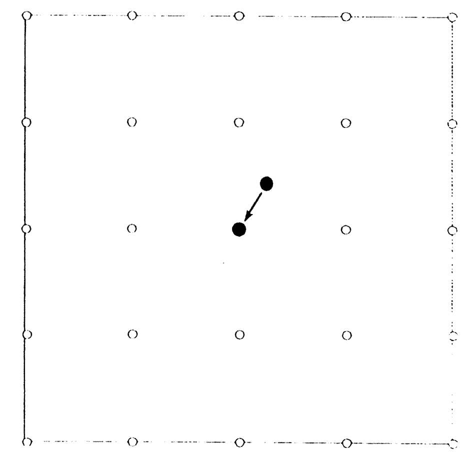

Linear Interpolation

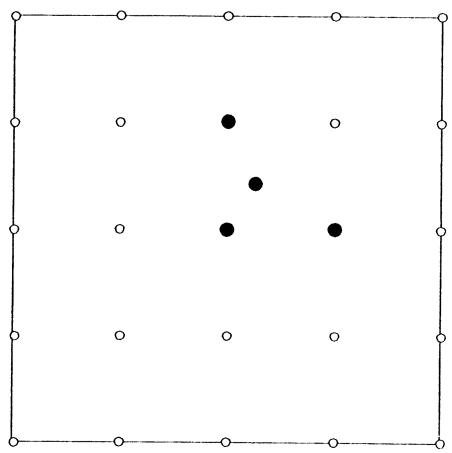

Optimization Systems Associates Inc.

Quadratic Interpolation

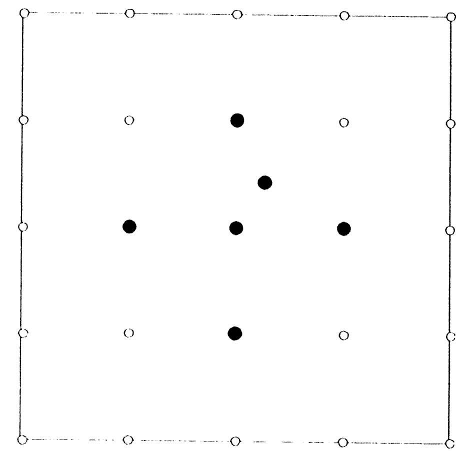

Potential Pitfalls Associated with Interpolation

interpolation may lead to distorted results especially for structures with resonance(s)

double stub test circuit

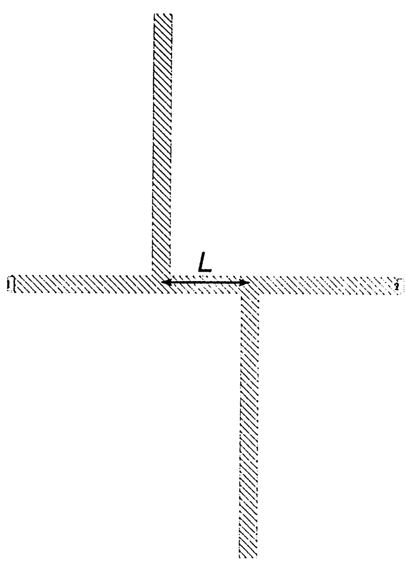

interpolate the parameter L between 30 mils and 35 mils (the grid size is 5 mils).

Linear Interpolation Based on *S* parameters

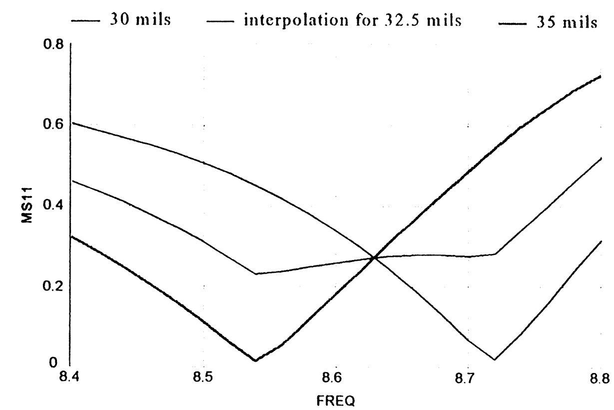

Linear Interpolation Based on *Y* Parameters

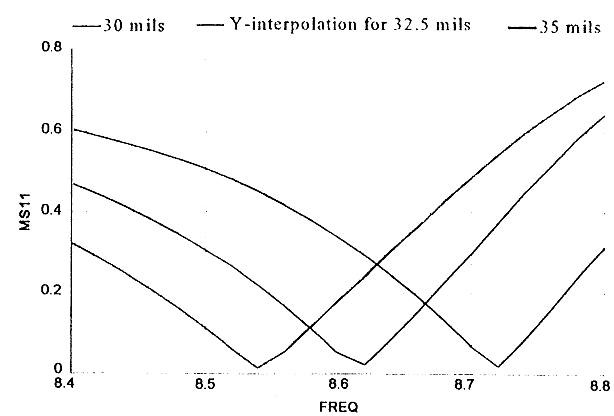

Y-Parameter-Interpolation May Also Have Problems

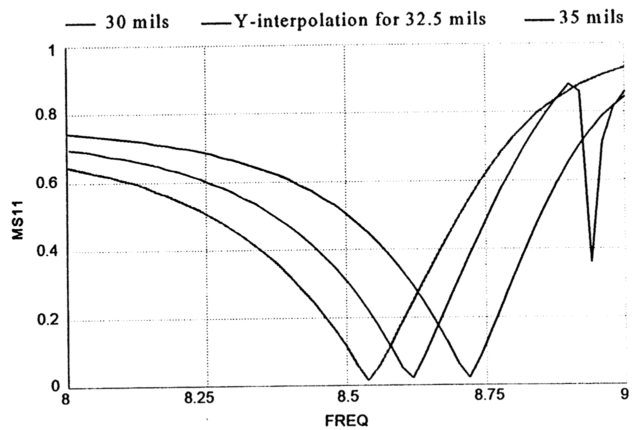

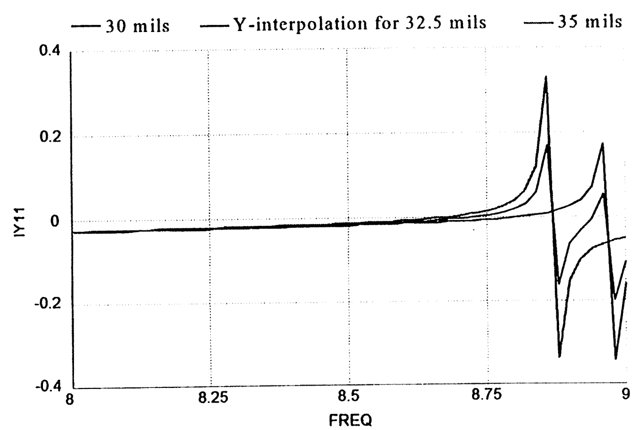

Empirical Circuit Model for Space Mapping

structure

empirical circuit model

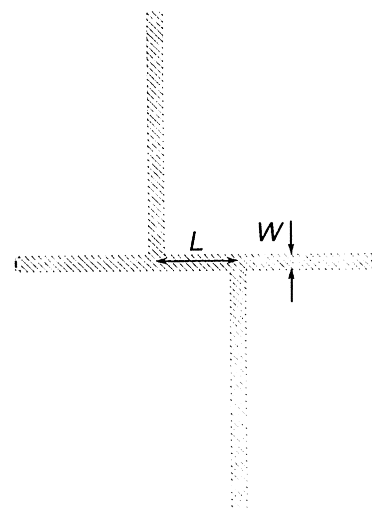

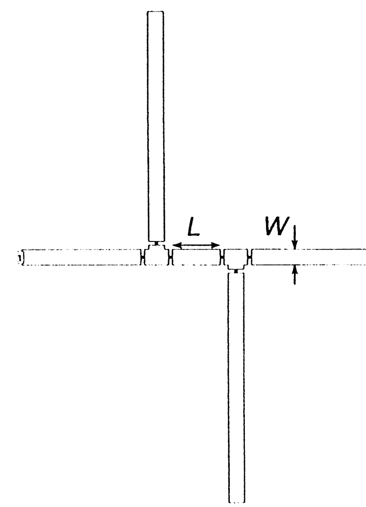

Parameter Extraction for Two On-Grid Points

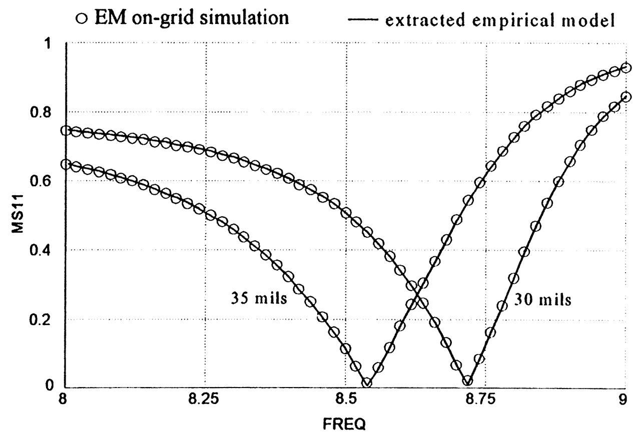

EM Parameters	
W	*L*
5 mils	30 mils
5 mils	35 mils

Empirical Model Parameters	
W	*L*
4.67 mils	32.1 mils
4.62 mils	37.2 mils

Optimization Systems Associates Inc.

Space Mapping for Response Interpolation

$$x_{em} \triangleq [\, L_{em} \,]$$

$$x_{os} \triangleq [\, W_{os} \quad L_{os} \,]^T$$

W_{em} is considered a constant since the interpolation is with respect to L_{em}

Space Mapping: $x_{os} = P(x_{em})$

parameter extraction: $R_{os}(x_{os}) \approx R_{em}(x_{em})$

base points: $L_{em} = 30$ mils and 35 mils

interpolation: $x^i_{os} = P(L_{em} = 32.5 mils)$

interpolated response: $R_{os}(x^i_{os})$

Space Mapping for Response Interpolation

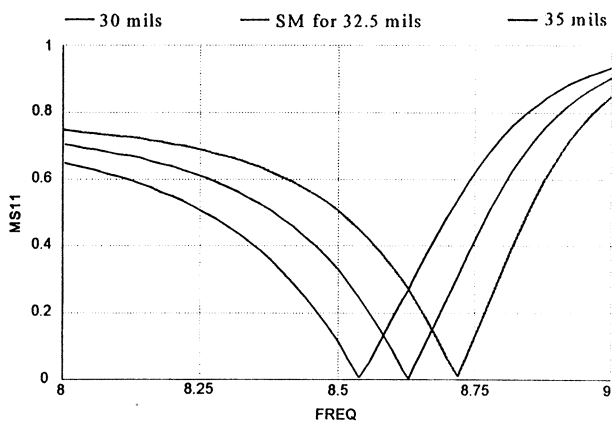

Conclusions

automated EM optimization is already a reality, providing solutions to practical problems

Geometry Capture™ empowers designers with user-definable capabilities never before considered possible

integrating EM and harmonic balance simulations elevates nonlinear circuit analysis and optimization to a new level of accuracy

Space Mapping™ is the key to combining previously disjoint simulation technologies, with wider applications yet to be explored

emerging new algorithms and implementations further improve the speed, robustness and user-friendliness of automated EM optimization

The Electromagnetic Analysis and Optimization of a Broad Class of Problems Using Companion Models

Anthony M. Pavio

Motorola Communications Semiconductor Products Division
5005 East McDowell Rd., E108
Phoenix, AZ 85008
602-244-3422

OVERVIEW

- METHOD OUTLINE AND ADVANTAGES
- NOTCH FILTER EXAMPLE
- DELAY LINE ANALYSIS AND OPTIMIZATION
- HIGH "Q" FILTER DESIGN
- CONCLUSION

METHOD OUTLINE

- THE CIRCUIT IS ANALYZED USING STANDARD LINEAR/ NONLINEAR SIMULATION TECHNIQUES.
- THE OPTIMIZED CIRCUIT VALUES (COMPANION MODEL) ARE MAPPED TO THE EM SIMULATOR.
- THE CIRCUIT MODEL VALUES ARE THEN ADJUSTED SO THAT THE SIMULATED PERFORMANCE MATCHES THAT OF THE FIRST PASS EM SIMULATION.
- THE CHANGE IN VALUES FROM THE COMPANION CIRCUIT MODEL ARE THEN USED TO UPDATE THE EM SIMULATOR FOR THE NEXT ITERATION STEP.

SIMPLIFIED EXAMPLE

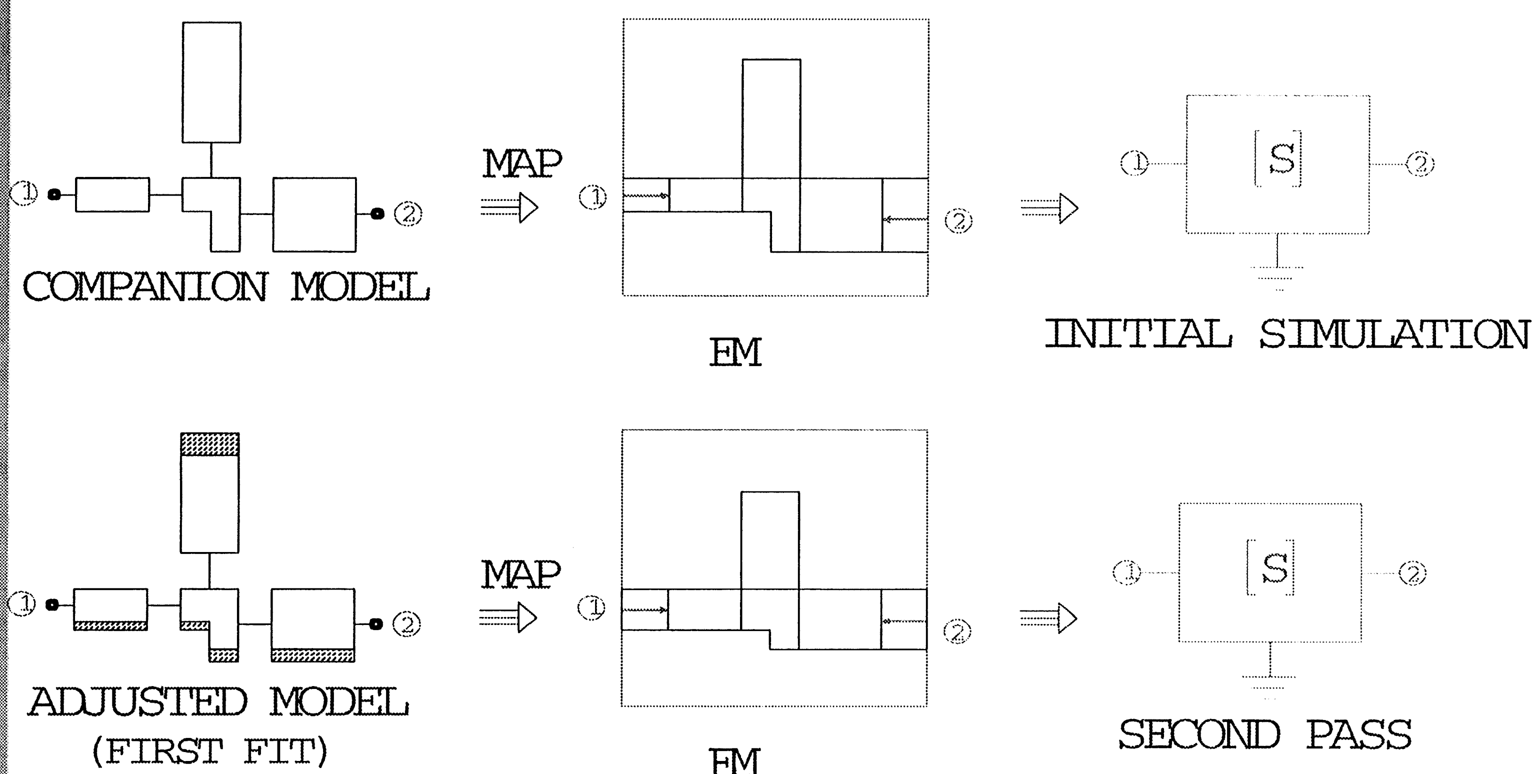

COMPANION CIRCUIT MODEL

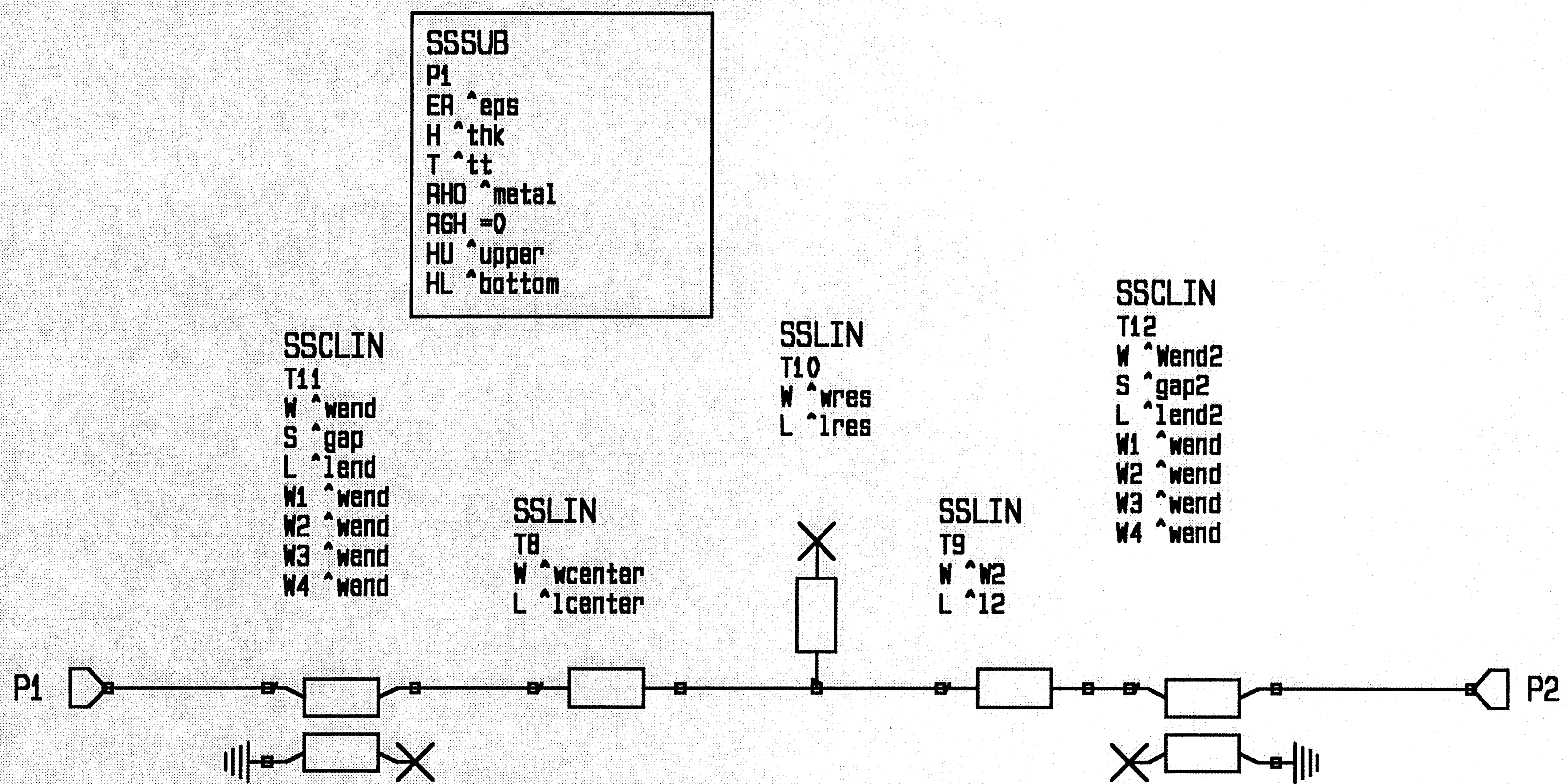

SUSPENDED SUBSTRATE NOTCH FILTER

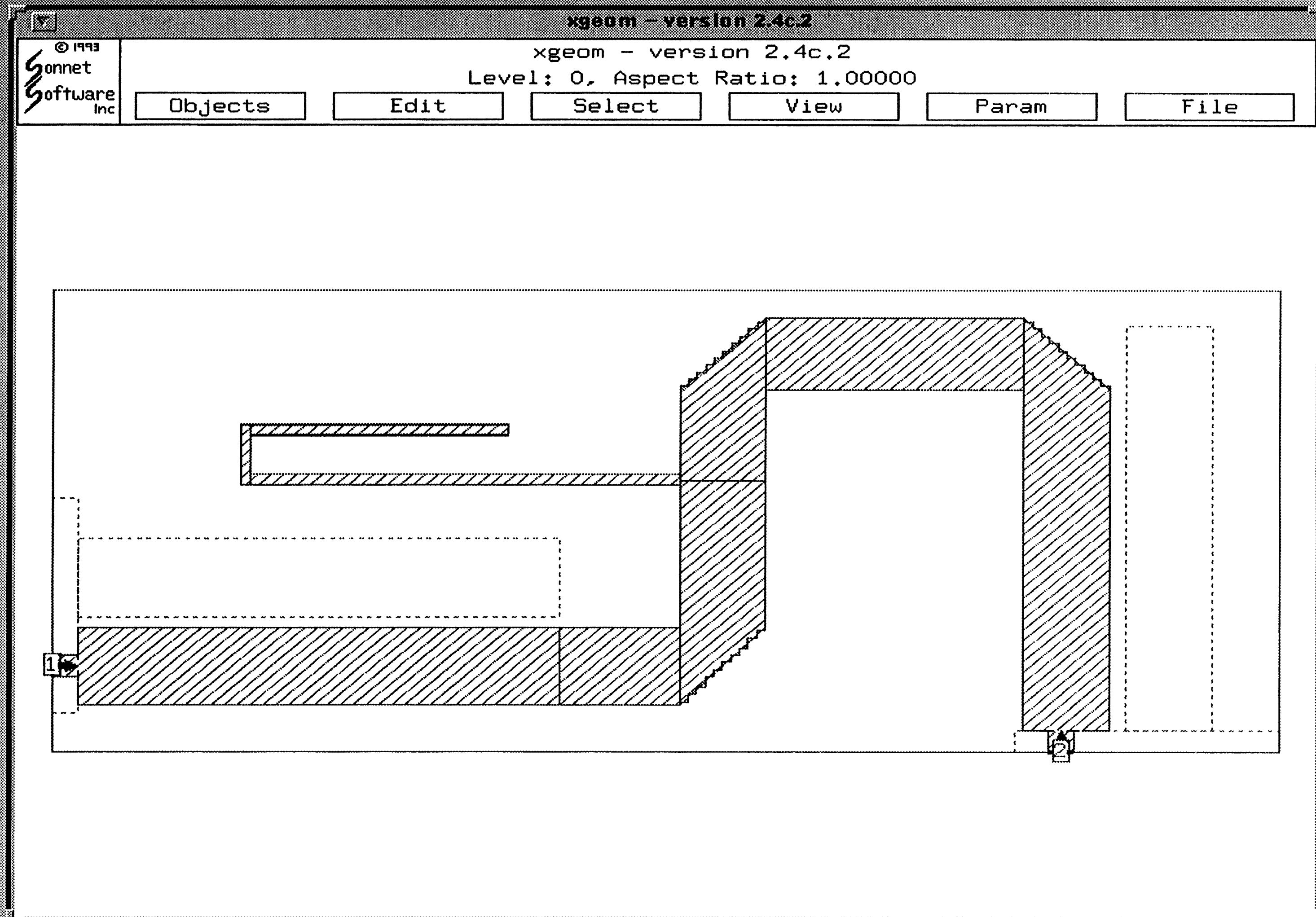

MODEL VERSUS EM SIMULATION FOR NOTCH FILTER

ANALYSIS # 1

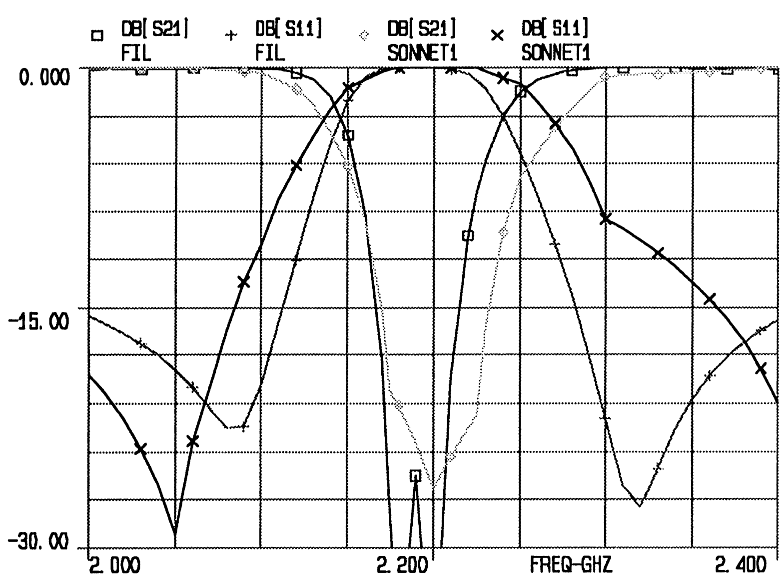

ANALYSIS # 2

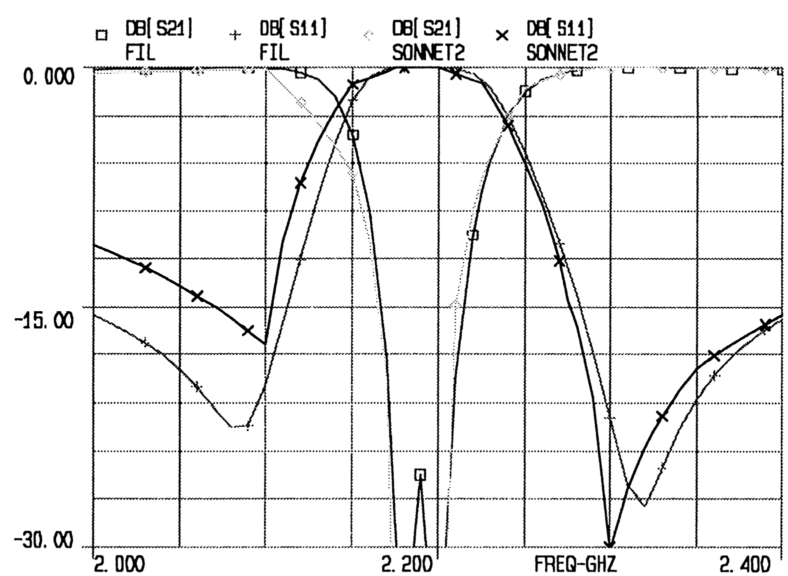

ITERATION MATRIX

	MODEL	FIT # 1	DELTA1	FIT # 2	DELTA2
WEND	220	220	0	220	0
LEND	1185	1160	25	1187	-2
GAP	29	23	6	29	0
WEND2	200	200	0	200	0
LEND2	1200	1192	8	1201	-1
GAP2	38	28	10	38	0
LCENTER	975	1008	-33	979	-4
LRES	1770	1754	16	1770	0
L2	960	957	13	958	2

DELAY LINE - COMPANION MODEL

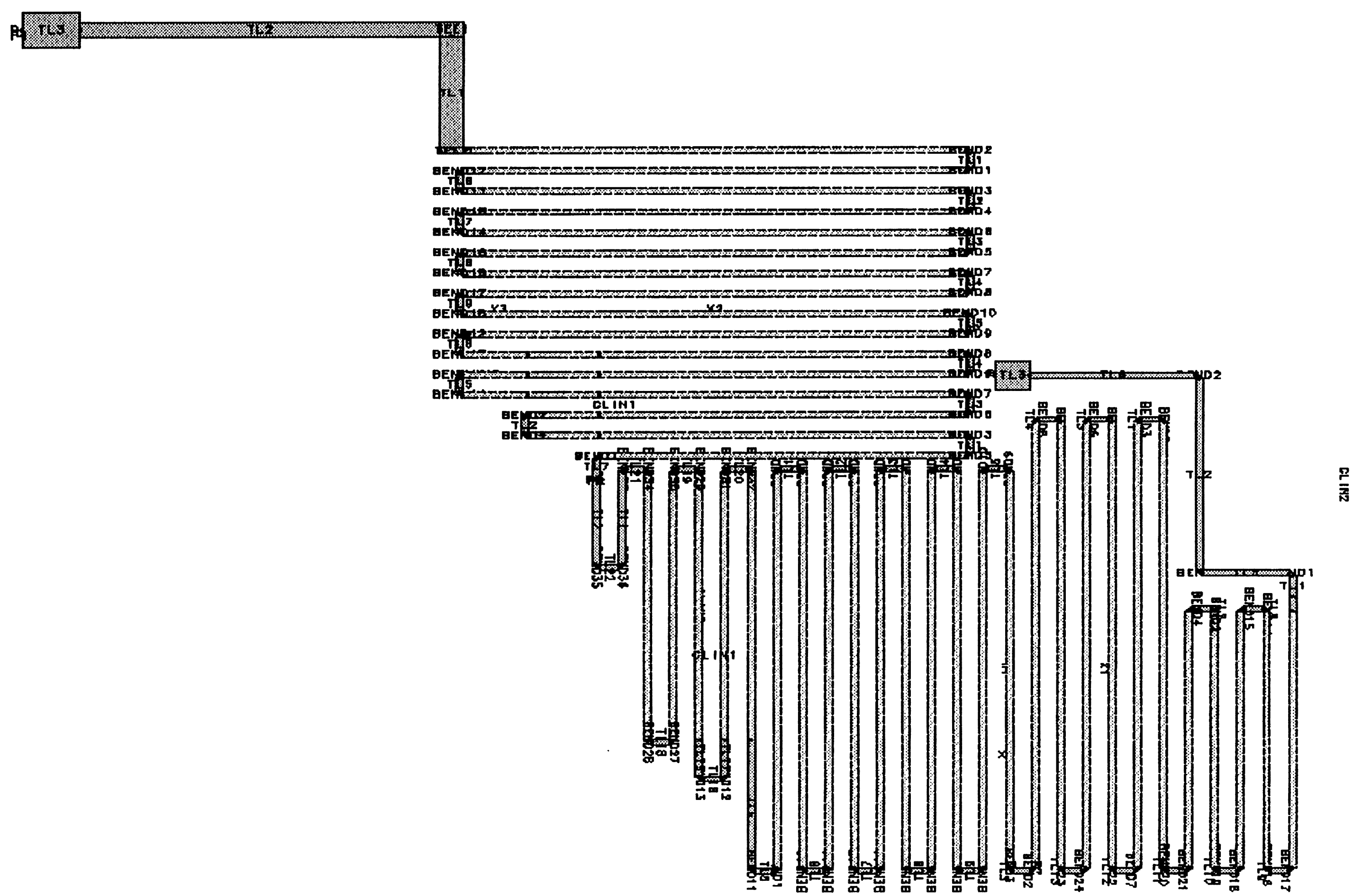

MOTOROLA
Communications, Power & Signal Technologies Group

Communications Semiconductor Products Division

9

STRUCTURES FOR EM ANALYSIS

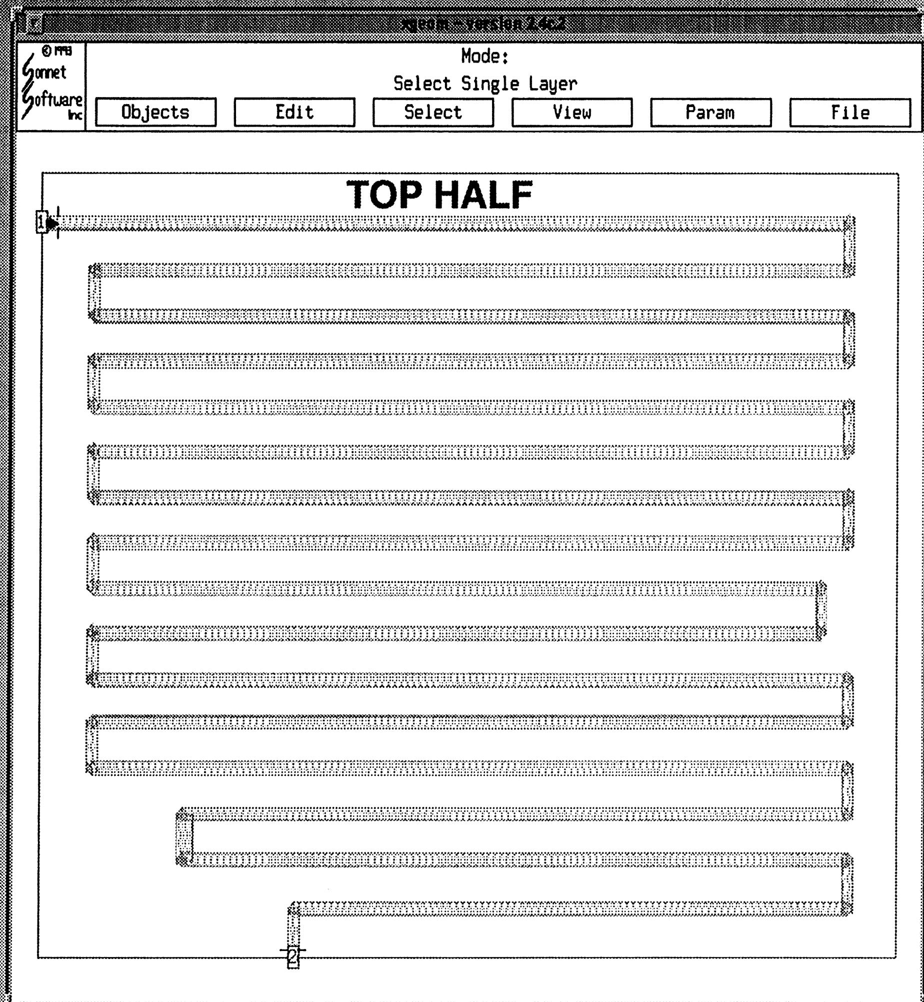

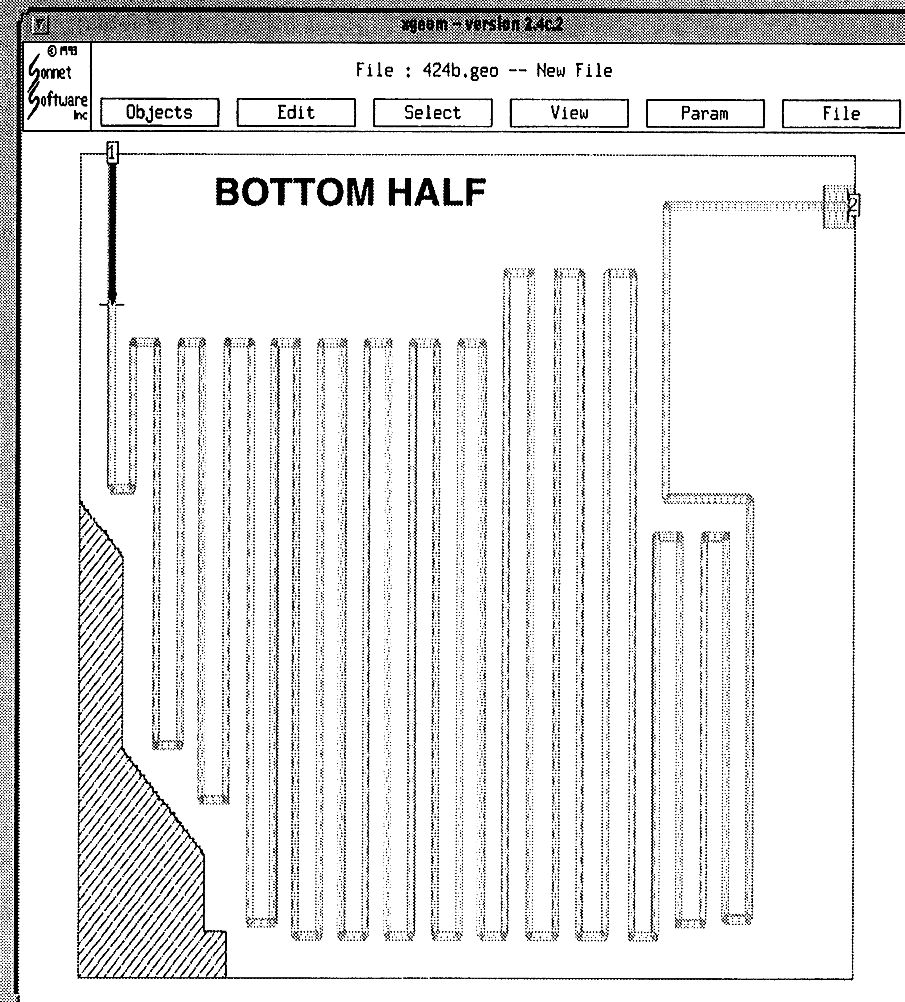

DELAY-LINE PHASE RESPONSE

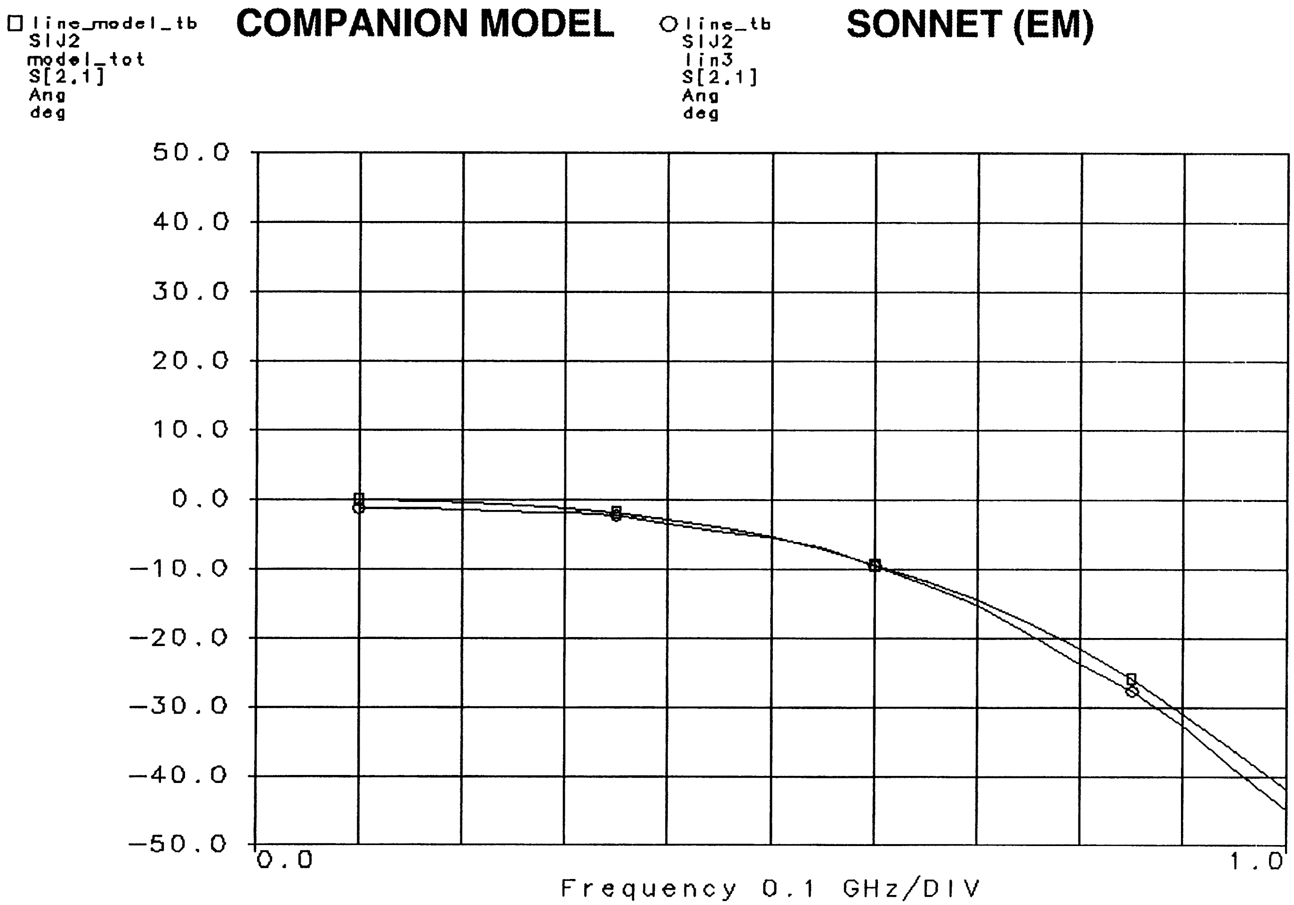

MITER OPTIMIZATION

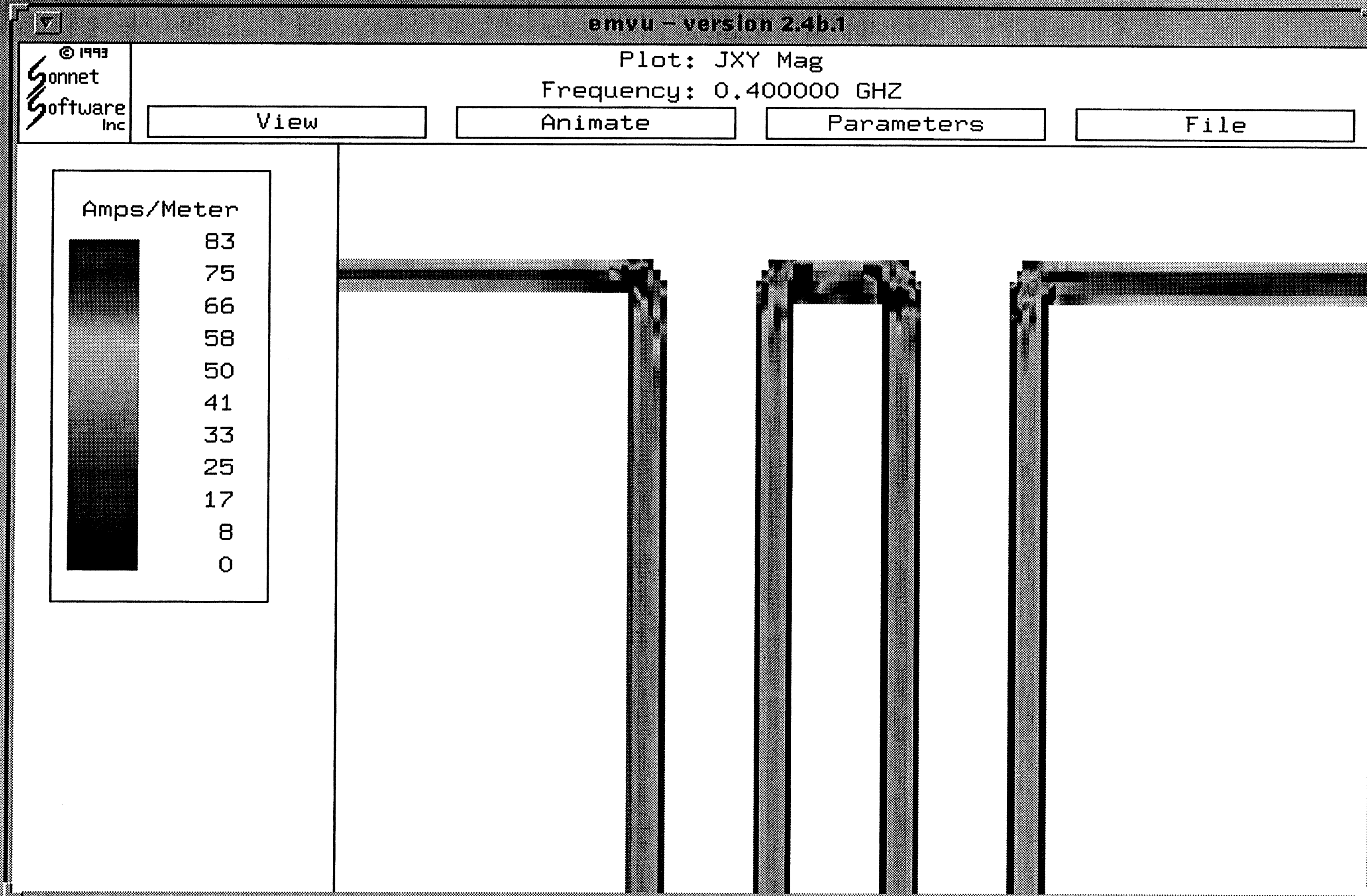

12

CLASSICAL INTERDIGITAL FILTER ANALYSIS

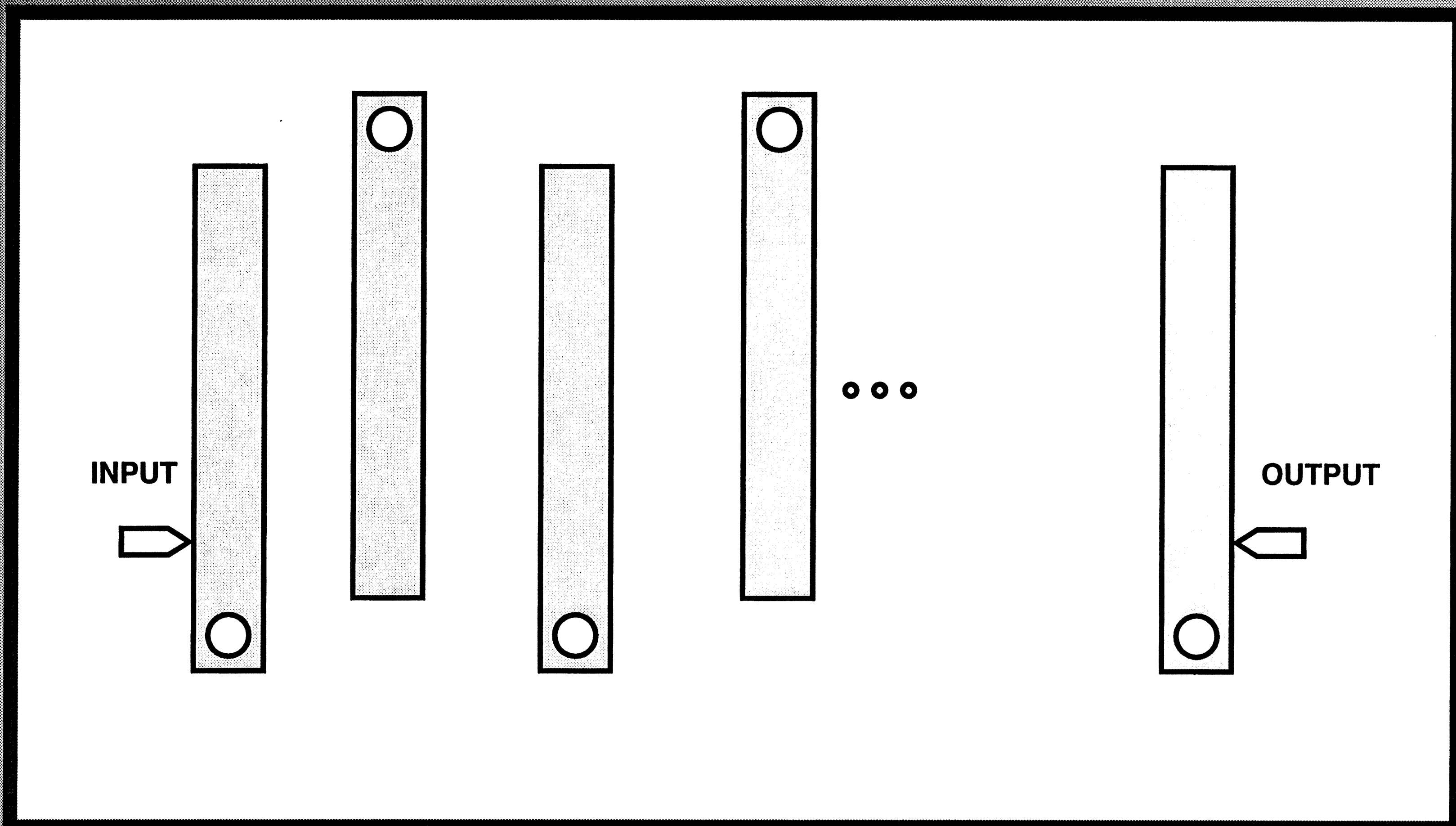

ALTERNATE FILTER ANALYSIS

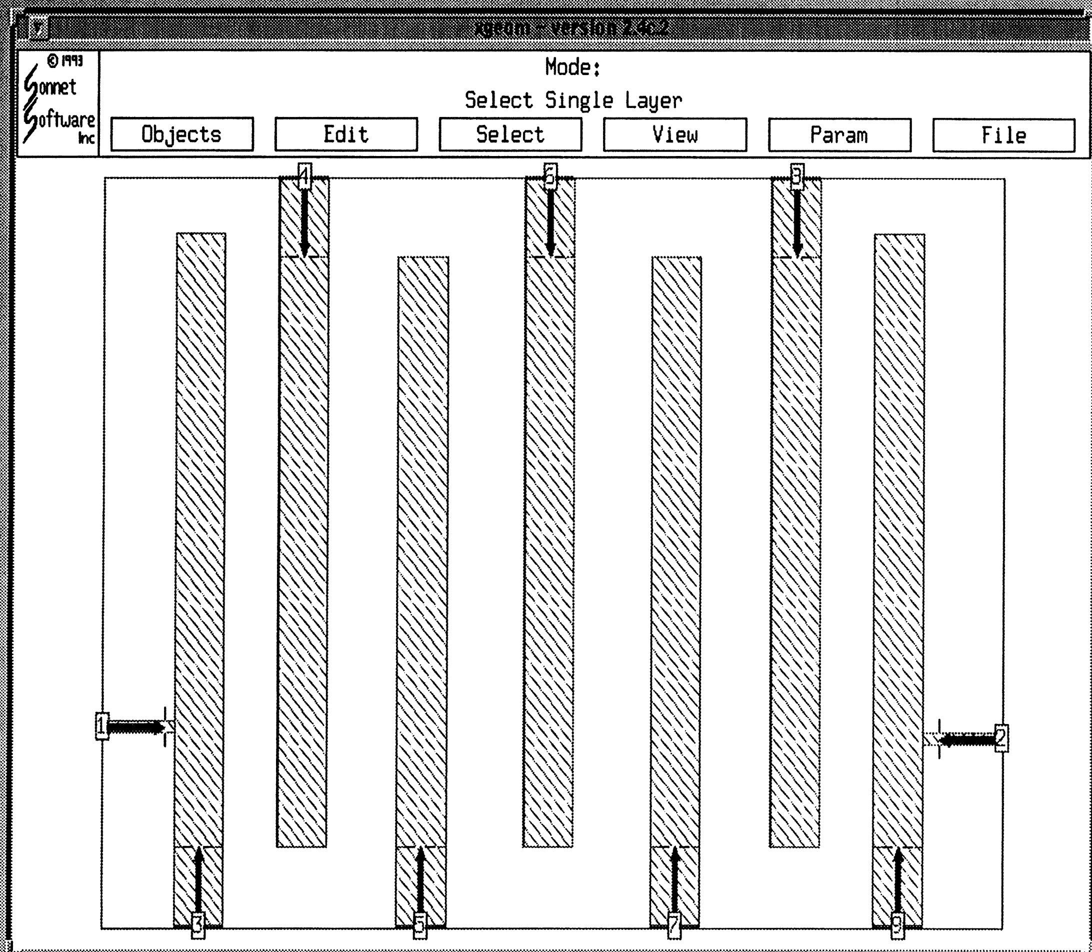

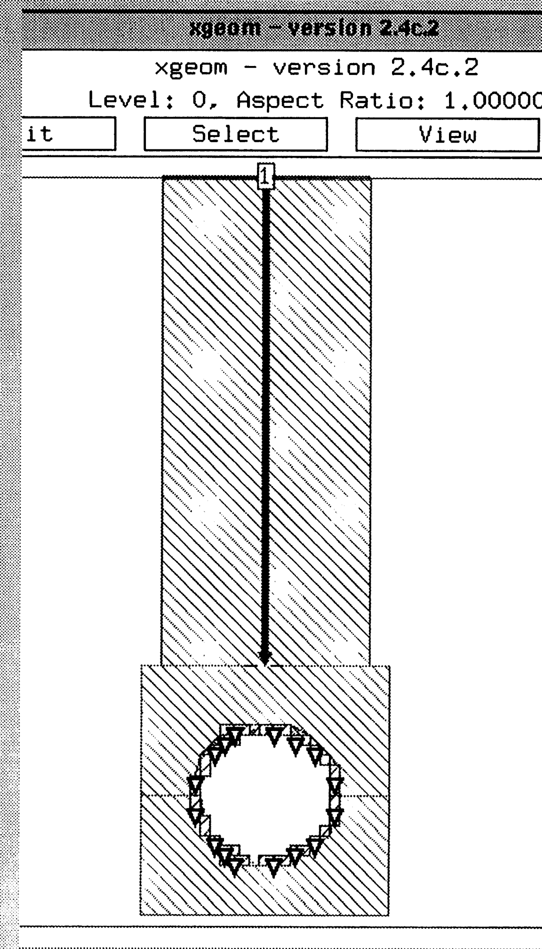

INTERDIGITAL 5 POLE FILTER COMPANION MODEL

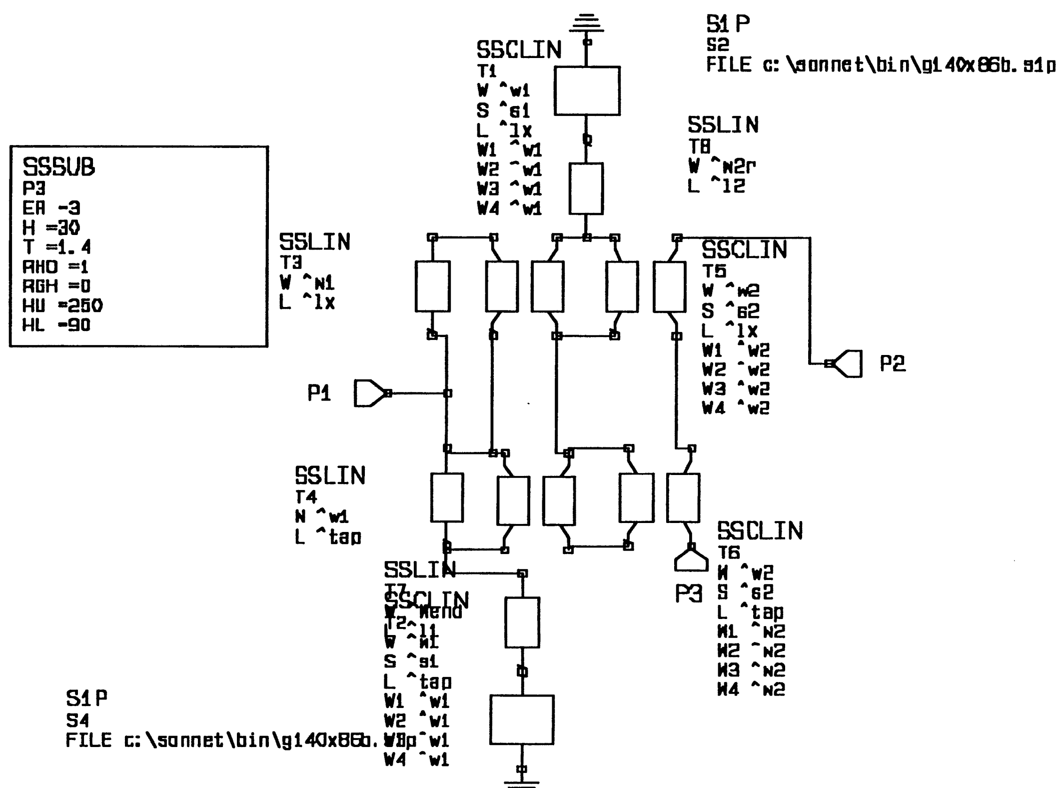

MODEL & EM ANALYSIS of 5 POLE INTERDIGITAL FILTER

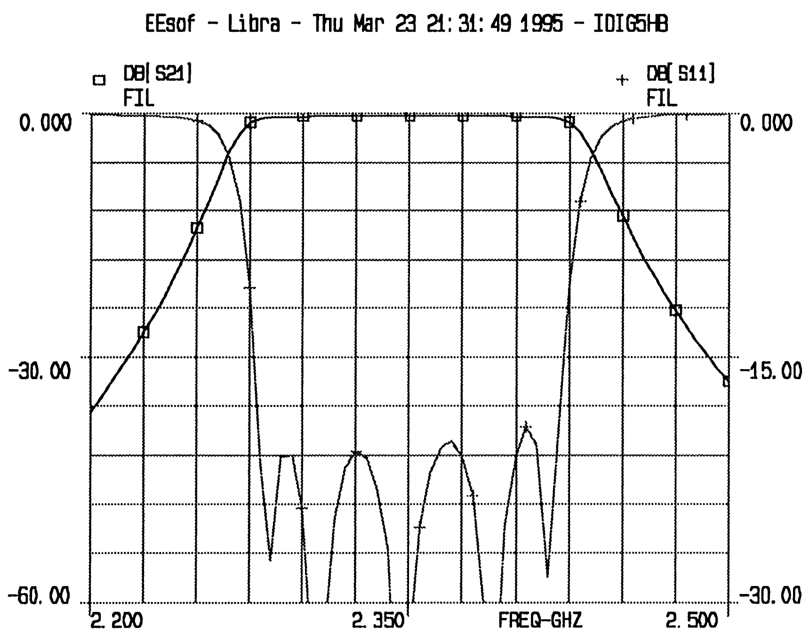

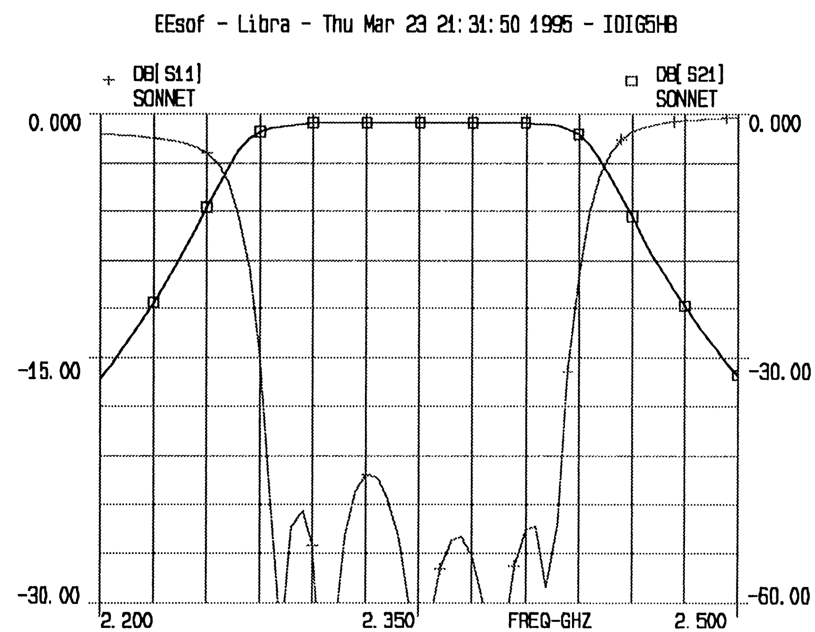

SUMMARY

- METHOD IS EASY TO APPLY USING MANUAL TECHNIQUES.
- SPECIAL STRUCTURES SUCH AS HIGH "Q" FILTERS AND DELAY LINES CAN BE RAPIDLY OPTIMIZED.
- ACTIVE DEVICES CAN BE ADDED TO SIMULATION.
- METHOD CAN BE EASILY AUTOMATED AND EXTENDED FOR ARBITRARY STRUCTURES.
- LARGE CIRCUITS SHOULD BE SEGMENTED AND SOLVED USING MULTIPLE PROCESSORS.

Automated Circuit Design Using Commercial EM Simulators

Corporate Research & Development

Presented by

Nitin Jain

Acknowledgment
Peter Onno, Eric Soshea, Peter Staecker and Gerry DiPiazza

Design Methods Utilizing EM Simulators

Corporate Research & Development

EM Simulators: HP's HFSS and Sonnet's Em

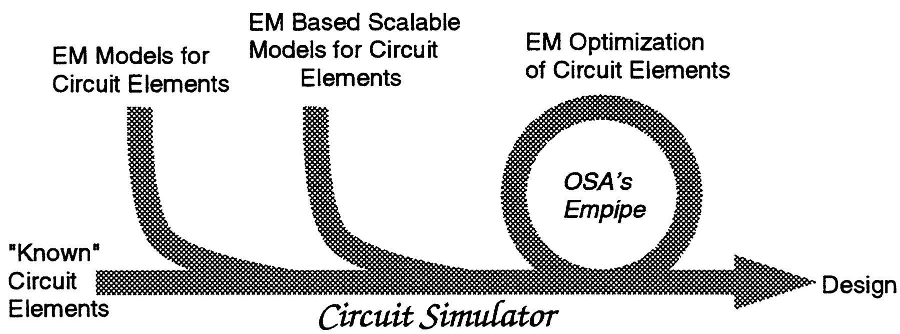

HP's MDS, EEsof libra, OSA's hope

Characteristics of the Design Methods

M/A-COM
Corporate Research & Development

- EM models of circuit elements
  - Quick and easy
  - Any EM simulator applicable
  - Portable and usable in different software and circuit files.
  - Allows no optimization of the EM simulated circuit element
- EM based scalable models of circuit elements
  - Scalable
  - Any EM simulator applicable
  - Portable between different simulation packages and circuits
  - Not all circuit elements have simple scalable equivalent circuits
- Automated EM optimization of circuit elements
  - Any-arbitrary structure can be optimized
  - Requires powerful optimizers
  - Prior knowledge of the existence of a solution
  - Computer intensive

Increasing Degree of Automation

Coax Surge Protector

M/A-COM
Corporate Research & Development

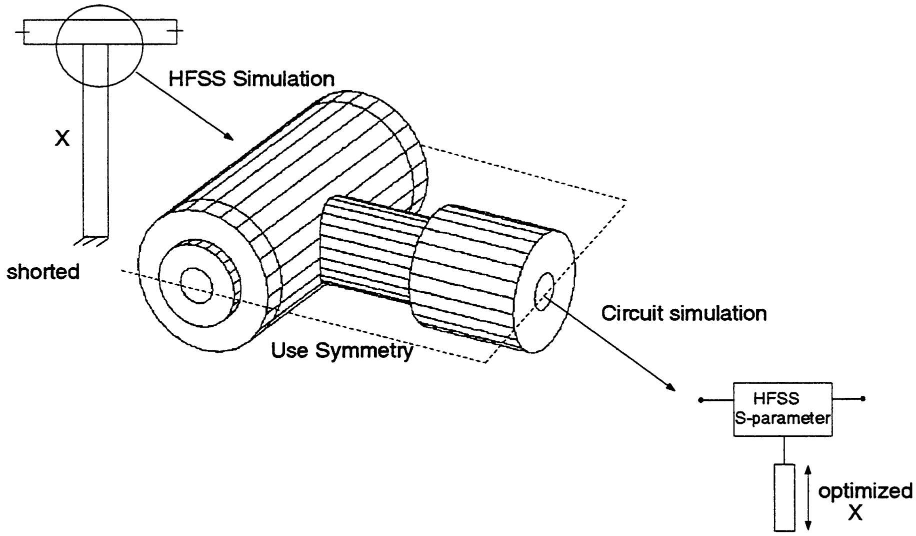

Design For a Surge Protector

Corporate Research & Development

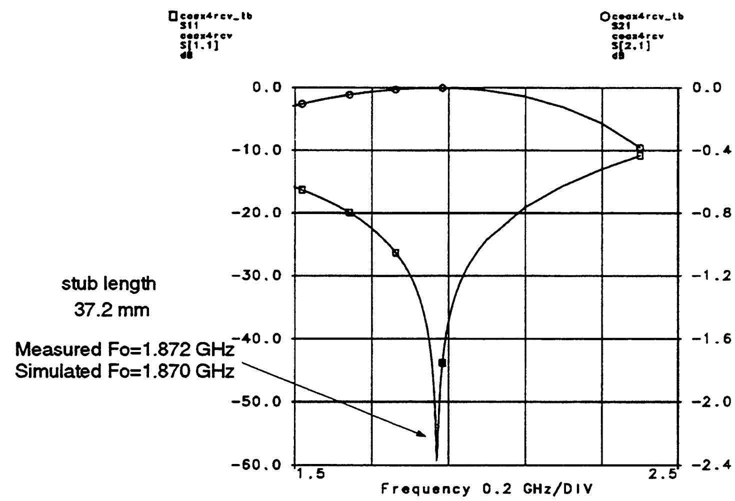

Fused Glass On Silicon

Corporate Research & Development

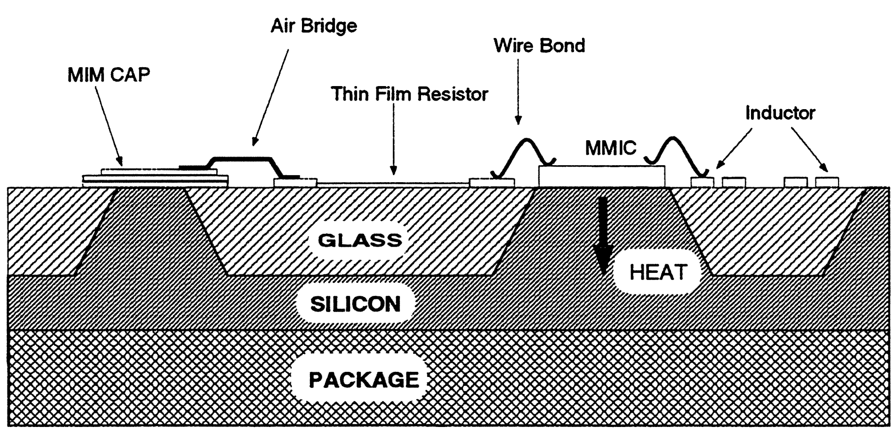

HMIC or GMIC Cross-Sectional View

Tapinductor's Xgeom Layout

Corporate Research & Development

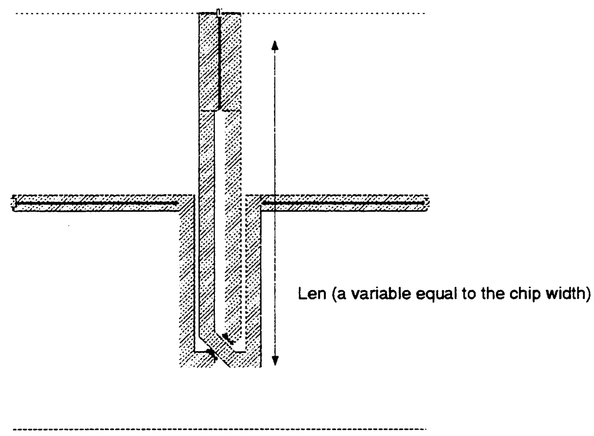

Tapinductor Equivalent Circuit

Corporate Research & Development

Equivalent Circuit Derivation

- SONNET's Em S-parameter imported to circuit simulator
- Even and odd mode analysis
- Equivalent circuit element extracted using YZ transformations
- Equivalent circuit element for three discrete "len" are interpolated.

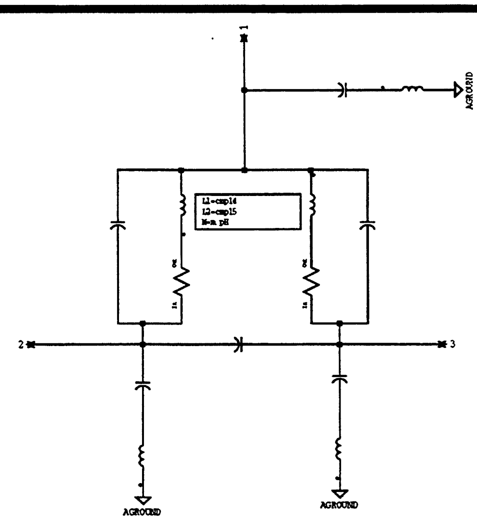

Tapinductor Test Reticle Layout

Corporate Research & Development

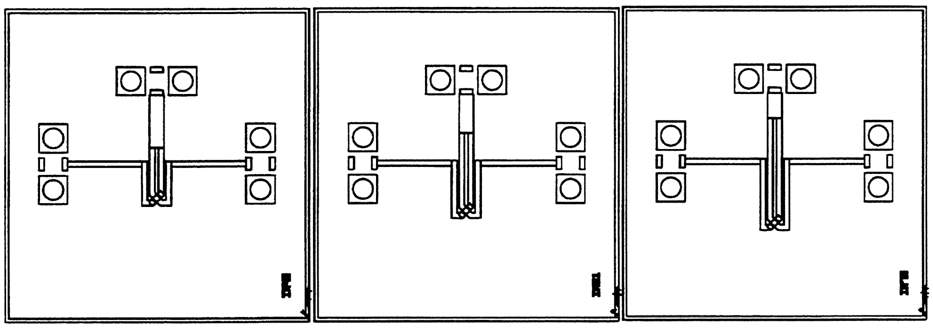

Tapinductor Measured Versus Simulated (1)

Corporate Research & Development

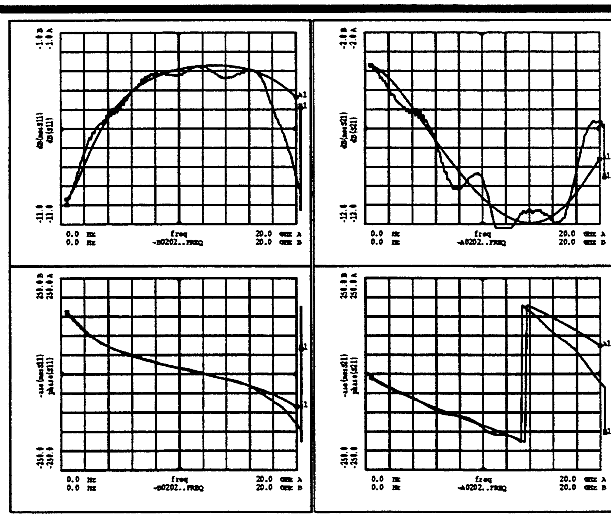

Tapinductor Len=67 mil

Other port parameters showed similar measured versus simulation match

Tapinductor Measured Versus Simulated (2)

M/A-COM Corporate Research & Development

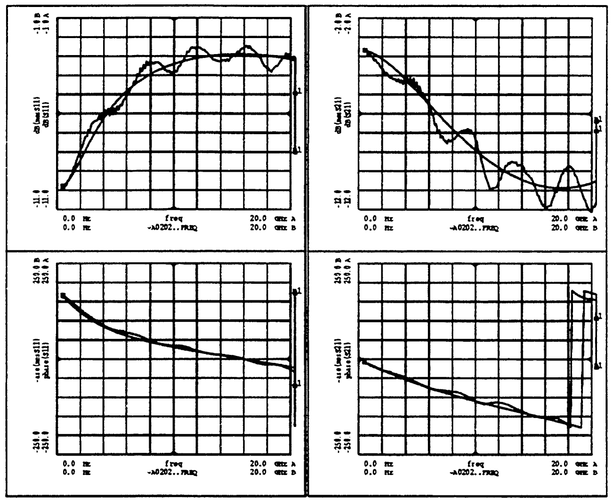

Tapinductor Len=46

11

Matched High Power SPDT Switch

M/A-COM Corporate Research & Development

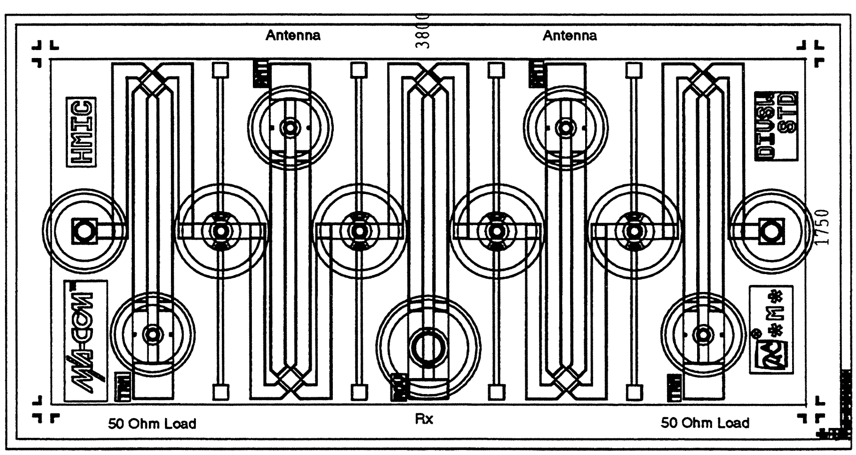

12

Measured And Simulated Performance Of the Switch

M/A-COM
Corporate Research & Development

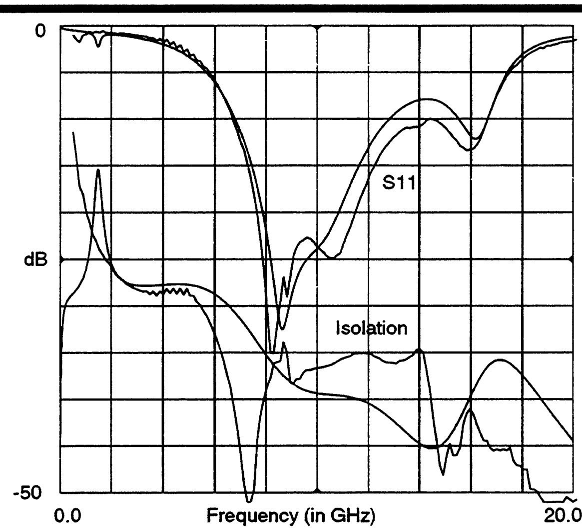

Ground Equalization Straps in CPWG

M/A-COM
Corporate Research & Development

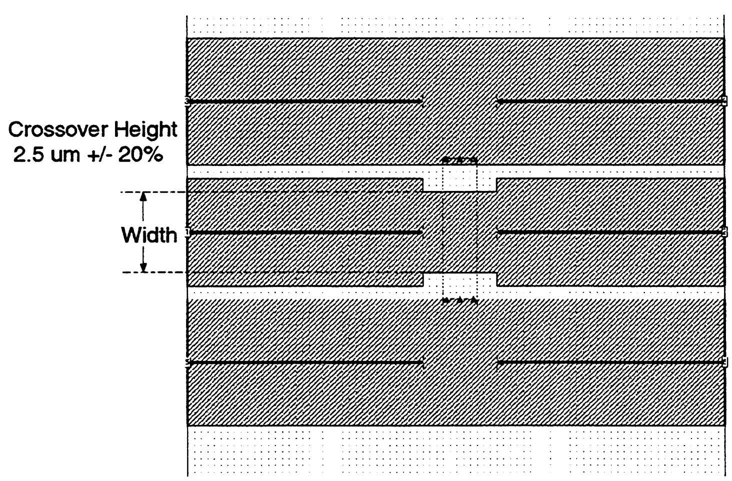

Automatic Optimization of CPWG Ground Straps

Corporate Research & Development

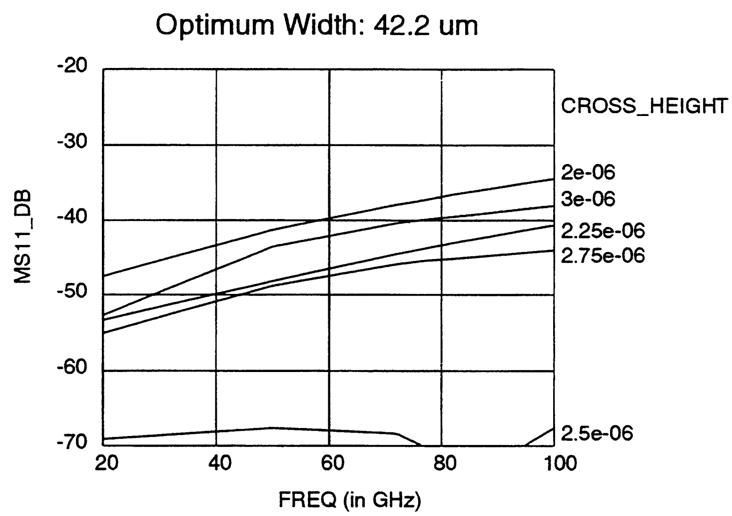

Conclusions

Corporate Research & Development

- Different degrees of automation possible
- Element models useful for circuit discontinuities
- Scalable element models useful for Hierarchical IC designs
- Automated EM optimization *useful* for multi-variant circuits
- More automation => more design freedom
  but ....
  more computer resources and lower model portability

Optimization of Microwave Structures using Time Domain TLM Electromagnetic Simulators

Wolfgang J.R. Hoefer

NSERC/MPR Teltech Research Chair in RF Engineering
Department of Electrical and Computer Engineering
POB 3055, MS 8610, University of Victoria
Victoria, British Columbia, V8W 3P6, Canada

Tel: (604) 721-6030
Fax: (604) 721-6230 or -6052
Email: WHoefer@ECE.UVic.CA

Abstract

Powerful workstations and massively parallel processors, in combination with advances in numerical field modeling and signal processing techniques, make it now feasible to design and optimize microwave structures directly with time and space discrete electromagnetic simulators. This opens the door for the automated design of structures with geometries that can only be handled with very general but numerically intensive methods, such as Transmission Line Matrix (TLM), Finite Difference - Time Domain (FD-TD) or Finite Element (FEM) methods.

This paper summarizes all the important features that must come together to form a powerful, efficient CAD system. First, the implementation of TLM algorithms on a massively parallel computer (DECmpp 12000), the technique of distributed computing in the UNIX environment, and the combination of TLM analysis with Prony's method as well as with autoregressive moving average (ARMA) digital signal processing for electromagnetic field modelling is described. By combining these advanced computation techniques, typical electromagnetic field modelling of microwave structures by TLM analysis can be accelerated by a few orders of magnitudes. Then, the combination of such a simulator with a commercial optimization program OSA90/hope™ via high speed data pipe is described. Finally, practical optimization examples are given, and the computational requirements as well as the execution speeds on various computer platforms are presented.

Since most of these details have been described in several publications, a list of references is provided below. The transparencies presented during the workshop are reproduced on the following pages.

Acknowledgement

This paper is based to a large extent on work performed by my research associates P. P.M. So and C. Eswarappa, as well as by numerous graduate students. Financial support by the Natural Sciences and Engineering Research Council of Canada, MPR Teltech Inc., The Science Council of British Columbia, and the University of Victoria is gratefully acknowledged.

Introduction

At present, field theory based microwave circuit CAD/CAM is performed in the frequency domain. This is more a matter of traditional practice and available computer power than a theoretical constraint. This paper reports the first successful combination of a frequency domain CAD program, OSA90/hope, with a massively parallel version of the time domain 3D-TLM electromagnetic field simulator in [1]. This technique increases the speed for the optimization of microwave structures.

The theory of the symmetrical condensed node 3D-TLM[i] method is well described in [2]. A 3D-TLM mesh is built by cascading a network of these nodes in the three dimensional space. To simulate electromagnetic wave propagation in the mesh, scattering and transfer of voltage impulses must be performed. A massively parallel implementation of this procedure is given in [3]. The parallel 3D-TLM module developed in this paper is divided into 3 programs — two serial and a parallel one; they are *3dtlm-pipe*, *3dtlm-server* and *mpl-server*, respectively. *3dtlm-pipe* is executed locally together with OSA90/hope on a HP 9000 series 700 workstation; *3dtlm-server* is executed remotely on a DEC5000/200 workstation, which is the front-end machine for the DECmpp 12000 massively parallel computer. *mpl-server* is executed on a DECmpp 12000 parallel computer. The serial and parallel programs communicate with each other via a few UNIX pipes, [4] and [5]. The serial programs are implemented in C++ to perform serial numerical operations such as discretization of geometrical parameters and computation of discrete Fourier transforms. The parallel program is implemented in MPL, a C like parallel programming language for DECmpp 12000, to perform computer time intensive 3D-TLM simulation.

Datapipe Feature of OSA90/hope

The Datapipe feature of OSA90/hope utilizes UNIX's interprocess communication facility, pipe, to establish high speed data connection between OSA90/hope and one or more external programs. Because UNIX's pipe is used, OSA90/hope can run on its host machine and control external programs running on the same or other machines. This allows CPU time intensive field simulation programs to run on a more powerful computer, such as the DECmpp 12000, [6].

OSA90/hope's Datapipe feature is built on top of the UNIX's pipe and a proprietary communication protocol, [7]. External programs must strictly comply with this protocol in order to work properly with OSA90/hope. Datapipe starts the external program as a child process and sets up a pipe connection between them. Once such a connection is properly established, OSA90/hope and its child process can begin to exchange data. OSA90/hope computes the inputs required by its child process according to their definitions and writes the data to the pipe. The child process reads the inputs from the pipe, carries out the requested calculations, and sends the output back to OSA90/hope. This interaction is illustrated in Figure 2.

The Datapipe feature of OSA90/hope is very good but not yet perfect for our application. One of the problems is that it has to send n requests to its child process if it needs n frequency responses. This is not a problem at all if both OSA90/hope and its child process are executed on the same computer. In our case, OSA90/hope and the parallel 3D-TLM program have to be executed on two different computers which are situated a few kilometers apart. In this case, network delay and overhead cannot be ignored. We have developed *3dtlm-pipe* to circumvent this problem.

i. From now on 3D-TLM means symmetrical condensed node 3D-TLM.

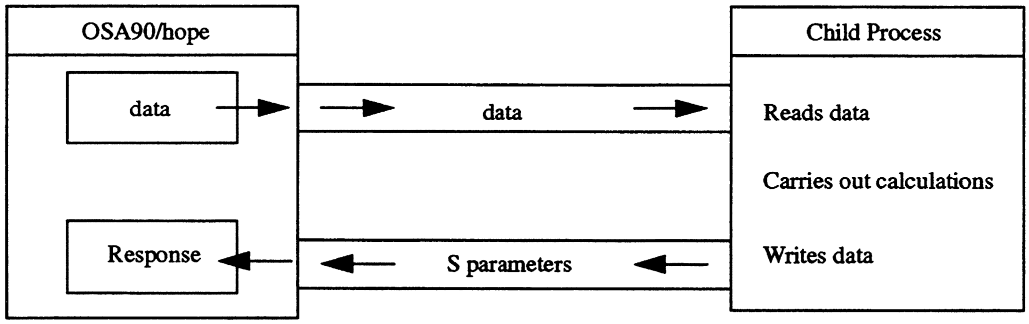

Figure 1 OSA90/hope computes the inputs required by the child process according to their definitions and writes the data to the pipe. The child process reads the inputs from the pipe, carries out the calculations, and sends the output back to OSA90/hope.

The Massively Parallel 3D-TLM Module

The massively parallel 3D-TLM module is divided into 3 programs — two serial and a parallel one; they are *3dtlm-pipe*, *3dtlm-server* and *mpl-server*, respectively. The serial and parallel programs communicate with each other via a few UNIX pipes. The serial programs are implemented in C++ to perform serial numerical operations such as discretization of geometrical parameters and computation of discrete Fourier transforms. The parallel program is implemented in MPL to perform parallel 3D-TLM simulation.

3dtlm-server is based on some source code extracted from the 3D-TLM Simulator in [1]. The graphical user interface module of that program is eliminated. Replacing it is a new module that reads geometrical and control data from the standard input stream; upon completion of the requested number of simulations, this module writes time and frequency domain result to the standard output stream if they are requested. The serial 3D-TLM number crunching part of this module is also replaced by a massively parallel program, *mpl-server*; which is based on some source code extracted from [3]. These two programs communicate with each other via UNIX pipes.

3dtlm-pipe is the program that make OSA90/hope and *3dtlm-server*, hence *mpl-server*, work together seamlessly. It provides a fully parameterized 3D-TLM component library for use in microwave circuit analysis and optimization with OSA90/hope. The user of OSA90/hope does not have to interact with *3dtlm-server* at all. He or she only has to work with the Datapipe syntax of OSA90/hope. Currently, the component library of *3dtlm-pipe* includes only three components for the rectangular waveguide environment. They are:

- resonant cavity,
- inductive iris bandpass filter, and
- inductive iris bandpass filter with two tuning screws.

Expanding this library to include more components is an easy task; the prerequisite is a basic knowledge of the 3D-TLM method and the C++ programming language. The interaction of OSA90/hope, *3dtlm-pipe*, *3dtlm-server* and *mpl-server* is depicted in Figure 2.

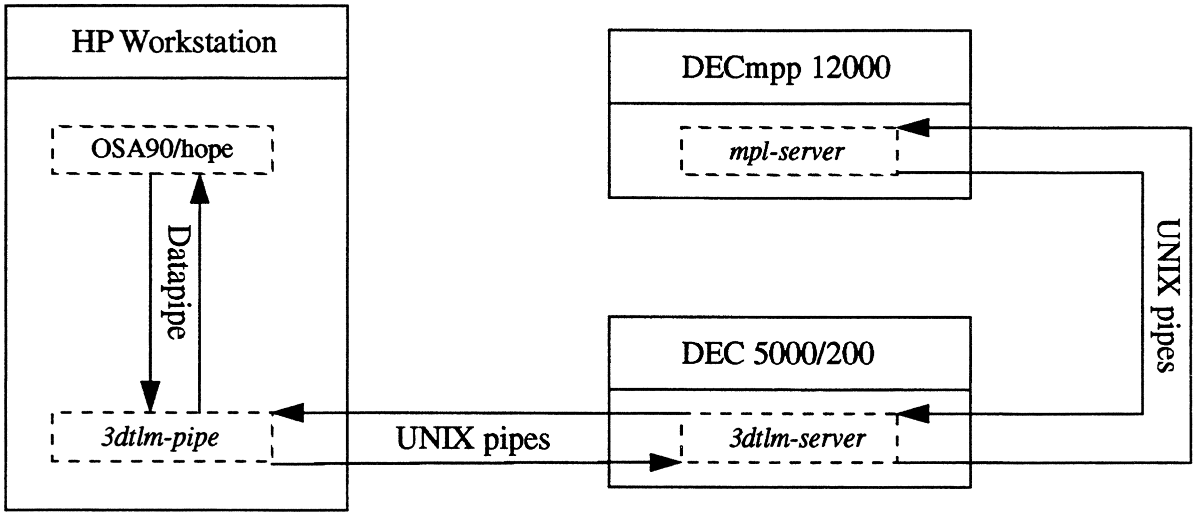

Figure 2 The interaction of OSA90/hope, *3dtlm-pipe*, *3dtlm-server* and *mpl-server.*

Comparison of Execution Speed of the Serial and Parallel 3D-TLM Simulation Modules

The performance of the parallel 3D-TLM simulation is quite impressive if the mesh dimensions of the problem to be solved are conformed to the processor dimensions of the parallel computer. The processor dimensions of the DECmpp 12000 available to us is 128×64, which gives a total of 8192 processors. Table 1 gives a quantitative comparison of the execution time of the serial and parallel 3D-TLM simulation modules on three workstations and a DECmpp 12000 parallel computer. In the serial cases, there is no *mpl-server* program; the 3D-TLM number crunching operation is done within the *3dtlm-server* program.

Computers	Execution time in seconds
DEC 5000/200 (DECmpp Front-end)	2580
IBM RS6000, Model 350 (42 MHz)	490
HP 9000, Series 7000, Model 755 (99 MHz)	368
DECmpp 12000	75

Table 1 Execution time of the serial and parallel 3D-TLM field simulation modules on three workstations and a parallel computer. The mesh size is 128×64×10; a mesh size of 128×64 in the *xy*-plane represents a full use of a DECmpp 12000 with 8192 processors. The number of time steps and frequency points are both 1000. The execution time shown above include all the network delay due to the piping operations depicted in Figure 2. This provides a clear picture of the required execution time for performing 3D-TLM field simulations on various hardware platforms.

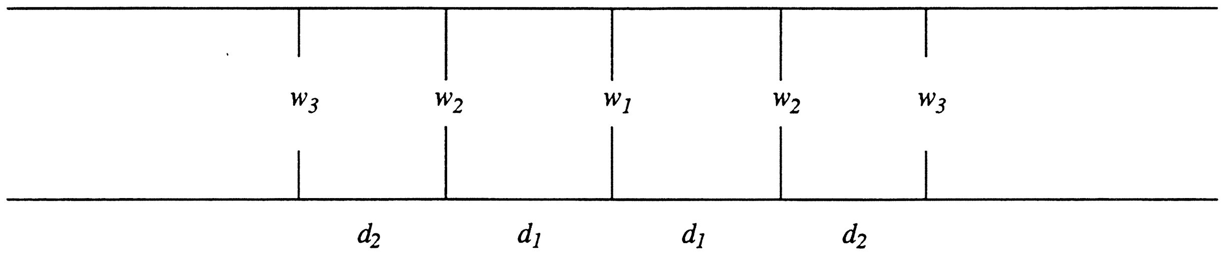

	Initial	30 Random	60 Random	90 Random
w_1 in Δl	2	4	4	4
w_2 in Δl	2	4	6	6
w_3 in Δl	2	10	10	10
d_1 in Δl	23	21	21	21
d_2 in Δl	23	23	22	23

Figure 3 The top view of an inductive iris bandpass filter. The initial and successive optimized values of the parameters are show in the above table, Δl=0.508mm. The desired center frequency is 33 GHz; the passband is from 32.5 GHz to 33.5 GHz. The optimization goal is to have minimum $|S_{11}|$ and maximum $|S_{21}|$ in the passband and vice

Simulation Examples

As a first example, the dimensions of an inductive iris bandpass filter is optimized with the random optimizer of OSA90/hope. The geometry and dimensional parameters of the filter are shown in Figure 5. The design specifications are:

- Center frequency — 33 GHz.
- Pass band — 32.5 to 33.5 GHz.
- Minimize $|S_{11}|$ and maximize $|S_{21}|$ in the passband and vice versa in the stopband

The initial length of the cavities is set to λ_g=11.81mm (rounded off to the nearest Δl). The initial width of the irises is chosen to be small so that the opening will not affect the characteristic of the resonators. The initial response of the filter is shown in Figure 2(a). The random optimizer of OSA90/hope is used to optimize the values of the parameters. The values of the parameters after 30, 60 and 90 simulations are shown in the table in Figure 5; their corresponding responses are shown in Figure 2(b), (c) and (d), respectively. The circuit file used for this optimization process is given in Figure 2.

The second example demonstrates the effect of inserting two tuning screws into the two center cavities of the filter in the above example. The location and depth of insertion are shown in Figure 3 together with the corresponding filter responses.

Circuit Files

The OSA90/hope circuit files for the examples are given in Figure 2.

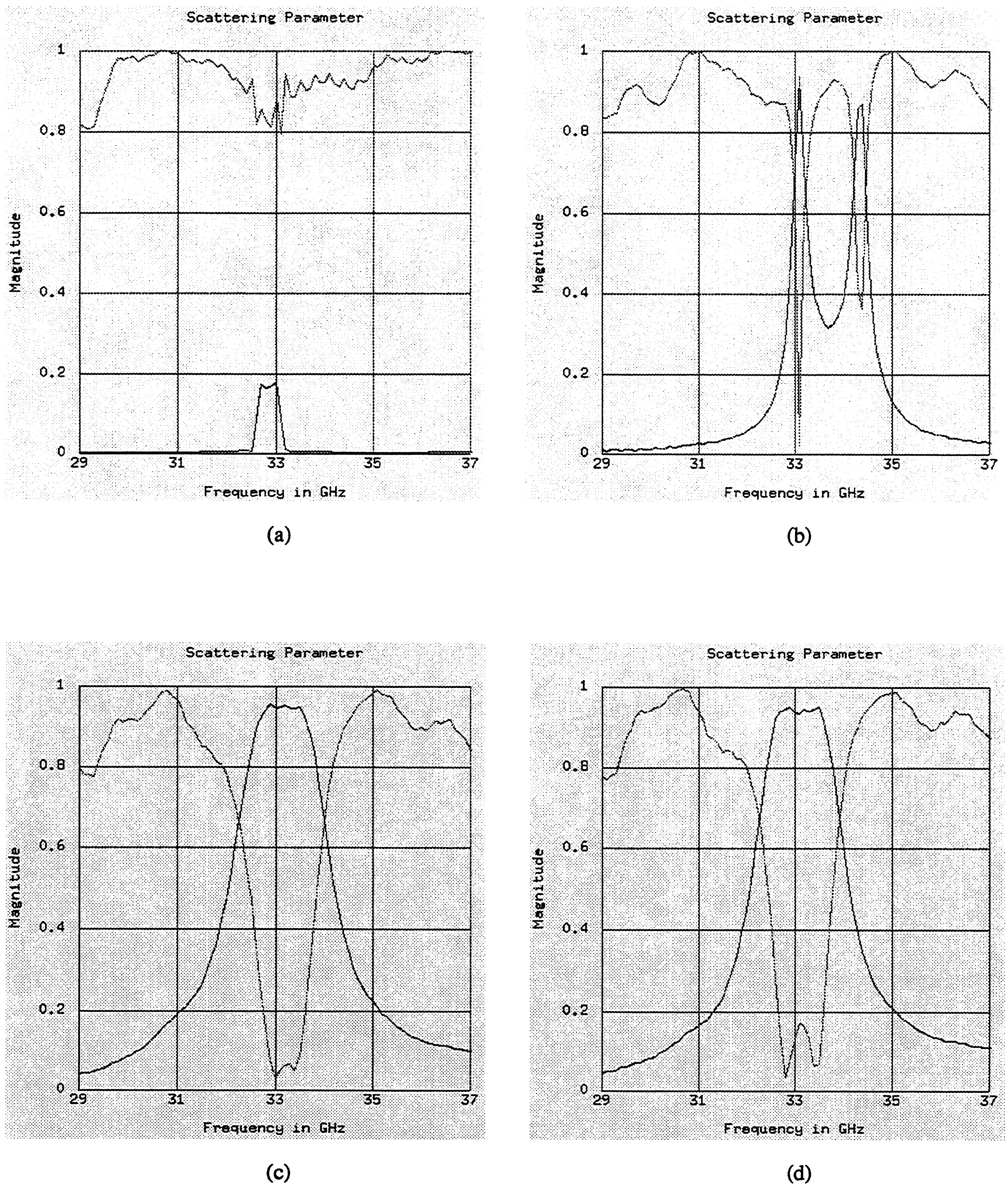

Figure 1 The responses of the inductive iris filter shown in Figure 5. (a) is the initial response; (b), (c) and (d) are the best responses after the 30th, 60th and 90th simulations with parameter values randomly chosen by the random optimizer of OSA90/hope.

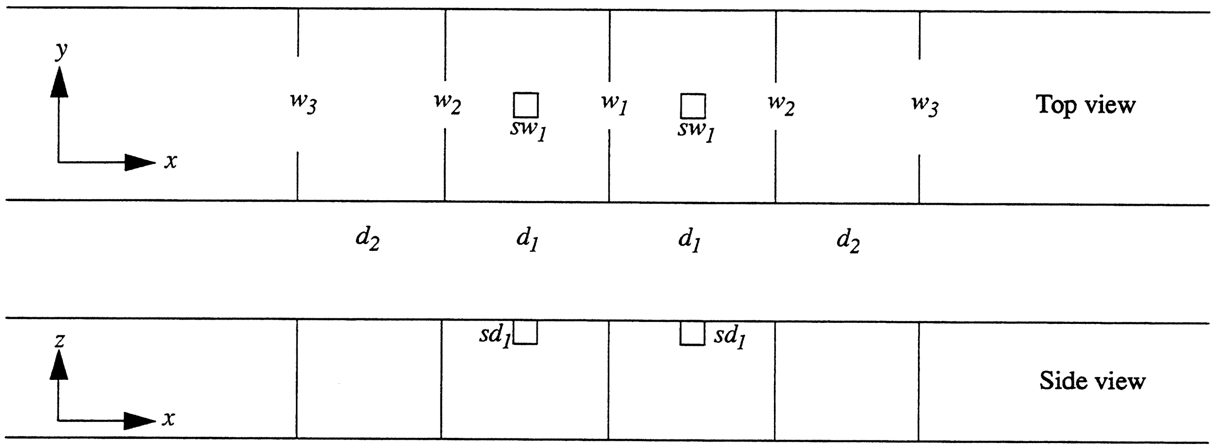

(a)

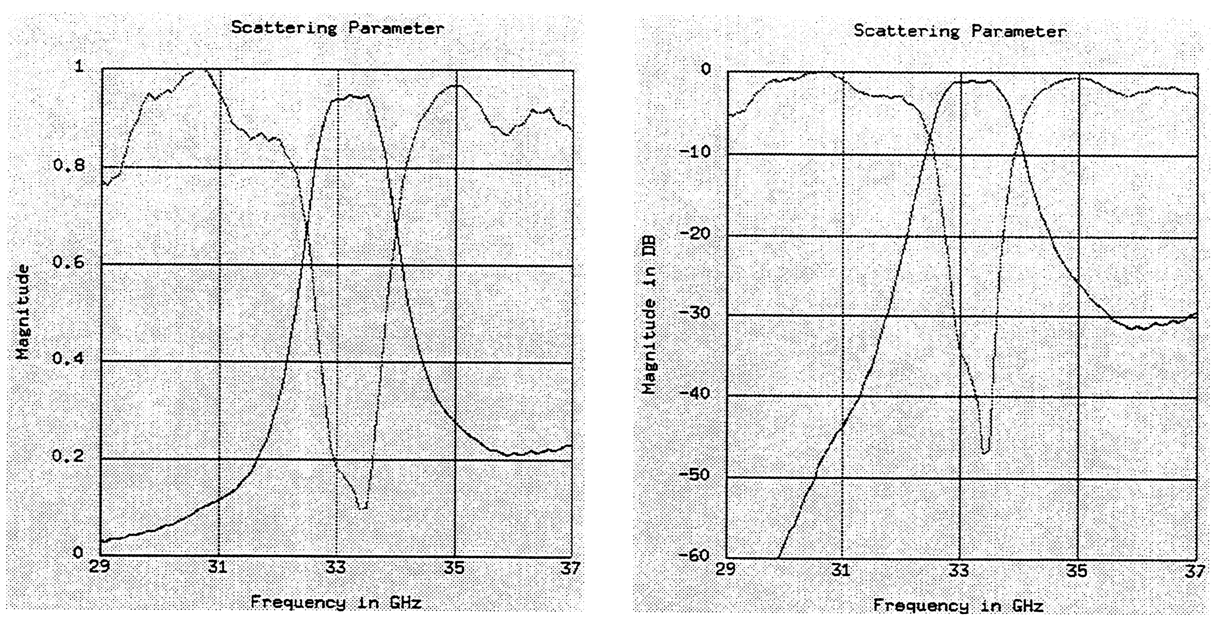

(b)

Figure 2 (a) Top and side views of a rectangular waveguide iris coupled bandpass filter. The values of w_1, w_2, w_3, d_1 and d_2 are given in the last column of the table in Figure 5. sw_1 and sw_1 are both 2 Δl.
(b) The response of the filter in (a) after 8000 time steps.

```
! File: Ind-Iris-Bandpass-Filter-1.ckt
!
Expression
 MF = 9;
 NY = 14;           NX = NY*MF;          NZ = 1;
 Y_DIM = 7.112e-3;
 X_DIM = Y_DIM*MF;
 Z_DIM = NZ*Y_DIM/NY;
 ER = 1.0;          UR = 1.0;            FC = 3;
 N_SIM = 8000;      N_F = 141;
 F_MIN = 26;        F_MAX = 40; ! GHz
 ELEM = 1; ! Inductive iris bandpass filter
 F0 = 33;           S11 = 1;             S21 = 2;
 v1 = ? 1  2  6?;
 v2 = ? 1  3  6?;
 v3 = ? 1  5  6?;
 u1 = ?18 21 24?;
 u2 = ?18 23 24?;
 W1 = Y_DIM*floor(v1)*2/NY;
 W2 = Y_DIM*floor(v2)*2/NY;
 W3 = Y_DIM*floor(v3)*2/NY;
 D1 = X_DIM*floor(u1)/NX;
 D2 = X_DIM*floor(u2)/NX;

 Datapipe: SIM FILE="3dtlm-pipe"
     N_INPUT =22 INPUT=(NX,NY,NZ,X_DIM,Y_DIM,Z_DIM,
                        ER,UR,FC,N_SIM,N_F,F_MIN,
                          F_MAX,FREQ,ELEM,F0,S11,W1,
                        W2,W3,D1,D2)
     N_OUTPUT=1 OUTPUT=(MAG_S11);

 Datapipe: SIM FILE=SAME
     N_INPUT =22 INPUT=(NX,NY,NZ,X_DIM,Y_DIM,Z_DIM
                        ER,UR,FC,N_SIM,N_F,F_MIN,
                          F_MAX,FREQ,ELEM,F0,S21,W1,
                        W2,W3,D1,D2)
     N_OUTPUT=1 OUTPUT=(MAG_S21);

 DB_S11 = 20*Log(MAG_S11);
 DB_S21 = 20*Log(MAG_S21);

End
```

```
! File: Ind-Iris-Bandpass-Filter-2.ckt
!
Expression
 MF = 9;
 NY = 14;           NX = NY*MF;          NZ = 7;
 Y_DIM = 7.112e-3;
 X_DIM = Y_DIM*MF;
 Z_DIM = NZ*Y_DIM/NY;
 ER = 1.0;          UR = 1.0;            FC = 3;
 N_SIM = 8000;      N_F = 141;
 F_MIN = 26;        F_MAX = 40; ! GHz
 ELEM = 2; ! Inductive iris bandpass filter with
           ! tuning two screws.
 F0 = 33;            S11= 1;             S21= 2;
 v1 = ? 1  2 6?;  v2 = ? 1  3  6?; v3 = ? 1 5 6?;
 u1 = ?18 21 24?; u2 = ?18 23 24?;
 sv1= ? 1  2 6?   sv2= ? 1  2  6?
 W1 = Y_DIM*floor(v1)*2/NY;
 W2 = Y_DIM*floor(v2)*2/NY;
 W3 = Y_DIM*floor(v3)*2/NY;
 D1 = X_DIM*floor(u1)/NX;
 D2 = X_DIM*floor(u2)/NX;
 SW1= Y_DIM*floor(sv1)*2/NY;
 SD1= Z_DIM*floor(sv2)/NZ;

 Datapipe: SIM FILE="3dtlm-pipe"
     N_INPUT =22 INPUT=(NX,NY,NZ,X_DIM,Y_DIM,Z_DIM,
                        ER,UR,FC,N_SIM,N_F,F_MIN,
                          F_MAX,FREQ,ELEM,F0,S11,W1,
                        W2,W3,D1,D2,SW1,SD1)
     N_OUTPUT=1 OUTPUT=(MAG_S11);
 Datapipe: SIM FILE=SAME
     N_INPUT =22 INPUT=(NX,NY,NZ,X_DIM,Y_DIM,Z_DIM
                        ER,UR,FC,N_SIM,N_F,F_MIN,
                          F_MAX,FREQ,ELEM,F0,S21,W1,
                        W2,W3,D1,D2,SW1,SD1)
     N_OUTPUT=1 OUTPUT=(MAG_S21);

 DB_S11 = 20*Log(MAG_S11);
 DB_S21 = 20*Log(MAG_S21);

End
```

Listing 1 The OSA90/hope circuit files for the examples given in this paper. The sweep, specification and control blocks are not shown here. The information for these blocks are given in the previous section.

Conclusion

A massively parallel 3D-TLM simulation module is developed in this paper to allow the use of the 3D-TLM numerical analysis together with OSA90/hope for microwave circuit analysis and optimization. This massively parallel 3D-TLM module is divided into 3 programs — two serial and a parallel one; they are *3dtlm-pipe*, *3dtlm-server* and *mpl-server*, respectively. The serial and parallel programs communicate with each other via a few UNIX pipes. The serial programs are implemented in C++ to perform serial numerical operations such as discretization of geometrical parameters and computation of discrete Fourier transforms. The parallel program is implemented in MPL to perform computer time intensive 3D-TLM simulation.

A comparison of the execution speed of the serial and parallel 3D-TLM simulation modules on three workstations and a DECmpp 12000 have been made. This provides a clear picture of the required execution time for performing 3D-TLM field simulations on various hardware platforms.

These programs integrate the 3D-TLM method with OSA90/hope via UNIX's pipe. In order to use OSA90/hope to optimize the geometry of microwave circuits, a microwave circuit component library with geometry parameterization in continuous Cartesian coordinates is implemented. Two examples are given to demonstrate the use of *3dtlm-pipe* and its component library.

This massively parallel 3D-TLM module is more than 30 times faster than its equivalent serial implementation running on a DEC5000/200 workstation. Therefore, it is feasible to optimize the geometry of microwave structures using 3D-TLM time domain field analysis without the need for equivalent circuits or lookup tables.

References

[1] P.P.M. So and W.J. R. Hoefer, *3D-TLM Time Domain Electromagnetic Wave Simulator for Microwave Circuit Modelling*, IEEE MTT-S, June 1991, Boston, MA.

[2] P. B. Johns, *A Symmetrical Condensed Node for the TLM Method*, IEEE Transactions on Microwave Theory and Techniques, vol. MTT-35, no. 4, pp. 370-377, April 1987.

[3] P.P.M. So, C. Eswarappa and W.J.R. Hoefer, *Transmission Line Matrix Method on Massively Parallel Processor Computers*, in 9th Annual Review of Progress in Applied Computational Electromagnetics Digest, pp.467-474, March 1993, Monterey, CA.

[4] P.P.M. So and W.J.R. Hoefer, *Distributed Computing for Transmission Line Matrix Method*, Second International Workshop on Discrete Time Domain Modelling of Electromagnetic Fields and Networks, October 1993, Berlin Germany.

[5] John J. Valley, *UNIX Programmer's Reference*, 1991, Que.

[6] P.P.M. So, W.J.R. Hoefer, J.W. Bandler, R.M. Biernacki and S.H. Chen, *Hybrid Frequency/Time Domain Field Theory Based CAD of Microwave Circuits*, in 23rd European Microwave Conference Digest, pp.218-219, September 1993, Madrid, Spain.

[7] S.H. Chen, *OSA90/hope™ Version 2.0 User's Manual* — May 1992, Optimization Systems Associates Inc., P.O. Box 8083, Dundas, Ontario, L9H 5E7, Canada.

Optimization of Microwave Structures using Time Domain TLM Electromagnetic Simulators

Wolfgang J.R. Hoefer

NSERC/MPR TELTECH Research Chair in RF-Engineering
Department of Electrical and Computer Engineering
University of Victoria, Victoria, British Columbia
Canada, V8W 3P6

WMFE: Automated Circuit Design using Electromagnetic Simulators
1995 IEEE-MTT Symposium, Orlando, Florida
May 15, 1995

Outline

- Introduction
- Huygens' Principle and TLM Processes
- Parallel Implementationof TLM Algorithms
- Distributed Computing Via UNIX's Pipe
- Prony's Method
- Autoregressive Moving Average (ARMA) Technique
- Simulation and Optimization Examples
- Conclusion

Introduction

- Field theory based microwave circuit CAD/CAM is mostly performed in the frequency domain.
- OSA90/hope is a commercially available CAD program that allows users to incorporate special elements into their circuit simulation using high speed UNIX pipe.
- Hence, OSA90/hope can run on its host machine and control external programs both in frequency and time domains running on other machines (such as DECmpp 12000).
- In order to control a time domain electromagnetic simulator with OSA90/hope, the geometry of the structure must be parameterized to allow geometry optimization.

Introduction (continued)

- A special software module has been designed to allow exchange of control and simulation data between the optimizer and the simulator.
- Since many computationally intensive analyses must be performed, a number of special features have been implemented to minimize computer time.
- These features include massively parallel and distributed computing, signal processing techniques.
- In this paper, the basic features of 2D and 3D TLM as well as various special acceleration techniques will be discussed.

Elementary 2D-TLM Processes

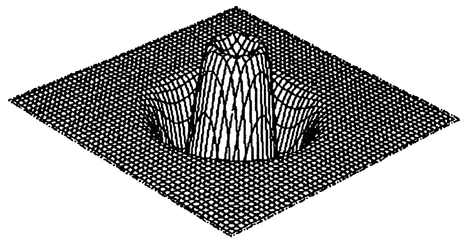

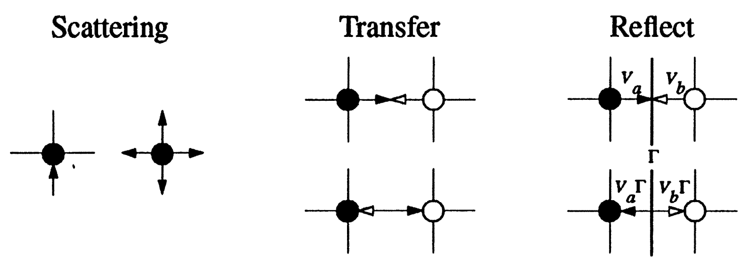

The DECmpp 12000

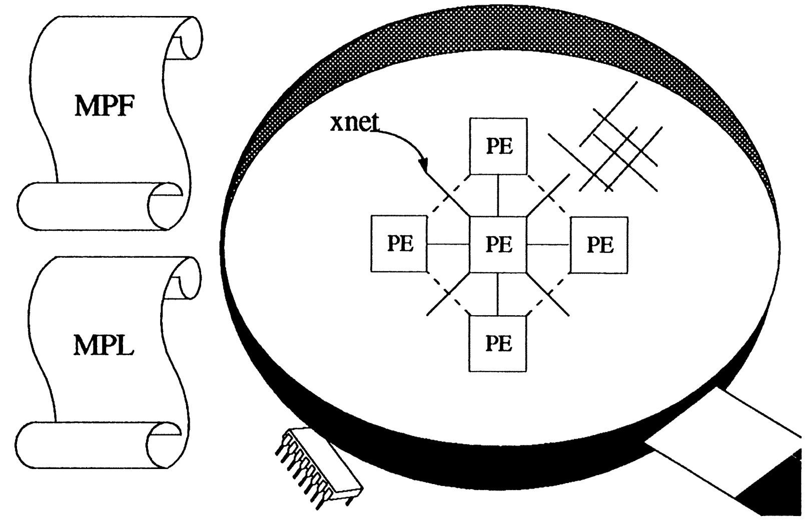

2D-TLM Scattering Algorithms

Series

```
Do x=1, NX
 Do y=1, NY
  Vz=0.5*(V1(x,y)+V2(x,y)+V3(x,y)+V4(x,y)
)
  V1(x,y) = Vz - V1(x,y)
  V2(x,y) = Vz - V2(x,y)
  V3(x,y) = Vz - V3(x,y)
  V4(x,y) = Vz - V4(x,y)
 End Do
```

Parallel

```
Vz = 0.5*(V1+V2+V3+V4)
V1 = Vz - V1
V2 = Vz - V2
V3 = Vz - V3
V4 = Vz - V4
```


2D-TLM Parallel Transfer Algorithm

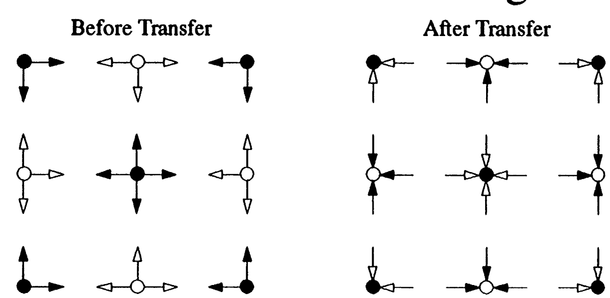


```
T1(1:NX,1:NY-1) = V1(1:NX,2:NY  )
T2(1:NX,2:NY  ) = V3(1:NX,1:NY-1)
Where (R1.EQ.0.0) V1=T2
Where (R3.EQ.0.0) V3=T1
T1(1:NX-1,1:NY) = V2(2:NX,  1:NY)
T2(2:NX,  1:NY) = V4(1:NX-1,1:NY)
Where (R2.EQ.0.0) V2=T2
Where (R4.EQ.0.0) V4=T1
```

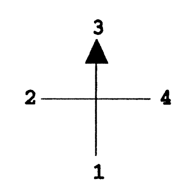

MPP 3D-TLM Mesh Implementation

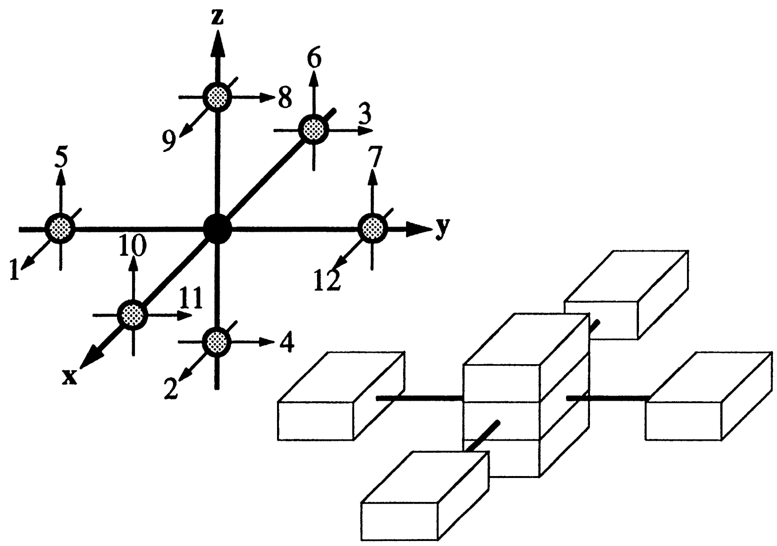

Optimization of Microwave Structures using Time Domain TLM Electromagnetic Simulators Wolfgang J.R. Hoefer

MPP 3D-TLM Mesh Implementation

```
        Integer    NX,NY,NZ
        Parameter  (NX=4,NY=4,NZ=4)
        Real       V1(NX,NY,NZ)
CMPF    MAP        V1(memory,xbits,ybits)
```

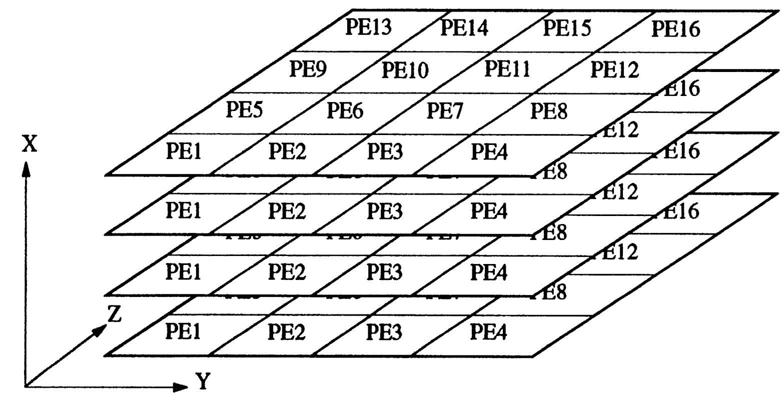

Optimization of Microwave Structures using Time Domain TLM Electromagnetic Simulators Wolfgang J.R. Hoefer

3D-TLM Transfer Algorithm

Parallel

```
for (z=0;z<z_size;z++){
  if (node[z].rx==NULL_REFL){
    swap(node[z].v6,xnetW[1].node[z].v10);
    swap(node[z].v3,xnetW[1].node[z].v11);
  }
  if (node[z].ry==NULL_REFL){
    swap(node[z].v5,xnetN[1].node[z].v7);
    swap(node[z].v1,xnetN[1].node[z].v12);
  }
  if (node[z].rZ==NULL_REFL){
    swap(node[z].v8,node[z+1].v4);
    swap(node[z].v9,node[z+1].v2);
  }
}
```


Optimization of Microwave Structures using Time Domain TLM Electromagnetic Simulators Wolfgang J.R. Hoefer

Distributed Computing

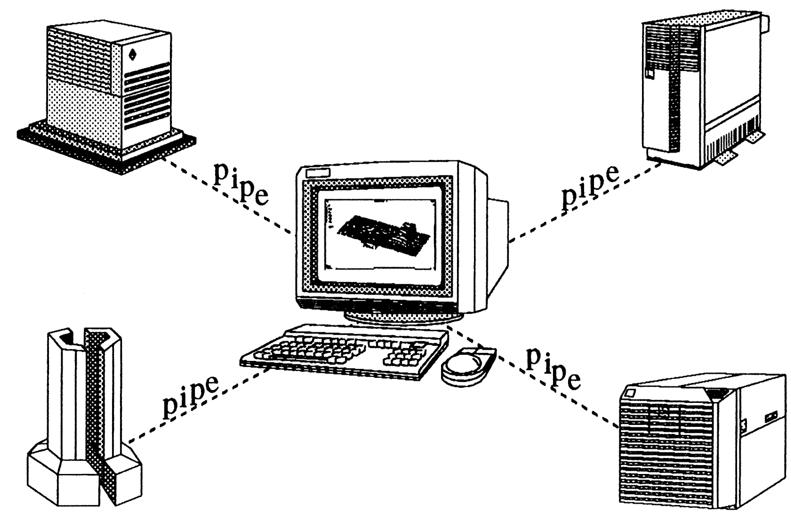

UNIX Piping Technique

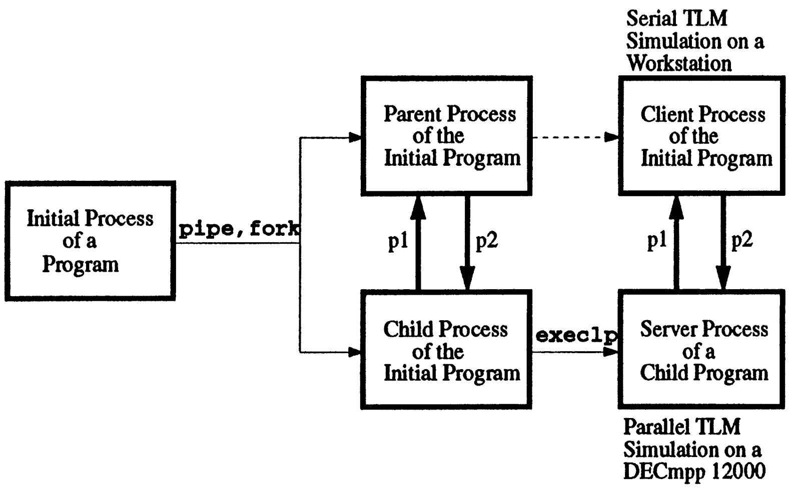

Interaction of Various UNIX Processes Via UNIX Pipes

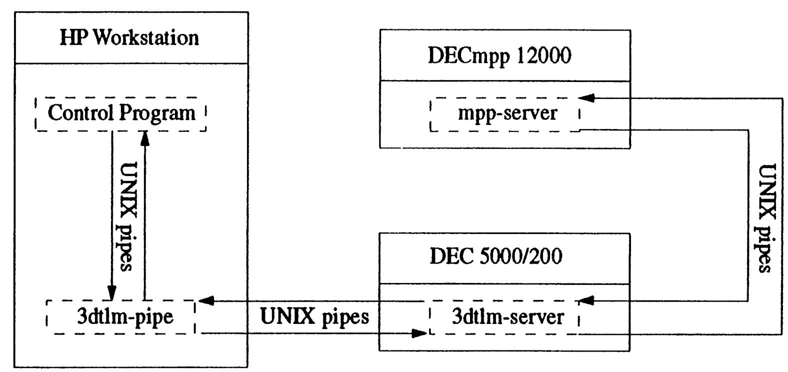

A Typical TLM Response

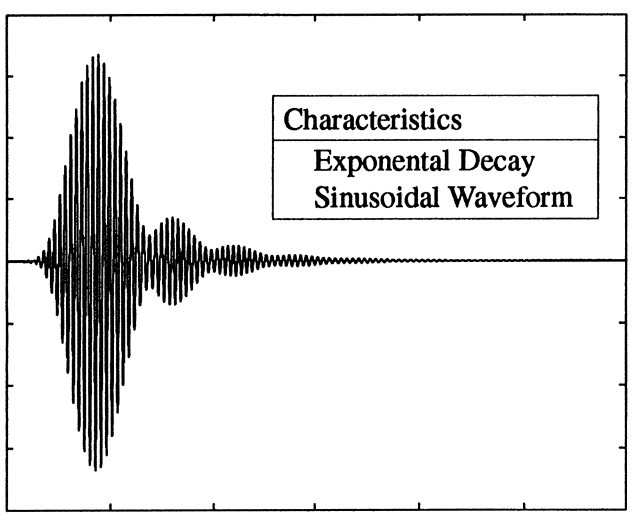

Prony's Method

$$u(n) = \sum_{k=1}^{q} A_k \, e^{-\alpha_k n\Delta t} \cos(2\pi f_k n\Delta t + \phi_k),\ n = 1, 2, \ldots, N$$

$$u(\omega) = \frac{1}{2}\sum_{k=1}^{q}\left(\frac{A_k e^{j\phi_k}}{\alpha_k + j(\omega - \omega_k)} + \frac{A_k e^{-j\phi_k}}{\alpha_k + j(\omega + \omega_k)}\right)$$

Where q is the number of resonant modes and the other modal parameters are:

Mode k	Amplitude A_k	Damping Factor [sec^{-1}] α_k	Phase [rad] ϕ_k	Frequency [GHz] f_k

Autoregressive Moving Average (ARMA)

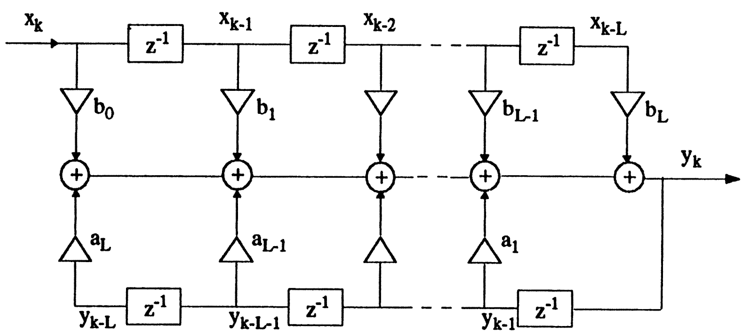

$$y_k = \sum_{n=0}^{L} b_n x_{k-n} - \sum_{n=1}^{L} a_n y_{k-n}$$

$$H(z) = \frac{Y(z)}{X(z)} = \frac{b_0 + b_1 z^{-1} + b_2 z^{-2} + \ldots + b_L z^{-L}}{1 + a_1 z^{-1} + a_2 z^{-2} + \ldots + a_L z^{-L}}$$

Time Domain Response of a Uniform Waveguide to a Cosine Modulated Gaussian Pulse Excitation

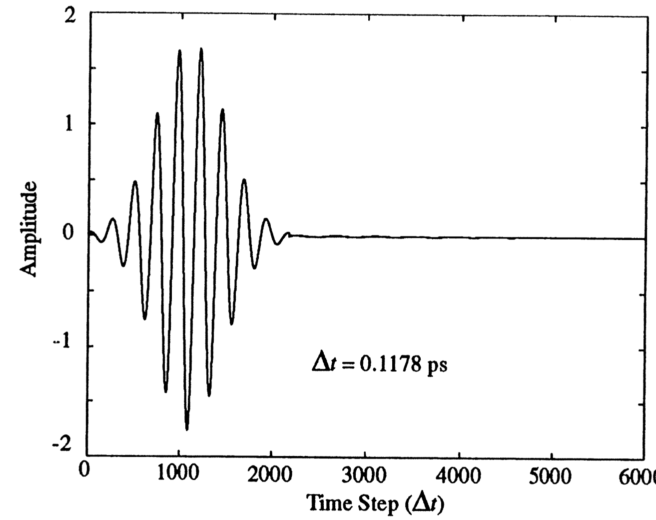

Frequency Domain Response of a Uniform Waveguide to a Cosine Modulated Gaussian Pulse Excitation

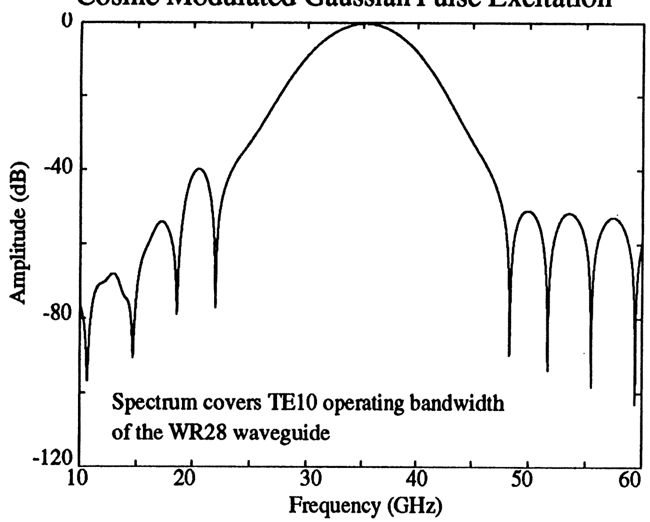

Optimization Example 1

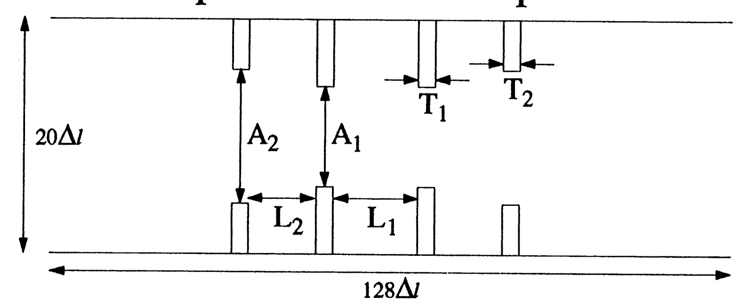

A bandpass filter in the WR28 rectangular waveguide, $\Delta l = 0.3556$ mm. Using single precision floating operation, the mesh requires 50K of RAM. The optimization goal is:

30.0 to 32.0 GHz step 0.1 GHz	S11=1	S21=0	weight=1
32.5 to 33.5 GHz step 0.1 GHz	S11=0	S21=1	weight=2
34.0 to 36.0 GHz step 0.1 GHz	S11=1	S21=0	weight=1

Time Domain Response at the Output of the Filter Obtained Using Direct TLM

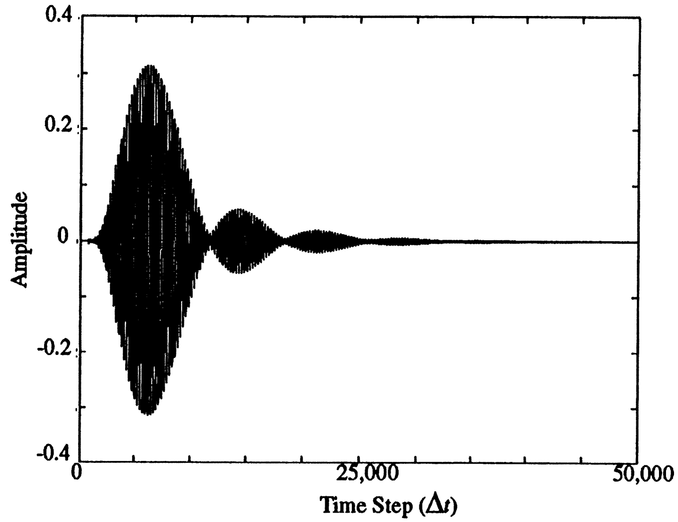

Time Domain Response at the Output of the Filter Obtained Using TLM with Prony's Method

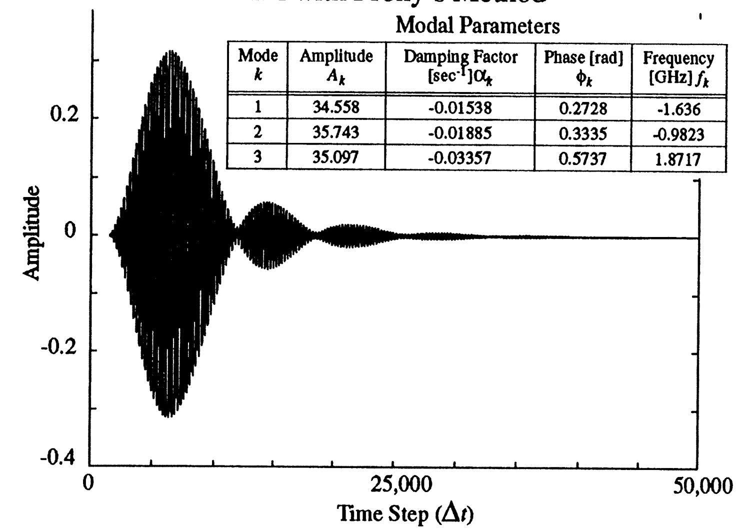

Modal Parameters

Mode k	Amplitude A_k	Damping Factor [sec^{-1}]α_k	Phase [rad] ϕ_k	Frequency [GHz] f_k
1	34.558	-0.01538	0.2728	-1.636
2	35.743	-0.01885	0.3335	-0.9823
3	35.097	-0.03357	0.5737	1.8717

Comparison of S-Parameters of the Filter Computed Using Prony's method and DFT of 12,000 and 50,000 Time Samples

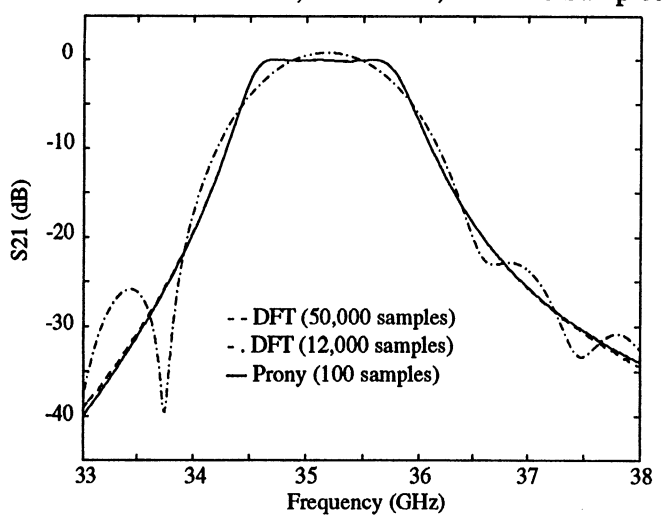

Comparison of S-Parameters of the Filter Computed Using ARMA and DFT of 50,000 Time Samples

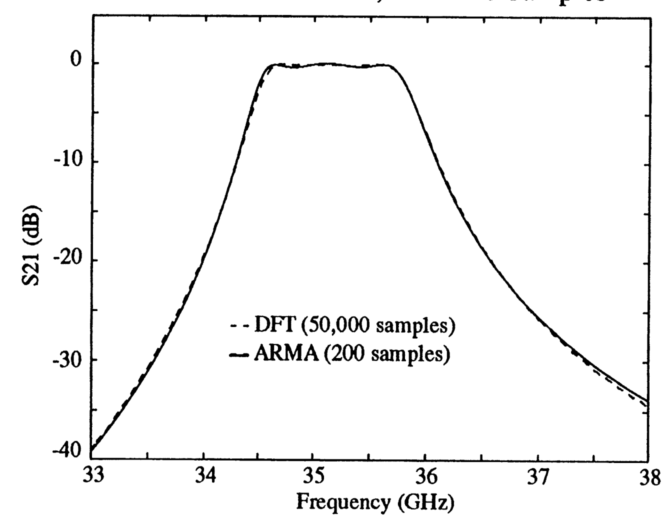

Initial Response (34 seconds/iteration)

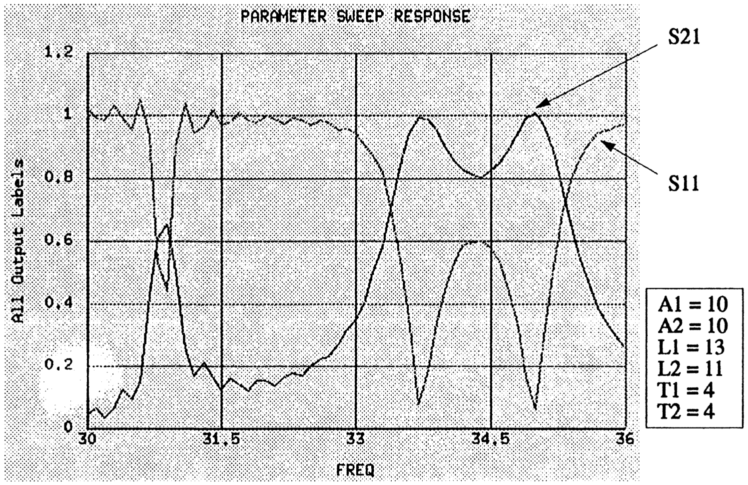

Intermediate Response (30 Iterations)

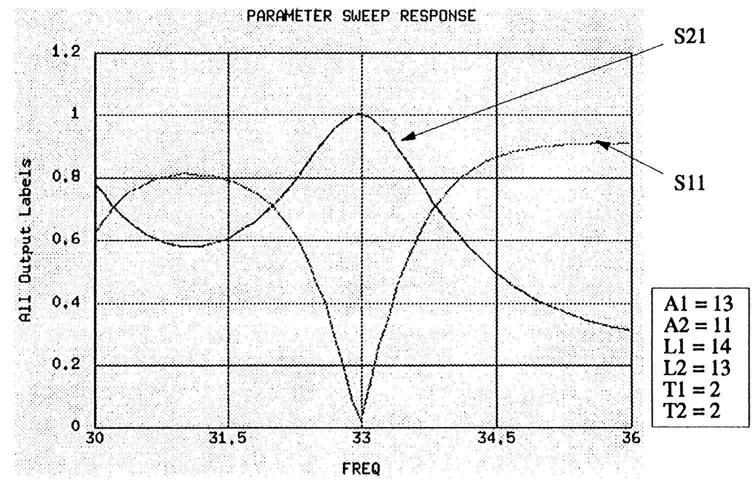

Intermediate Response (60 Iterations)

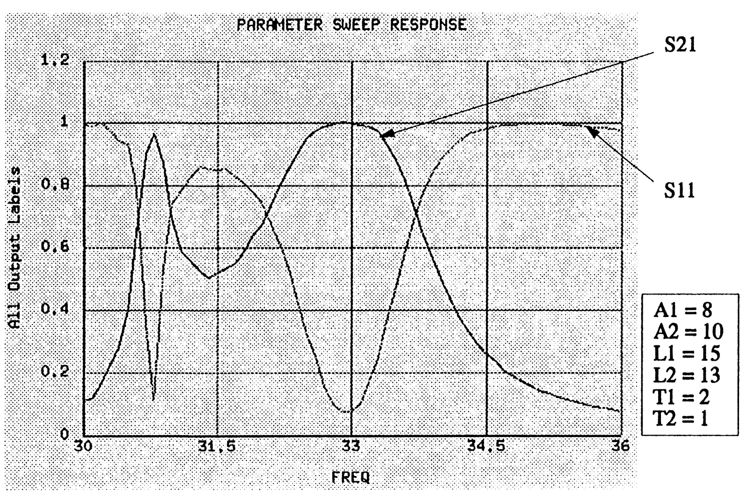

Optimized Result (180 Iterations)

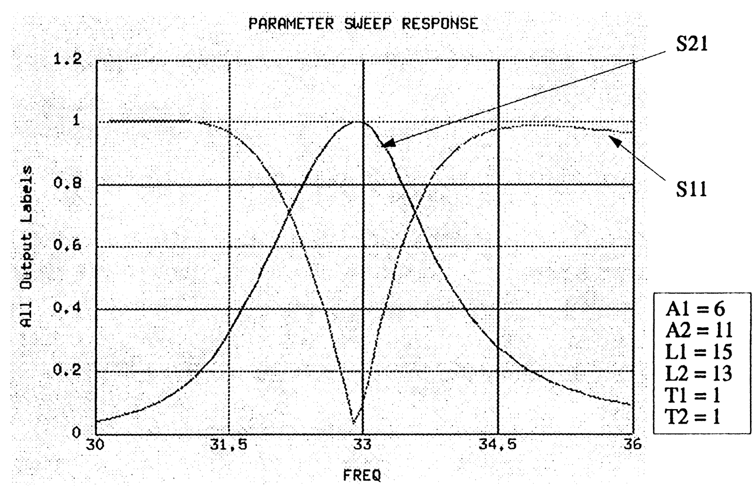

Optimization Example 2

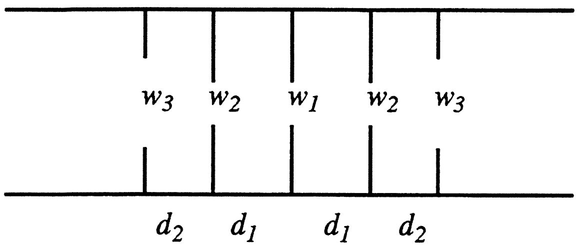

	Initial	30 steps	60 steps	90 steps
w_1 in Δl	2	4	4	4
w_2 in Δl	2	4	6	6
w_3 in Δl	2	10	10	10
d_1 in Δl	23	21	21	21
d_2 in Δl	23	23	22	23

$\Delta l = 0.508$mm

Initial Response

Scattering Parameters

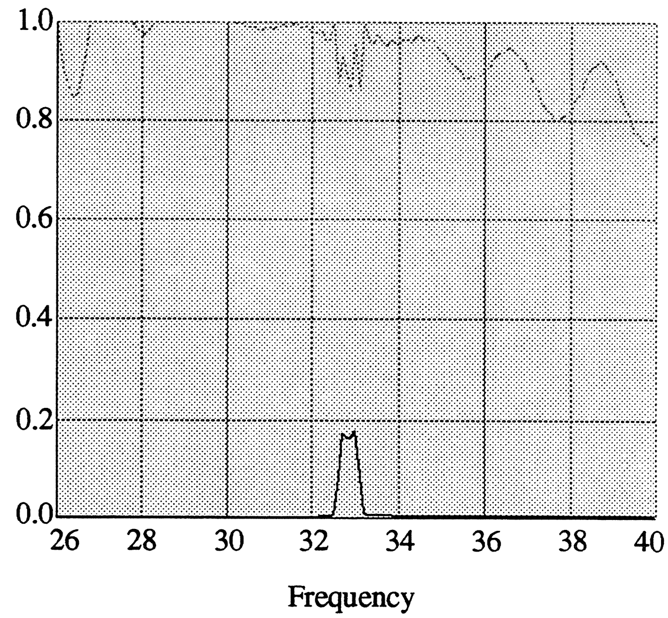

After 30 Steps

Scattering Parameters

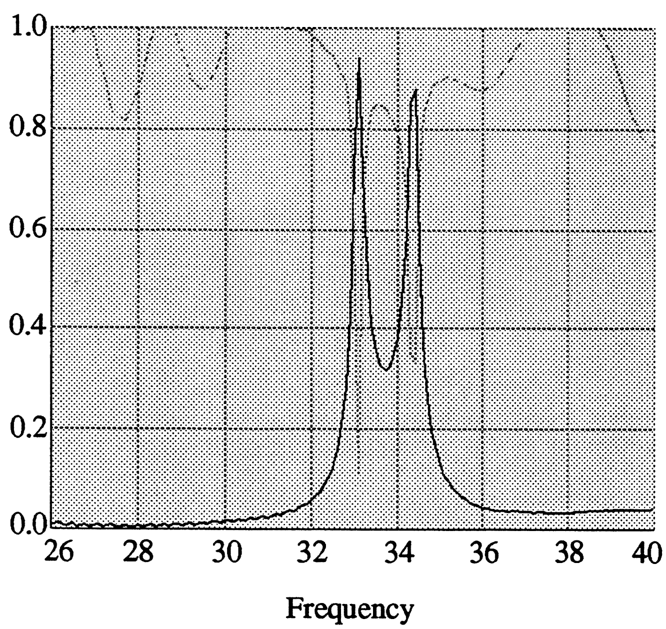

After 60 Steps

Scattering Parameters

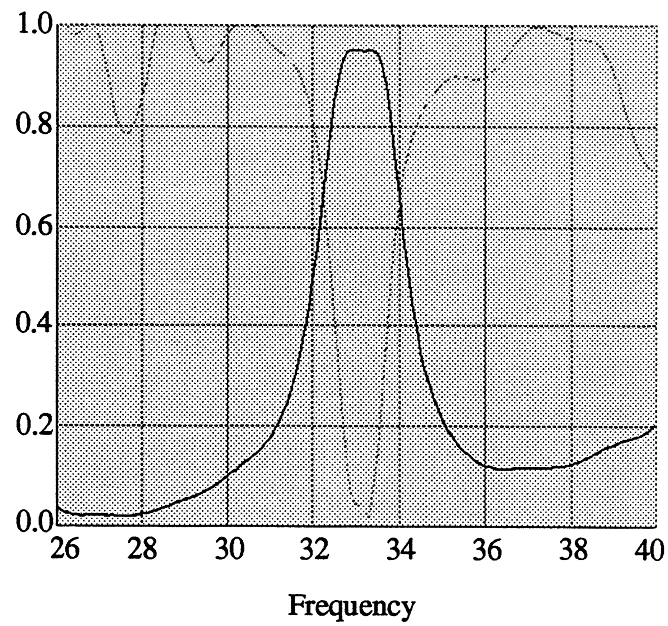

After 90 Steps

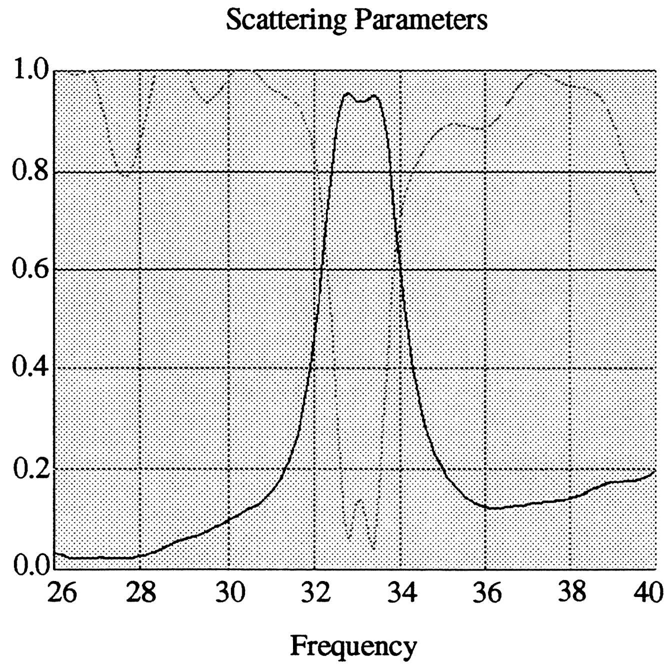

Double Resolution Result

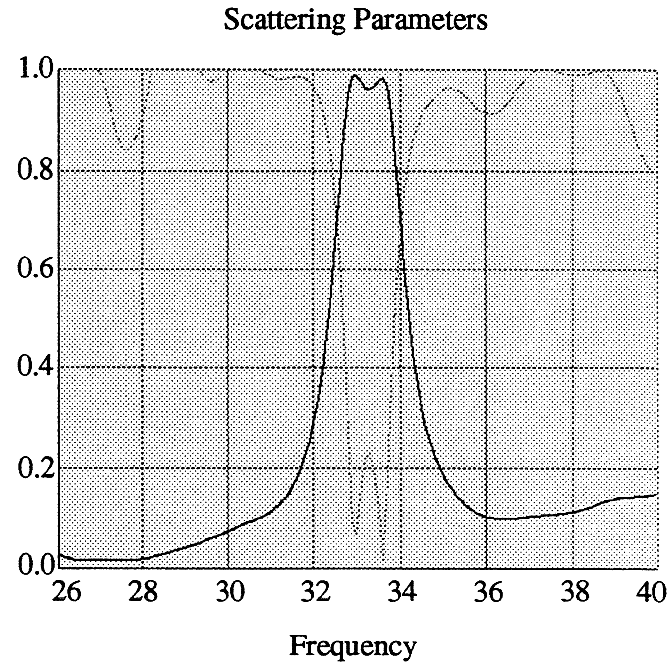

Quadruple Resolution Result

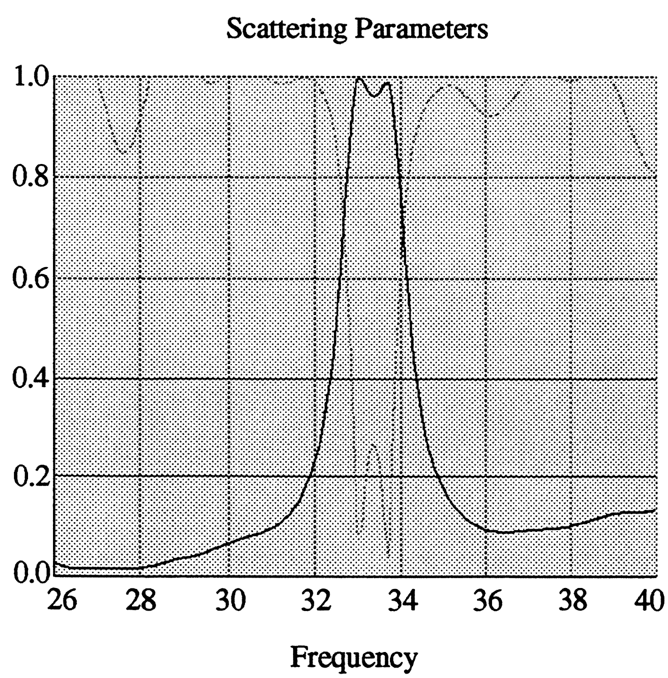

Some Data of Interest

Computer	CPU time (sec.)
Slow RISC Workstation	2580
Medium speed Workstation	490
High speed Workstation	368
DECmpp 12000	75

- Execution time of a serial and a parallel 3D-TLM field simulation module on three workstations and a parallel computer. The mesh size is 128×64×10; a mesh size of 128×64 in the *xy*-plane represents a full use of a DECmpp 12000 with 8192 processor. The number of time steps and frequency points are both 1000.
- The execution time shown above include all the network delays due to the piping operations.

Estimated 3D Requirements

- The difference in simulation speed between our 2D and 3D simulators for a 20×128 mesh is about 4 times.
- The memory requirement for a 3D-TLM simulation is 180K bytes.
- It is possible to use 3D simulation, say for a 10×20×128 mesh, for the previous example; the estimated execution time per iteration and memory requirement would be:

  10×4×34 = 1360 seconds, and
  10×180 = 1800 K bytes.

Advantages

- A single time domain field analysis yields information at an arbitrary number of frequency points within the desired bandwidth.
- Band limited excitation can be used to reduce unwanted frequency components with a corresponding gain in computer time, i.e. faster convergence.
- The computer expenditure depends mainly on the size of the computational domain and not on the geometrical simplicity of the geometry.

Disadvantages

- Practitioners must grasp both the frequency and time domain concepts.
- There are no standard protocols for pipe communication in CAD/CAM system, which makes porting of the field simulators among them difficult.
- Powerful computers, preferably computers with massively parallel processors, with large amounts of memory and fast CPU are needed to run the field-based simulator.

Conclusions

- Successful linking of time domain electromagnetic field simulator (TLM) with a frequency domain CAD program (OSA90/hope) via datapipe has been demonstrated.
- The network piping feature allows OSA90/hope to control the TLM simulators which may run on massively parallel computers or workstations.
- The computational effort required for time domain simulation is larger than that for a specialized frequency domain simulator, however, it is independent of the geometrical complexity and offers considerably more flexibility. Further work is directed towards development of a more efficient TLM-Pipe software.

University of Perugia

Slide No. 1

Automated Design of Waveguide Components based on 3D Mode Matching and Adjoint Network Method

R. Sorrentino
University of Perugia
Italy

University of Perugia

OUTLINE of PRESENTATION

Slide No. 2

- Introduction
- 3-D mode matching method
- Generalized multiport representation
- The Adjoint Network Method
- Examples
- Conclusions

University of Perugia

WAVEGUIDE DISCONTINUITIES AND COMPONENTS

Slide No. 3

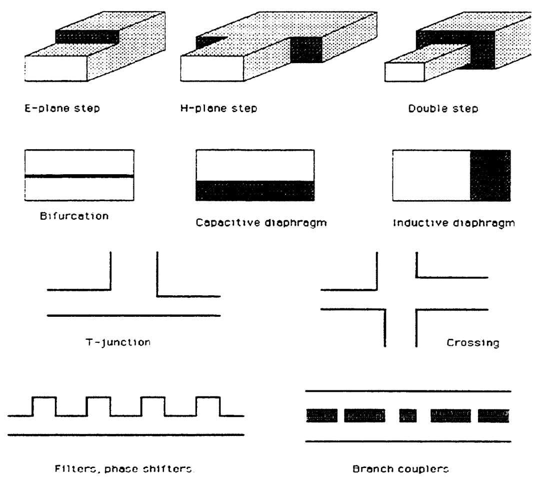

University of Perugia

CONVENTIONAL MODE-MATCHING TECHNIQUE

Slide No. 4

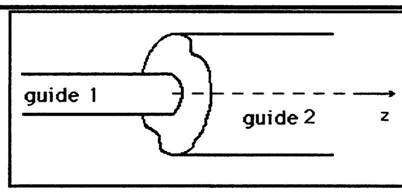

1. **EXPAND THE EM FIELD AT BOTH SIDES OF THE DISCONTINUITY IN TERMS OF WAVEGUIDE MODES**

normal modes: $\mathbf{h}_p = \mathbf{z}_o \times \mathbf{e}_p$

$$\mathbf{E}_t^{(i)} = \sum_{p=0}^{P-1} V_p^{(i)} \mathbf{e}_p^{(i)}(x,y) \; ; \quad \mathbf{H}_t^{(i)} = \sum_{p=0}^{P-1} I_p^{(i)} \mathbf{h}_p^{(i)}(x,y)$$

2. **MATCH THE FIELDS AT THE INTERFACE**

3. **USE MODE ORTHOGONALITY TO OBTAIN A LINEAR SYSTEM OF EQUATIONS IN THE EXPANSION COEFFICIENTS**

$$[V_1] = [W]^T [V_2]$$

$$[I_2] = [W] [I_1]$$

University of Perugia

CASCADED DISCONTINUITIES
The GSM Approach

Slide No. 5

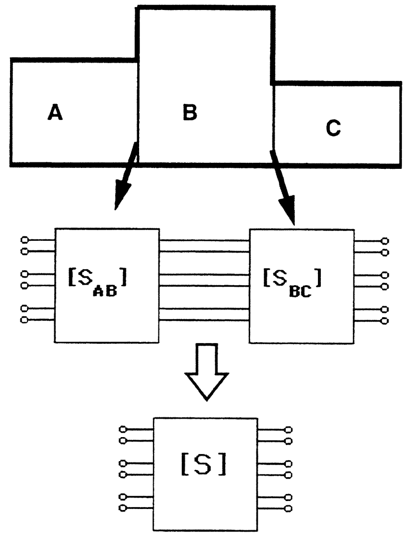

University of Perugia

CASCADED DISCONTINUITIES:
The GAM Approach

Slide No. 6

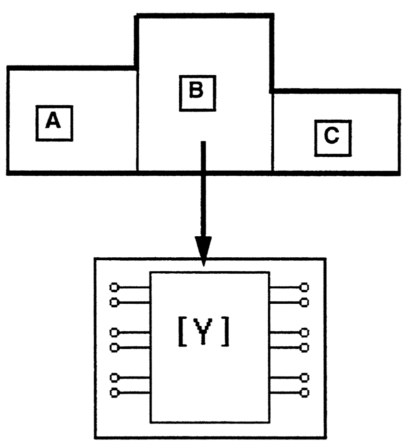

From the step equations one obtains directly the admittance matrix of the 'B' cell <u>with no matrix inversion</u>

$$\begin{bmatrix} I_A \\ I_C \end{bmatrix} = [Y] \begin{bmatrix} V_A \\ V_C \end{bmatrix}$$

University of Perugia

GENERALIZED ADMITTANCE MATRIX OF A 3-D MICROWAVE NETWORK

Slide No. 7

THE MAGNETIC FIELD IS GIVEN BY:

$$\mathbf{H}(\mathbf{r}) = j\omega\varepsilon \oint_S \mathbf{n}\times\mathbf{E}(\mathbf{r}')\, \underline{\mathbf{G}}(\mathbf{r},\mathbf{r}')\, dS' = j\omega\varepsilon \sum_{i=1}^{N_P} \int_{S_i} \mathbf{n}\times\mathbf{E}(\mathbf{r}')\, \underline{\mathbf{G}}(\mathbf{r},\mathbf{r}')\, dS'$$

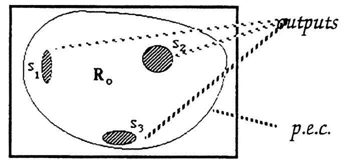

ELECTRIC FIELD AT THE OUTPUTS:

equivalent voltages

$$\mathbf{n}\times\mathbf{E}^{(i)} = \sum_{k=1}^{N_i} V_k^{(i)} \phi_k^{(i)}$$

equivalent currents

$$I_k^{(i)} = \int_{S_i} \mathbf{H}(\mathbf{r})\, \phi_k^{(i)}(\mathbf{r})\, d\mathbf{r}$$

One obtains:

$$I_m^{(j)} = \sum_{i=1}^{N} \sum_{k=1}^{N_i} Y_{mk}^{(ji)} V_k^{(i)}$$

with

$$Y_{mk}^{(ji)} = \int_{S_j} \int_{S_i} \phi_m^{(j)}(\mathbf{r}) \cdot \underline{\mathbf{G}}(\mathbf{r},\mathbf{r}') \cdot \phi_k^{(i)}(\mathbf{r}')\, d\mathbf{r}\, d\mathbf{r}'$$

generalized admittance matrix

University of Perugia

Segmentation with triangular elements

Slide No. 8

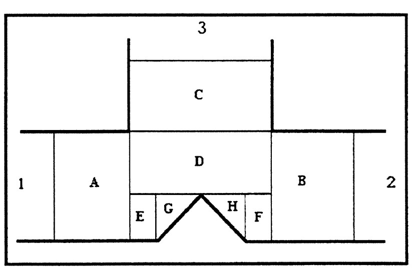

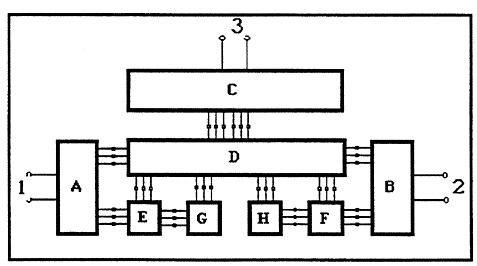

COMPENSATED T-JUNCTION

EQUIVALENT CIRCUIT

University of Perugia

Conventional vs 3D Mode Matching

Slide No. 9

1. Conventional MM (GSM):

Boundary conditions imposed at the discontinuities using the 2D eigenmodes of the wave guides

2. 3D MM (GAM):

B.C. imposed on portions of the boundary using 3D eigensolutions (resonant modes)

University of Perugia

A 6-port Branch Coupler:
Conventional Mode Matching (GSM)

Slide No. 10

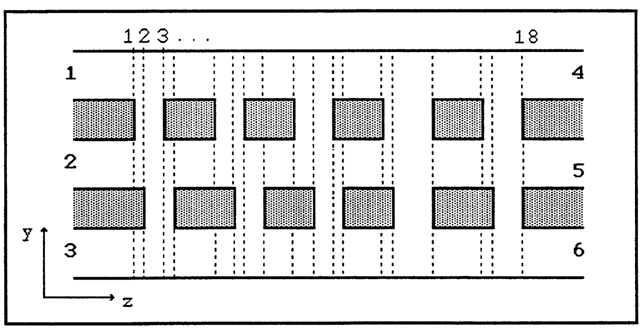

1 multiport associated to each discontinuity:
- **18 cascaded discontinuities (n-furcations)**
- **18 cascaded multiport networks**
- **Overall equivalent circuit changes during optimization**

University of Perugia

A 6-port Branch Coupler: 3D Mode Matching

Slide No. 11

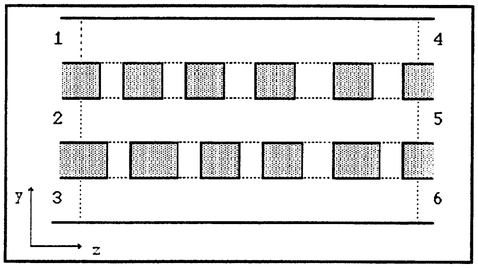

Equivalent circuit

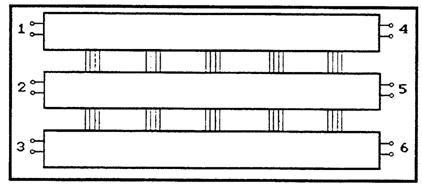

- Low number of discontinuities, thus of multipor
- Simple general equivalent network
- 8 times faster than GSM

University of Perugia

The Adjoint Network Method

Slide No. 12

Ext.Port

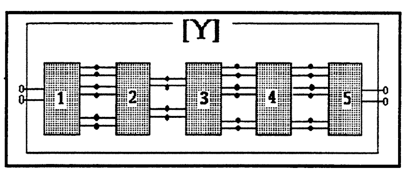

Ext.Port 2

For a reciprocal network, the adjoint network coincides with the original network

The gradient of [Y] is expressed in terms of the gradients of the Np subnetworks

$$\frac{\partial \hat{Y}_{jk}}{\partial x_m} = \sum_{i=1}^{N_p} (\mathbf{V}_i^T)_j \frac{\partial \mathbf{Y}_i^T}{\partial x_m} (\mathbf{V}_i)_k$$

- (Vi)j: voltages at subnetwork i for excitation at the external port j;
- Yi : admittance matrix of the ith subnetwork
- All (Vi)j are computed by the same system of eqns. <u>Only one analysis needed</u>
- Yi and its derivatives can be evaluated analytically!
- Conventionally x_m is an electrical parameter (e.g. line length, etc.), but can also be a geometrical parameter!

University of Perugia

Advantages and Disadvantages

Slide No. 13

PRO's

- Finite difference computation of derivatives is avoided
- Only one full analysis is needed instead of $N_{par}+1$

CONs

- Analytical effort required to evaluate the derivatives of the constituent networks

University of Perugia

A quotation

Slide No. 14

"There seems little doubt, from the circuit designer's point of view at any rate, that the introduction of the adjoint network method by Director and Rohrer is a turning point in computer-aided design"

J.W. Bandler and R.E. Seviora, MTT. Trans., Dec 1970

University of Perugia

Optimization by 3-D Mode Matching and ANM

Slide No. 15

1. The microwave structure is segmented into a number of simple cells
2. Generalized multiport representation for each cell using a generalized mode matching technique
3. Rigorous network representation of the overall structure
4. Gradient computation using Adjoint Network, i.e. by a single analysis
5. <u>CPU saving proportional to Nvar+1</u>

University of Perugia

OPTIMIZING A BANDPASS FILTER

Slide No. 16

FILTER STRUCTURE:

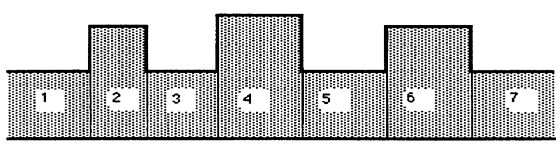

EQUIVALENT CIRCUIT:

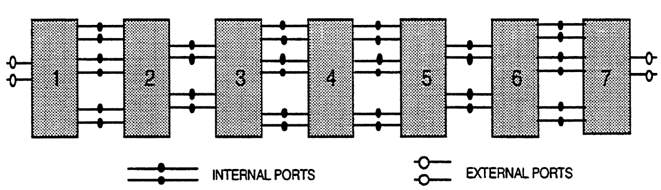

University of Perugia

OPTIMIZING A BANDPASS FILTER
(CONT.'D)

Slide No. 17

OBJECTIVE FUNCTION:

$$F = \sum_{i=1}^{NF} [K_{1i}(|s_{11}(f_i)| - |s_{11}^{ob}|)^2 + K_{2i}(|s_{21}(f_i)| - |s_{21}^{ob}|)^2]$$

The objective function is minimized by a quasi-Newton strategy making use of its derivatives with respect to the geometrical parameters.

Derivatives are computed by the ANM rather than by finite differences

University of Perugia

A bandpass filter

Slide No. 18

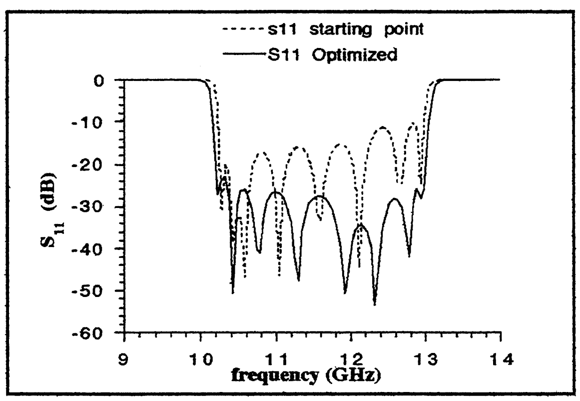

Simulations performed on 486 33MHz PC:
Convergence reached in 200 iterations.
Time per iteration: 10 sec with the ANM
116 sec with FD

University of Perugia

Waveguide bandpass filter with H-plane irises

Slide No. 19

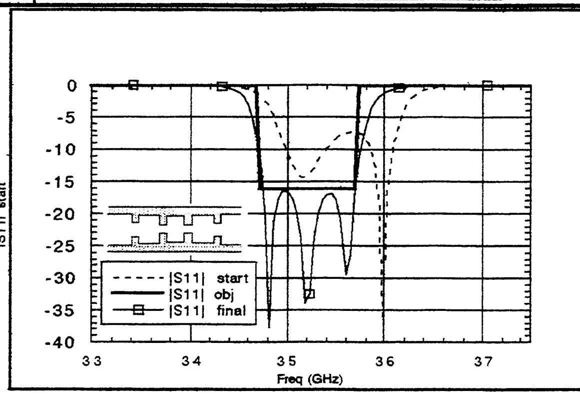

6 geometrical parameters
52 iterations (3120 single analyses and 18.720 derivatives)
12' CPU on 486 33 MHz IBM compatible PC

University of Perugia

E-plane 0-dB branch guide coupler

Slide No. 20

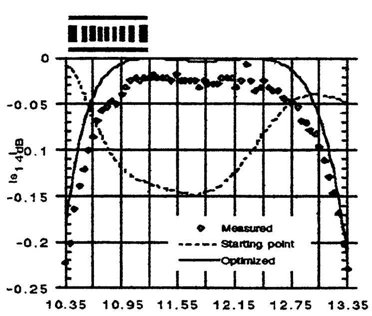

COUPLING

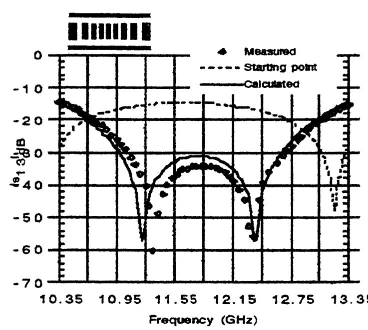

TRANSMISSION

- **8 branches**
- **13 optimization variables**

University of Perugia

3-dB H-plane branch coupler

Slide No. 21

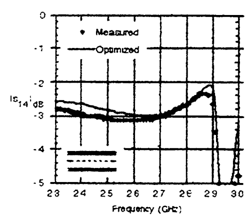

COUPLING

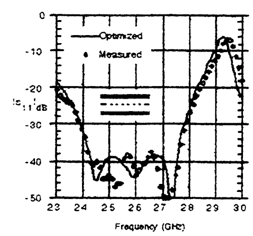

INSERTION LOSS

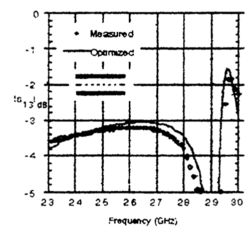

ISOLATION

University of Perugia

CONCLUSIONS

Slide No. 22

- MM technique generalized to 3-D structures
- Segmentation into simple volume elements
- Rigorous network representation of the microwave structure
- Application of ANM for efficient optimization: speed upfactor proportional to Npar+1
- Applicable to waveguides and MMIC's

IEEE MTT-S Workshop WMFE parallel to the IMS 1995, Orlando, Florida, May 15, 1995
Automated Circuit Design using Electromagnetic Simulators

Interactive Use of 2D and 2.5D EM Tools in (M)MIC Design

R.H. Jansen, RWTH Aachen, Institute of Technology, Aachen, Germany
P. Hildenhagen, Jansen Microwave GmbH, Aachen, Germany
Dan G. Swanson, Jr., Watkins Johnson Company, Palo Alto, CA, USA

Abstract - Optimization directly using 2D EM tools has been used with excellent success over about three years for high-order mmwave interdigital, edge-coupled and compensated coupled filter design. High-speed 2.5 D EM has been implemented for direct interactive design providing further flexibility and allowing fast broadband simulation of user-defined conductor configurations up to the level of geometrical complexity of full high-order filters. 2D and 2.5 D EM implementation details, applications and results are discussed.

EFFICIENT DESIGN OF RECTANGULAR AND CIRCULAR WAVEGUIDE COMPONENTS USING MODE-MATCHING SIMULATORS IN COMMON CIRCUIT CAD TOOLS

F. Arndt, Th. Sieverding, U. Papziner, T. Wolf

Microwave Department, University of Bremen
P.O. Box 330 440
Kufsteiner Str., NW1, D-28359, Bremen, Germany
Tel.: +49 (421) 218-2495 /-2242, Fax: +49 (421) 218-3601
E-mail: fritz.arndt@physik.uni-bremen.de, siever@hf-technik.uni-bremen.de

Abstract **- Efficient mode-matching waveguide elements are presented for the user-friendly use in common circuit theory CAD packages. This hybrid mode-matching/circuit theory CAD approach allows the accurate and fast design of a comprehensive class of rectangular and/or circular waveguide components by combining advantageously the accuracy of the rigorous electromagnetic simulators with the efficiency of matured and well-established circuit theory design instruments. The efficiency of the hybrid CAD method is demonstrated at typical design examples which are calculated by using the mode-matching waveguide elements in powerful circuit CAD packages, such as TOUCHSTONE^{TM} by hp-EEsof and OSA90/hope^{TM} by Optimization Systems Associates (OSA) Inc. Because these waveguide elements are conveniently available as additions to the usual element catalogs of the CAD packages, no special knowledge of the field theory behind the models is required by the user.**

I. INTRODUCTORY REMARKS

INCREASING PROGRESS in modern communication systems, such as satellite or high-capacity microwave radio relay links, has prompted the need for the accurate design of high performance waveguide components for many different applications [1] -[4]. Recent advances in the development of efficient circuit theory CAD tools and the progress in modern waveguide fabrication techniques have stirred, therefore, the interest in interfacing rigorous electromagnetic simulators into common CAD frameworks. Moreover, with the availability of powerful low-cost workstations, the storage and cpu time requirements of appropriate electromagnetic methods are no longer a limiting factor for applying advanced field theory subroutines for portions in the design that need it.

Although complete numerical 3D analysis techniques, such as the finite element [5] or finite difference approach, are commercially available for some time, the analytical mode-matching method [2] - [4], [6] -[10] proves faster and more efficient for analyzing and optimizing waveguide components that are composed of the important class of stepped discontinuities. Moreover, nearly all standard waveguide components can be decomposed into a few basic key-building blocks. Their combination with homogeneous waveguide sections of finite lengths by using the overall full-wave modal scattering [6] - [10], or admittance matrix [3], [4], formulation achieves the rigorous modeling of nearly all common structures for the microwave designer.

Many common waveguide components, such as filters, multiplexers, transformers, however, include sections where the higher-order modes evanesce to a negligible value. The most prudent approach for fast but reliable design tools for this class of waveguide components is, therefore, to solve only the critical pieces (e.g. windows or obstacles of finite thickness) by rigorous mode-matching subroutine files by including there all necessary higher-order modes, and combining them with the fast circuit theory technique (i.e. merely with the fundamental mode network) of available standard CAD programs. Moreover, this approach allows the application of matured yield optimization techniques and the utilization of the familiar graphics environment of common CAD software.

II. Short Overview of the Theory

Although the mode-matching waveguide elements are conveniently available as additions to the usual element catalogs of the CAD packages, and no special knowledge of the details of the field theory behind the models is required by the user when applying these elements, a short overview of the theory may nevertheless elucidate the efficiency and accuracy of the models.

The required basic key-building blocks for the formulation of the mode-matching waveguide element set are: The asymmetric rectangular waveguide double-plane step discontinuity [6], the asymmetric rectangular to circular, and circular to circular waveguide step discontinuities [8] (note that these asymmetric step discontinuities already inlude the full information required for general multiport transitions, cf. [3]), the general six-port cross [10], the general planar boundary contour mode-matching (BCMM) discontinuity [12], and the T-junction circular waveguide to side coupled rectangular waveguide [13].

The full set of TE_{mn} and TM_{mn} modes in all sections is required in order to model adequately the composed mode-matching waveguide elements. The principle of the mode-matching technique is shortly described at the example of the step discontinuities rectangular to rectangular or circular waveguide. For a more detailed description, the reader is referred to the available literature, [6] -[13].

For the waveguide subregion under consideration, the fields [6] - [11]

$$\vec{E}^\nu = \frac{1}{j\omega\epsilon}\nabla \times \nabla \vec{A}_e^\nu + \nabla \times \vec{A}_h^\nu,$$
$$\vec{H}^\nu = -\frac{1}{j\omega\mu}\nabla \times \nabla \vec{A}_h^\nu + \nabla \times \vec{A}_e^\nu, \tag{1}$$

are derived from the z-components of the electric and magnetic vector potentials A_e, A_h, respectively,

$$\vec{A}_{hz} = \sum_{i=0}^{N_h} Q_{hi}T_{hi}(a_{hi}e^{-\gamma_{hi}z} + b_{hi}e^{+\gamma_{hi}z}),$$
$$\vec{A}_{ez} = \sum_{i=1}^{N_e} Q_{ei}T_{ei}(a_{ei}e^{-\gamma_{ei}z} - b_{ei}e^{+\gamma_{ei}z}), \tag{2}$$

where a_i, b_i are the still unknown eigenmode amplitude coefficients of the forward ($-$) and backward ($+$) waves in z direction, $\gamma_{h,e}$ are the propagation factors of the N_h and N_e considered TE_{pq} and TM_{pq} modes, respectively, where i stands for p, q. $Q_{h,e}$ is the normalization factor, and $T_{h,e}$ are the cross-section eigenfunctions for the rectangular or circular waveguide, respectively.

By matching the tangential field components at all interfaces at the individual step discontinuities, the wave amplitude coefficients of equation (2) can be related to each other after multiplication with the appropriate orthogonal functions. This yields the corresponding key-building block modal scattering matrix, where one of the advantages of the mode-matching method is that the coupling matrices are given in analytical form, cf. [6] - [11].

For modeling the composite mode-matching waveguide elements, such as irises of finite thickness, the generalized S-matrix technique is used [6] - [12], which combines the key-building block modal S-matrices with those of the additional building block elements, such as empty waveguide of finite length. A modified algorithm [7] requires only the inversion of a quadratic submatrix of reduced order.

Computer subroutines for the current about thirty available mode-matching waveguide elements for use with common CAD circuit theory software have been implemented. These include: step discontinuity rectangular or circular to rectangular or circular waveguide (2 to 5 ports), rectangular or circular iris (up to 4 apertures) in rectangular or circular waveguides, rectangular waveguide n-furcation (2 to 5 ports), E-plane and H-plane corners and T-junctions, E- and H-plane crosses, the trivial homogeneous empty waveguide of finite length, the short-circuited and matched waveguide. All concerned mode-matching waveguide elements are of finite thickness and/or arbitrary location. The full set of modes may be included for any element up to 150 TE_{mn}- and 150 TM_{mn}-modes, which guarantees a high accuracy of the results if required. Moreover, it is possible to calculate each element with an individual number of modes, if desired, independently from the other elements.

The mode-matching waveguide elements are available in the form of FORTRAN subroutine object files that may be implemented into common circuit CAD software within the UNIX environment, such as TOUCHSTONE^{TM} by hp-EEsof and OSA90/hope^{TM} by Optimization Systems Associates Inc. The desired waveguide structure may then be built up by using the implemented waveguide elements in the usual manner with the help of the familiar circuit CAD software . The scattering parameters of all building block elements are internally normalized to the wave impedances of all considered modes, and all ports are automatically matched.

Although the individual mode-matching waveguide building block elements are modeled rigorously by including a desired number of modes, the combination of the elements in the common circuit CAD software, for instance for a series of transformer steps, is carried out by the fundamental mode. Since for sufficiently separated discontinuities (more than about one quarter of the guide wavelength) all evanescent higher-order modes are adequately decayed, this hybrid approach, however, is accurate for the most common structures (such as filters, transformers, multiplexers).

The computing time depends on the number of modes that are taken into account and on the computer used. For example, a typical computing time for analyzing a three-resonator metal insert filter with 15 modes is about 1 second for each frequency point on a typical workstation with 10 Mflops.

III. RESULTS

The copies of the viewgraphs of the following pages demonstrate the efficiency of the mode-matching waveguide elements which have been implemented already as additions to the catolog elements of TOUCHSTONE^{TM} and OSA90/hope^{TM}.

New mode-matching waveguide elements are in preparation and have already been tested successfully: Circular waveguide with side coupled rectangular waveguide, and a general boundary contour mode-matching element. These elements allow the modeling of still more complicated structures, such as mitered waveguide corners, rounded resonator sections, irises of more general shape, and orthomode transducers.

IV. CONCLUSION

Efficient mode-matching waveguide elements are developed for the user-friendly use in common circuit theory CAD packages on usual workstations. This hybrid mode-matching/circuit theory CAD approach allows the accurate and fast design of a comprehensive class of rectangular and/or circular waveguide components, such as filters, multiplexers, and transformers.

Acknowledgment

The authors acknowledge the kind support of this challenging project by hp-EEsof and by Optimization Systems Associates Inc. Their powerful CAD tools TOUCHSTONE^{TM} and OSA90/hope^{TM}, respectively, are very appropriate for the convenient implementation of the mode-matching waveguide elements. This novel combination yields an reliable, powerful and efficient tool for the waveguide designer. The authors thank Mr. Hirsekorn and Prof. Bandler for their valuable help.

References

[1] C. KUDSIA, R. CAMERON, W.-C. TANG, "Innovations in microwave filters and multiplexing networks for communications satellite sytems ", IEEE Trans. Microwave Theory Tech., vol. MTT-40, pp. 1133 - 1149, June 1992.

[2] U. ROSENBERG, W. HAEGELE, "Consideration of parasitic bypass couplings in overmoded cavity filter designs ", IEEE Trans. Microwave Theory Tech., vol. MTT-42, pp. 1301 - 1306, July 1994.

[3] W. HAUTH, R. KELLER, U. PAPZINER, R. IHMELS, T. SIEVERDING, F. ARNDT, "Rigorous CAD of multiport coupled rectangular waveguide components", in Proc. 23rd European Microwave Conf., Madrid, Sept. 1993, pp. 611 - 614.

[4] F. ALLESANDRI, M. DIONIGI, R. SORRENTINO, M. MONGIARDO, "A fullwave CAD tool of waveguide components using a high speed direct optimizer", in IEEE MTT-S Int. Symp. Digest, pp. 1539-1542, May 1994.

[5] Z.J. CENDES, J.-F. LEE, "The transfinite element method for modeling MMIC devices", IEEE Trans. Microwave Theory Tech., vol. MTT-36, pp. 1639-1649, Dec. 1988.

[6] H. PATZELT, F. ARNDT, "Double-plane steps in rectangular waveguides and their application for transformers, irises, and filters", IEEE Trans. Microwave theory Tech., vol. MTT-30, pp. 771-776, May 1982.

[7] T. SIEVERDING, F. ARNDT, "Field theoretic CAD of open or aperture matched T-junction coupled rectangular waveguide structures", IEEE Trans. Microwave Theory Tech., vol. MTT-40, pp. 353-362, Feb. 1992.

[8] F. ARNDT, U. PAPZINER, "Modal-S-matrix design of microwave filters composed of rectangular and circular waveguide elements", in IEEE MTT-S Int. Symp. Digest, pp. 535-538, June 1991.

[9] T. SIEVERDING, U. PAPZINER, T. WOLF, F. ARNDT , "New mode-matching building blocks for common circuit CAD programs ", Microwave Journal, vol. 36, pp. 66-79, Dec. 1993.

[10] T. SIEVERDING, F. ARNDT, "Rigorous analysis of the rectangular waveguide six-port cross junction", IEEE Microwave and Guided Wave Letters, vol. 3, pp. 224-226, July 1993.

[11] T. SIEVERDING, F. ARNDT, "Combined circuit-/field-theory CAD procedure for manifold multiplexers with circular cavities", in Proc. 24th European Microwave Conference, Cannes, pp. 437-442, Sept. 1994.

[12] J. REITER, F. ARNDT, "A full-wave boundary contour mode-matching method (BCMM) for the rigorous CAD of single and cascaded optimized H-plane and E-plane bends", in IEEE MTT-S Int. Symp. Digest, pp. 1021-1024, May 1994.

[13] P. KRAUSS, F. ARNDT, "Rigorous mode-matching method for the modal analysis of the T-junction circular to sidecoupled rectangular waveguide", accepted for the MTT-S Symposium 1995, Orlando.

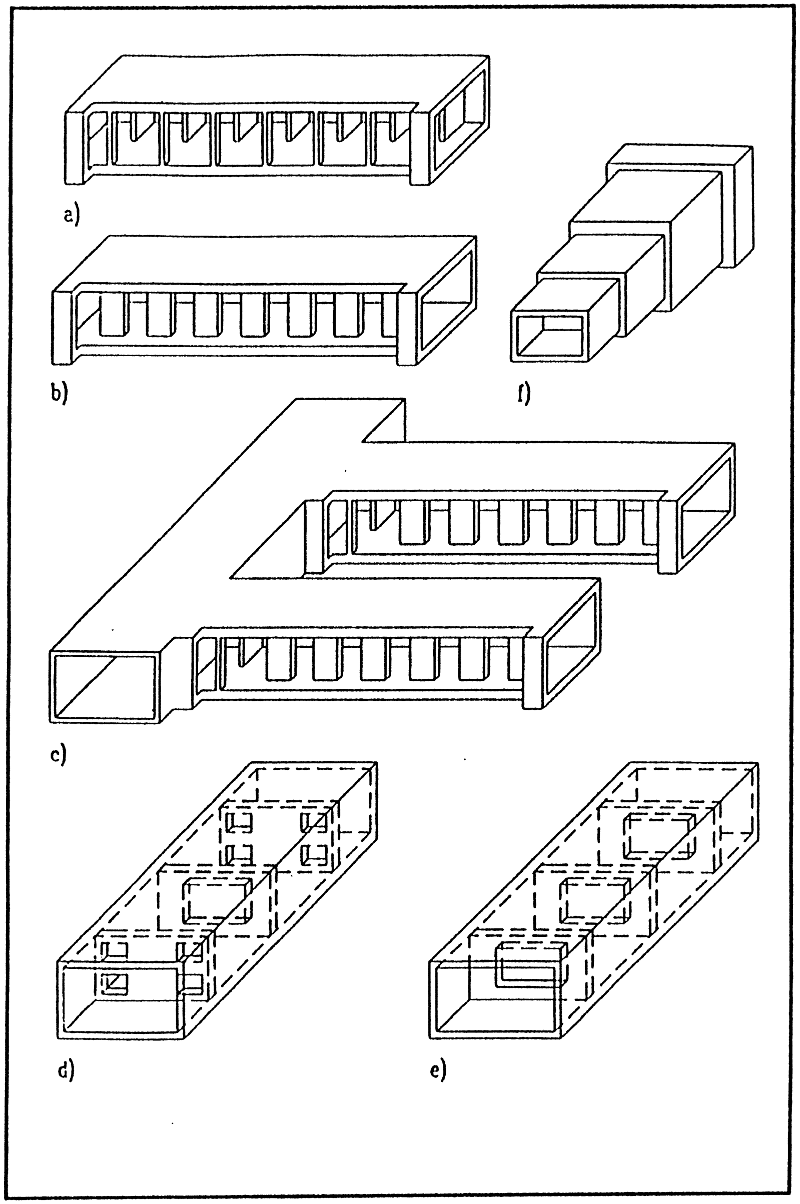

a)
b)
c)
d)
e)
f)

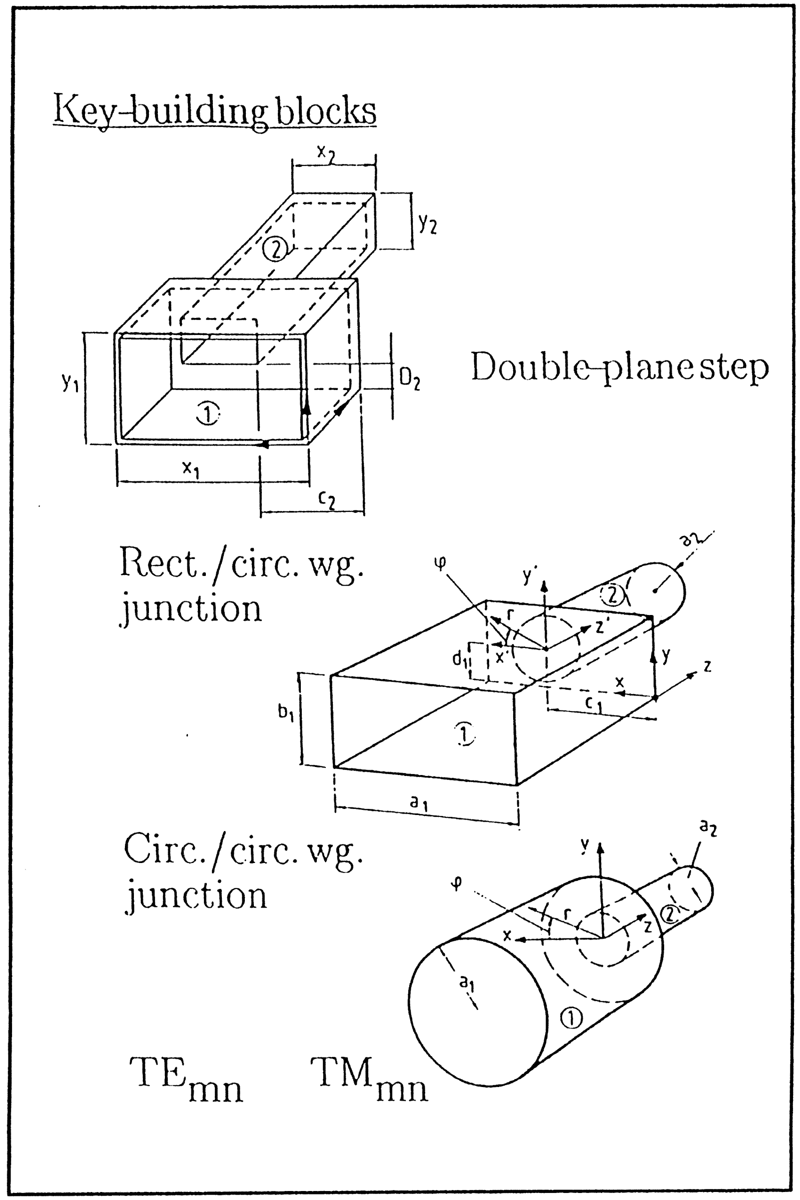

Key-building blocks
x2
y2
y1
x1
c2
D2
Double-plane step
Rect./circ. wg.
junction
φ
y'
z'
r
x'
d1
y
z
x
c1
b1
a1
a2
Circ./circ. wg.
junction
TEmn
TMmn

Six-Port Cross-Junction

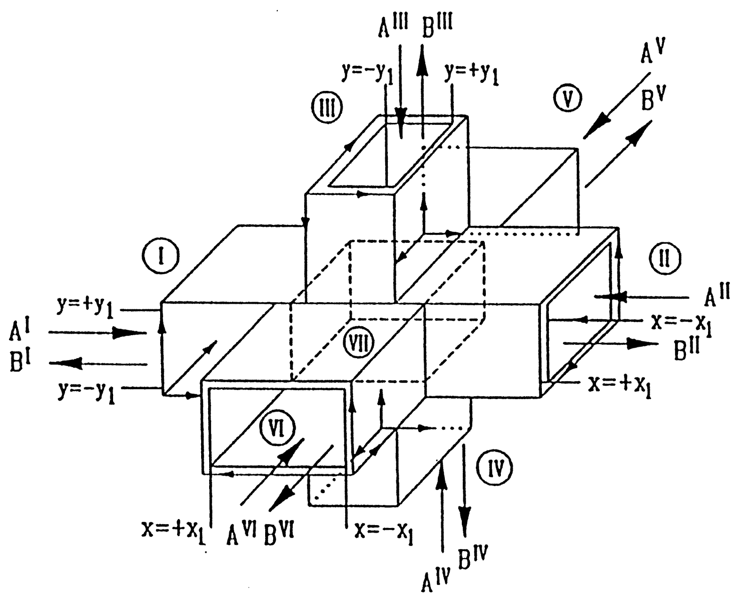

THEORY

3D-(Scattering) Problems
Homogenous Waveguide Discontinuity

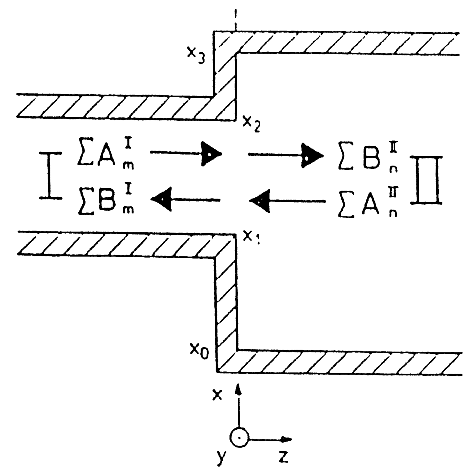

Basic Steps for Deriving the S-Matrix

1) Field expansion in the orthogonal modes on both sides
2) Normalization to the complex power
3) Field continuity along the common interface
4) Application of the orthogonal property
5) Adequate rearranging of the equations

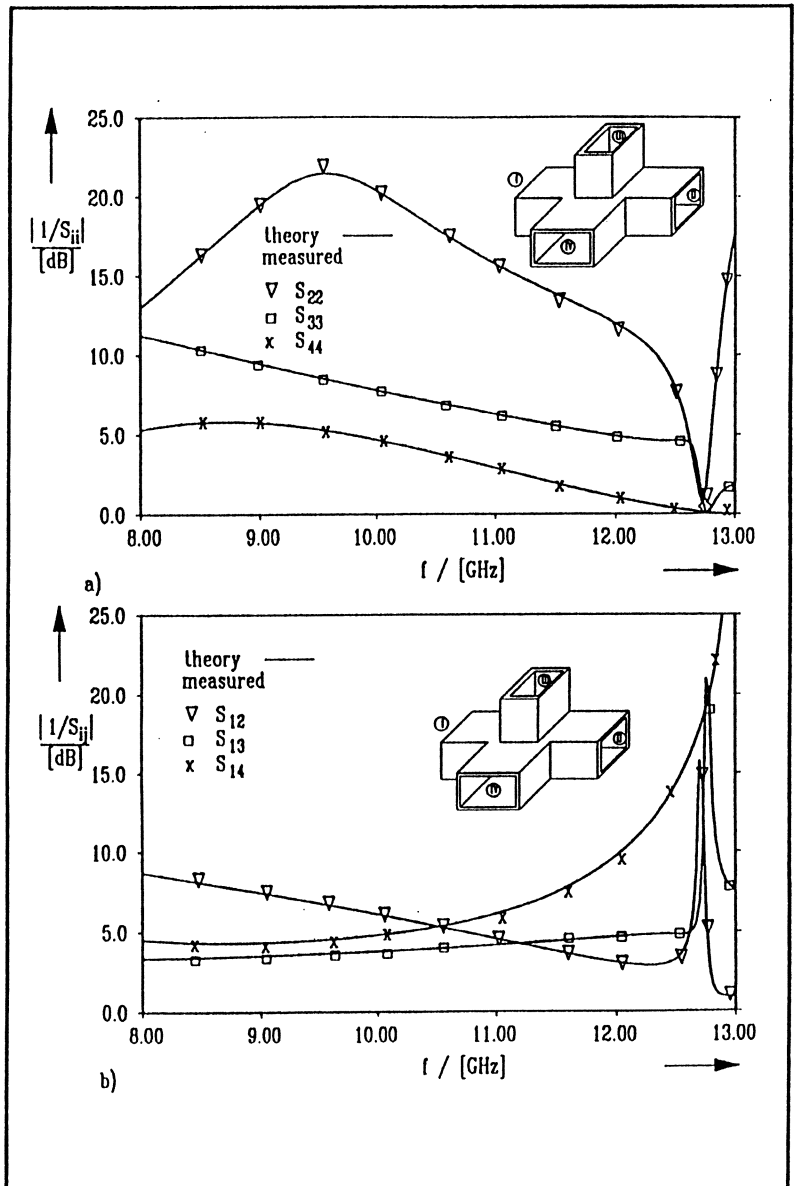

|1/S_ii| [dB]
25.0
20.0
15.0
10.0
5.0
0.0
8.00
9.00
10.00
11.00
12.00
13.00
f / [GHz]
theory
measured
S22
S33
S44
a)
|1/S_ij| [dB]
theory
measured
S12
S13
S14
b)

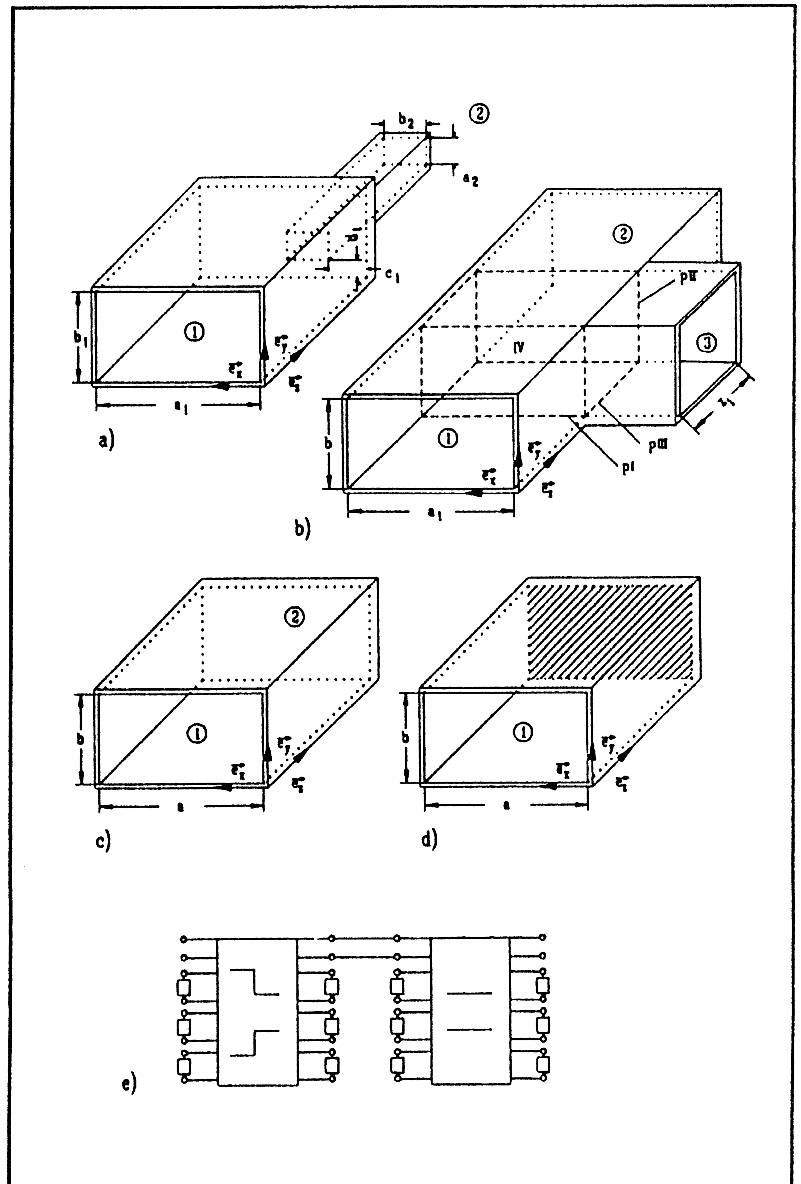

a)
b)
c)
d)
e)

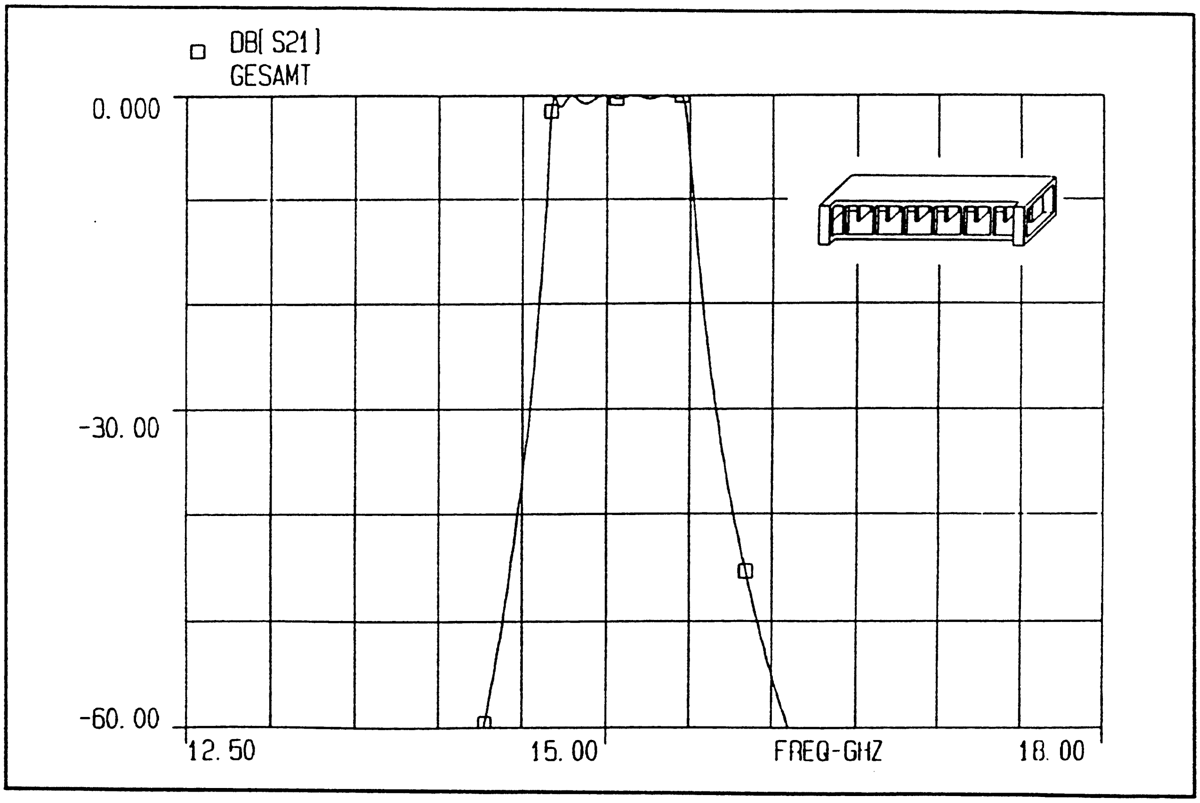

DB[S21]
GESAMT
0. 000
-30. 00
-60. 00
12. 50
15. 00
FREQ-GHZ
18. 00

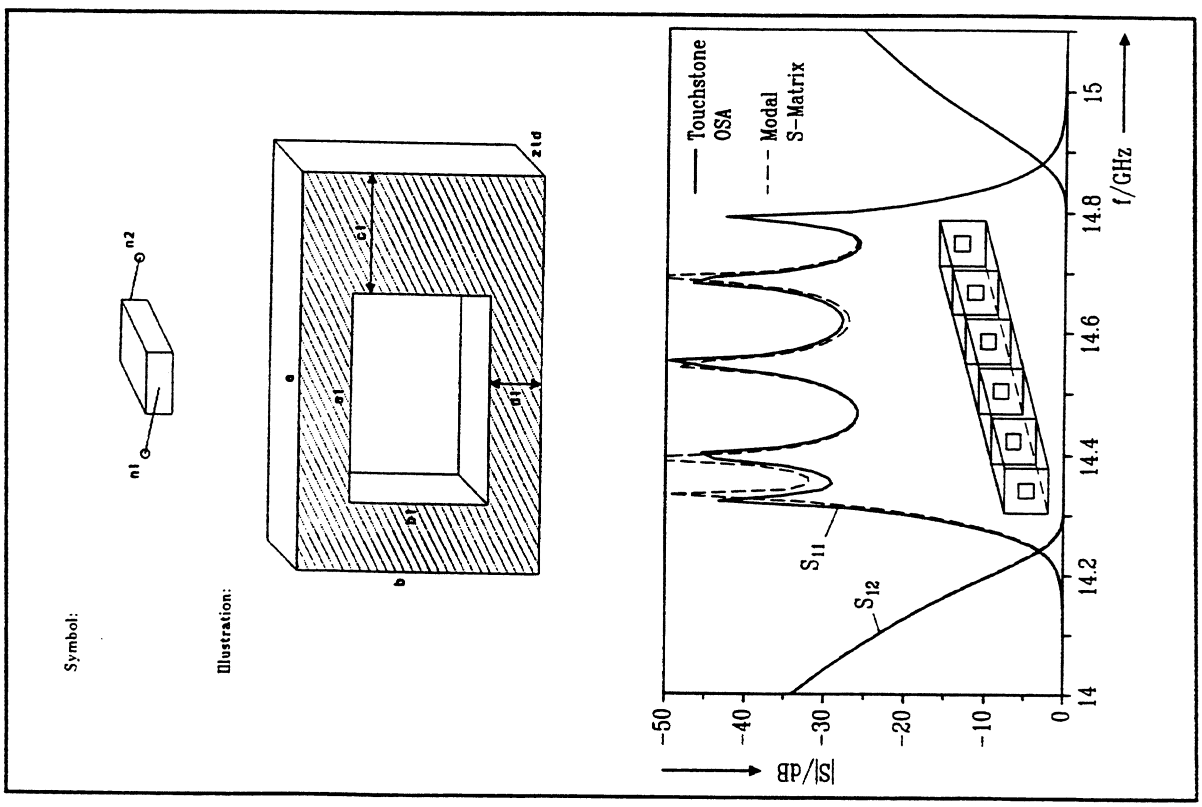

Symbol:
Illustration:
n1
n2
Touchstone OSA
Modal S-Matrix
S11
S12
|S|/dB
f/GHz
-50
-40
-30
-20
-10
0
14
14.2
14.4
14.6
14.8
15

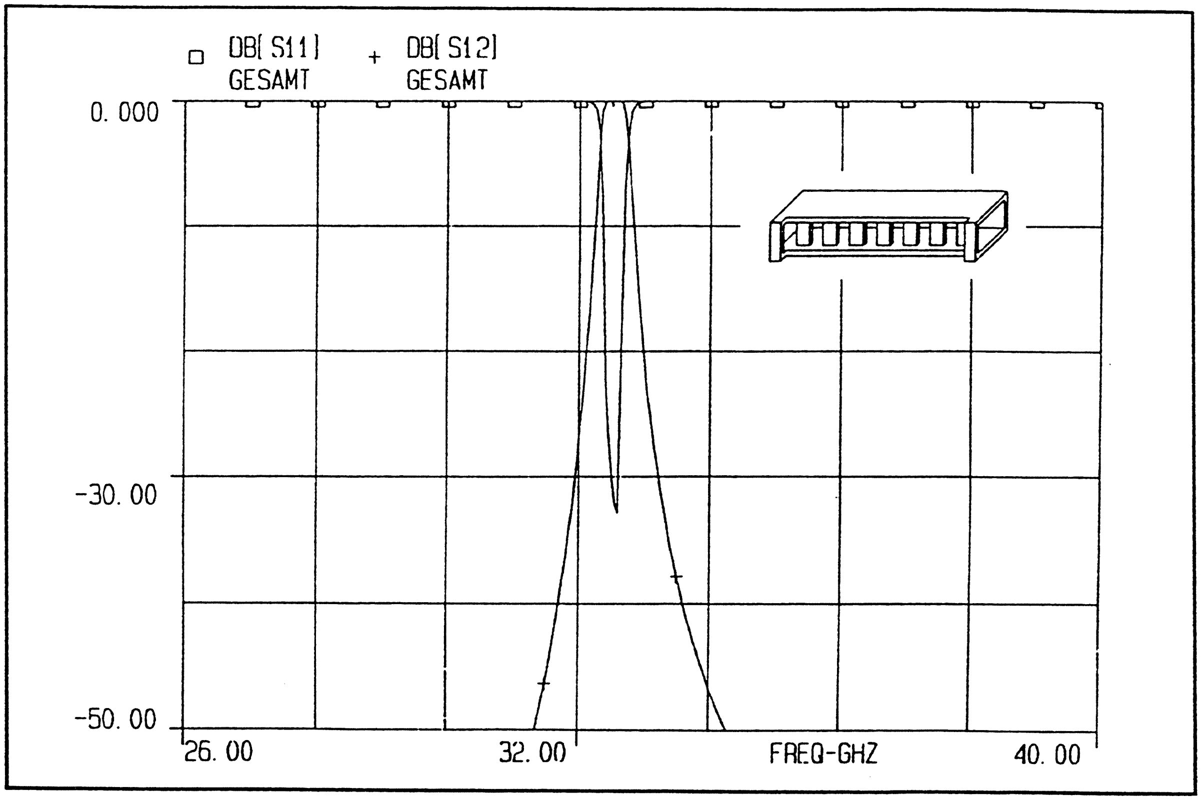
DB[S11]
GESAMT
DB[S12]
GESAMT
0.000
-30.00
-50.00
26.00
32.00
FREQ-GHZ
40.00

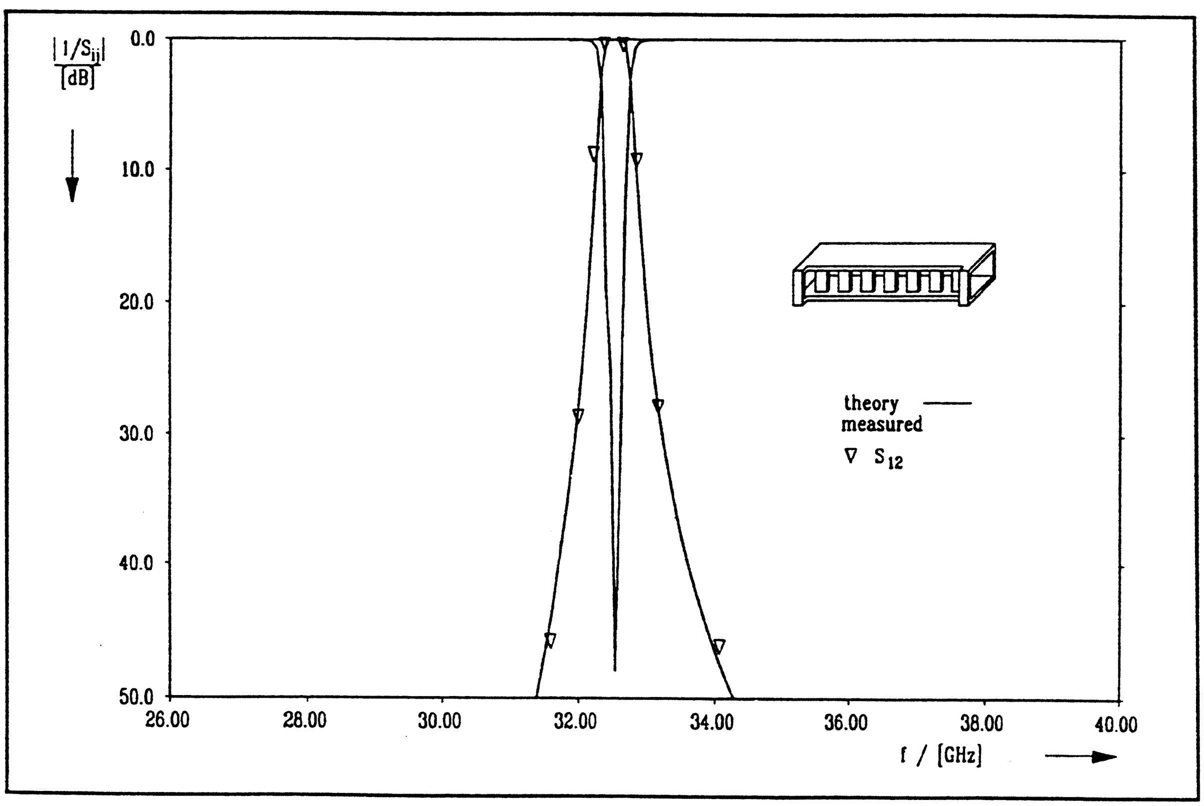
|1/Sij|
[dB]
0.0
10.0
20.0
30.0
40.0
50.0
26.00
28.00
30.00
32.00
34.00
36.00
38.00
40.00
f / [GHz]
theory
measured
∇ S12

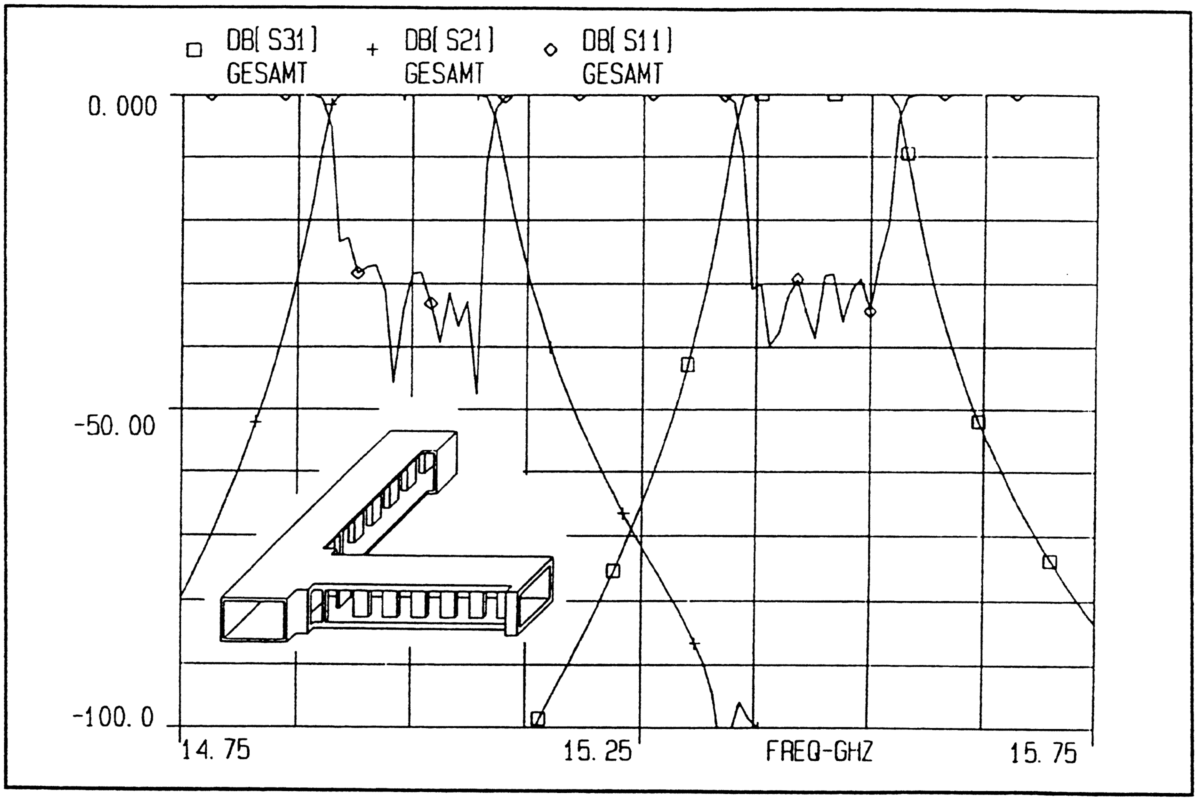

DB[S31] GESAMT
DB[S21] GESAMT
DB[S11] GESAMT
0. 000
-50. 00
-100. 0
14. 75
15. 25
FREQ-GHZ
15. 75

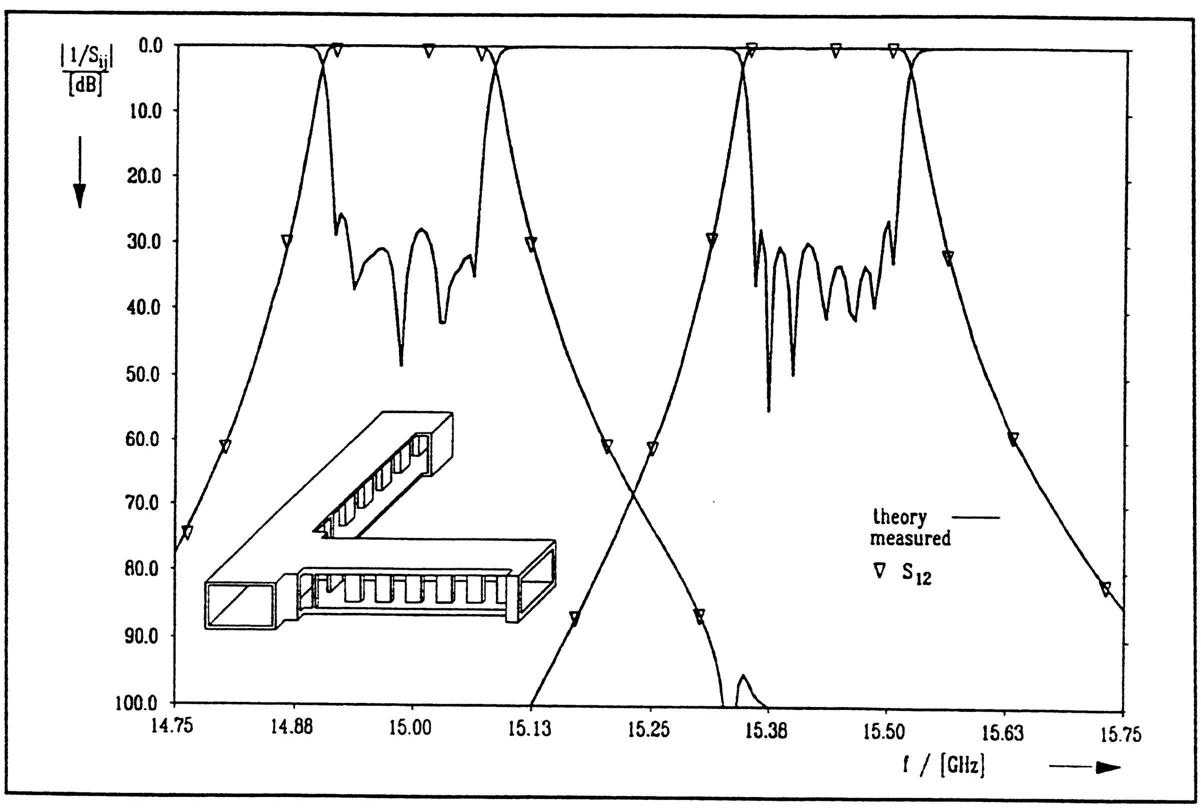

|1/Sij| [dB]
0.0
10.0
20.0
30.0
40.0
50.0
60.0
70.0
80.0
90.0
100.0
14.75
14.88
15.00
15.13
15.25
15.38
15.50
15.63
15.75
theory
measured
∇ S12
f / [GHz]

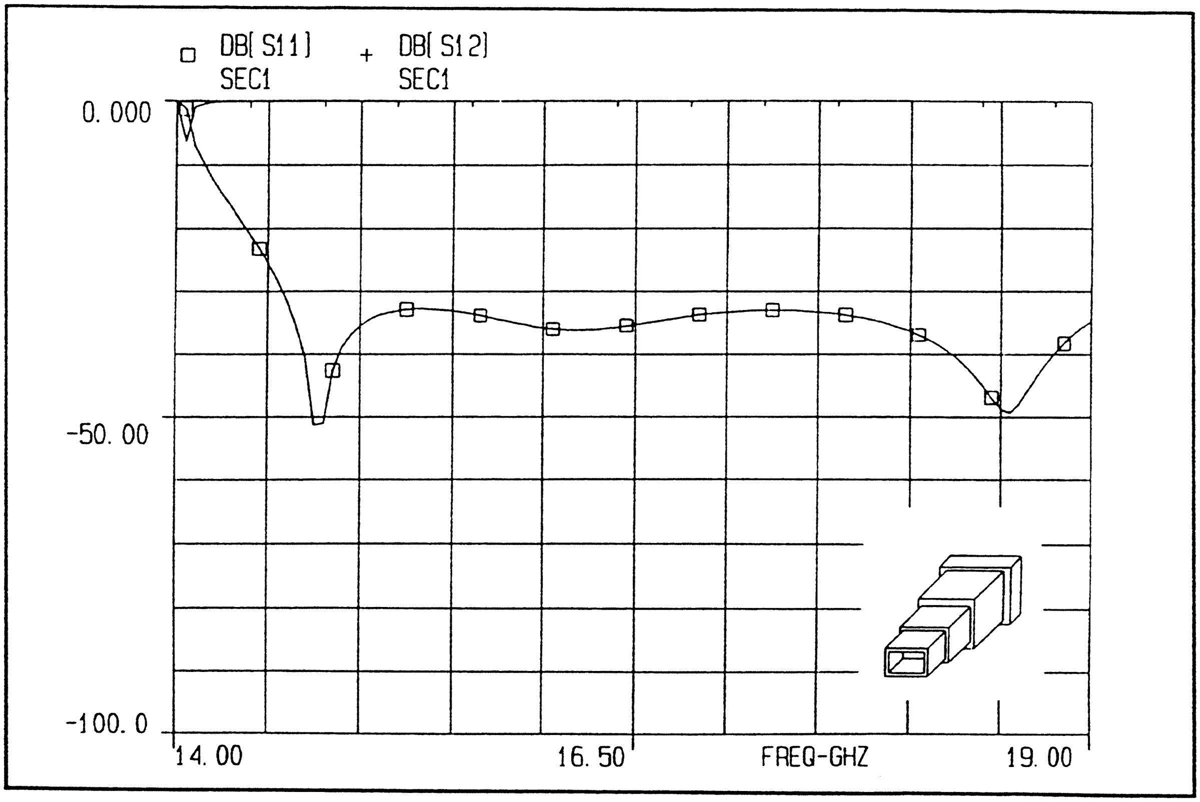

DB[S11]
SEC1
DB[S12]
SEC1
0. 000
-50. 00
-100. 0
14. 00
16. 50
FREQ-GHZ
19. 00

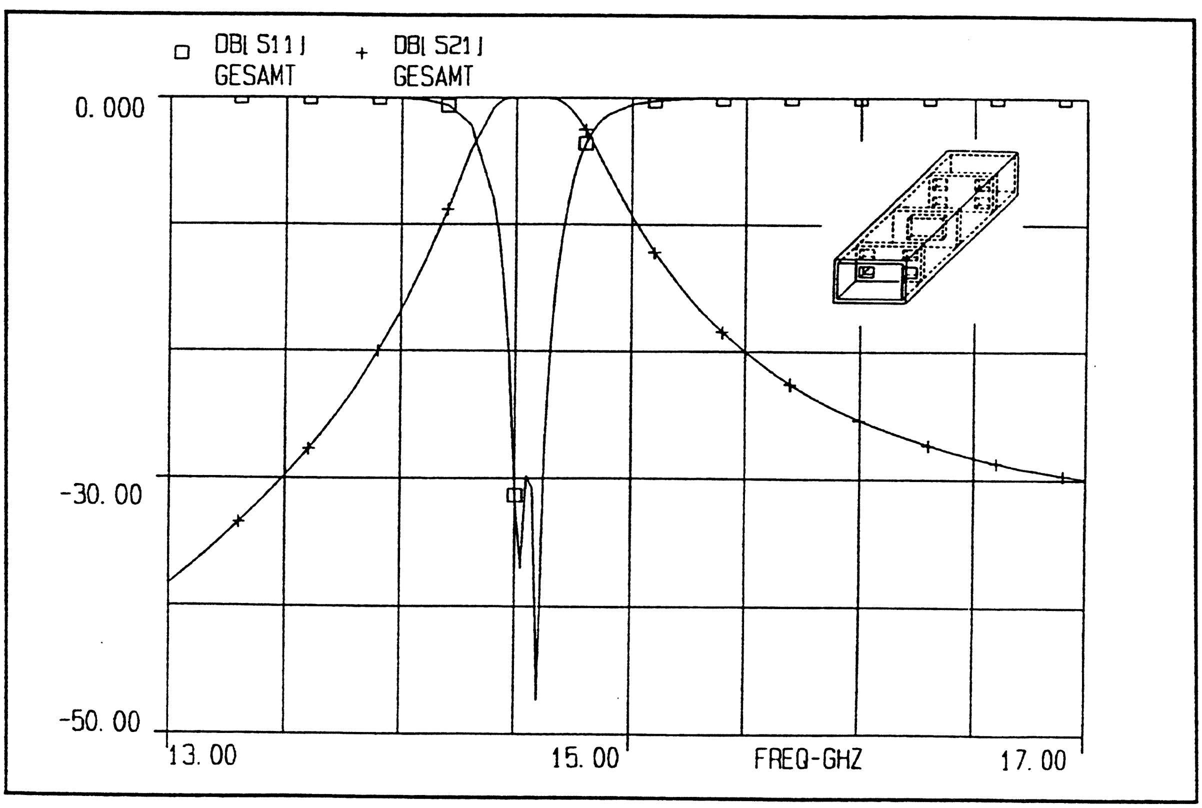

DB[S11]
GESAMT
DB[S21]
GESAMT
0. 000
-30. 00
-50. 00
13. 00
15. 00
FREQ-GHZ
17. 00

Symbol Illustration:

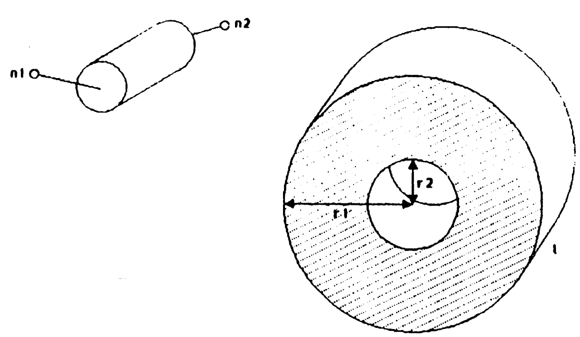

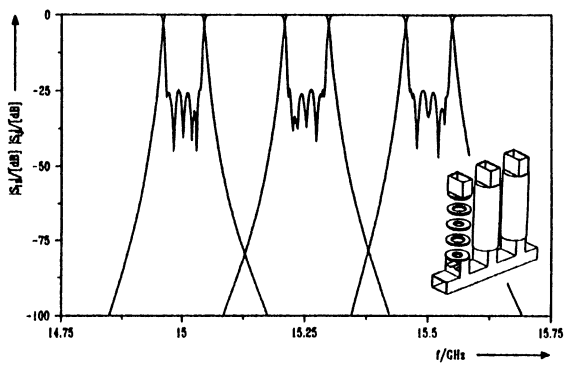

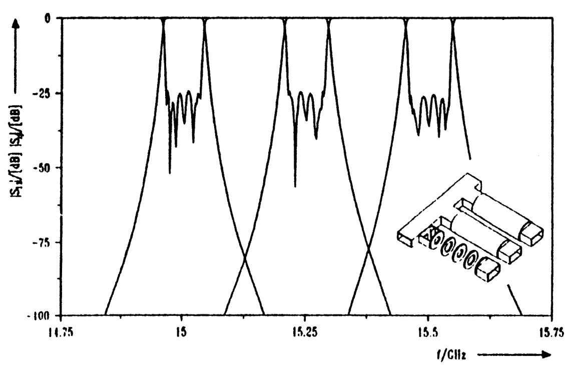

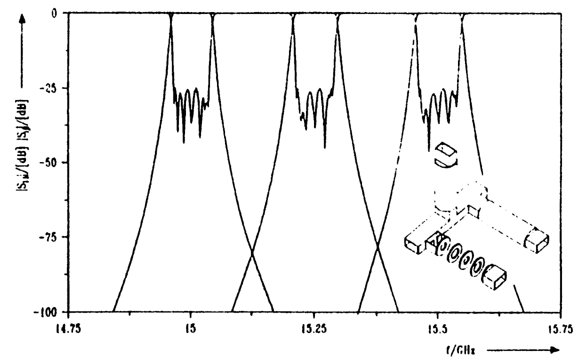

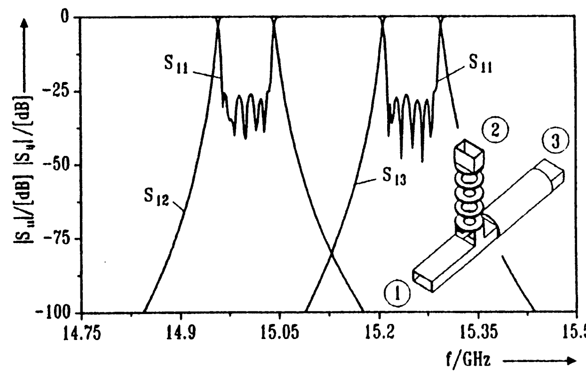

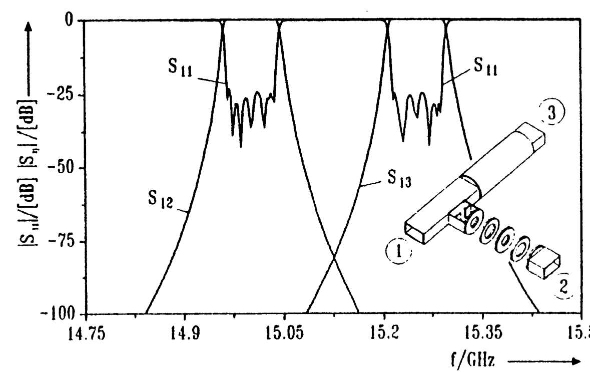

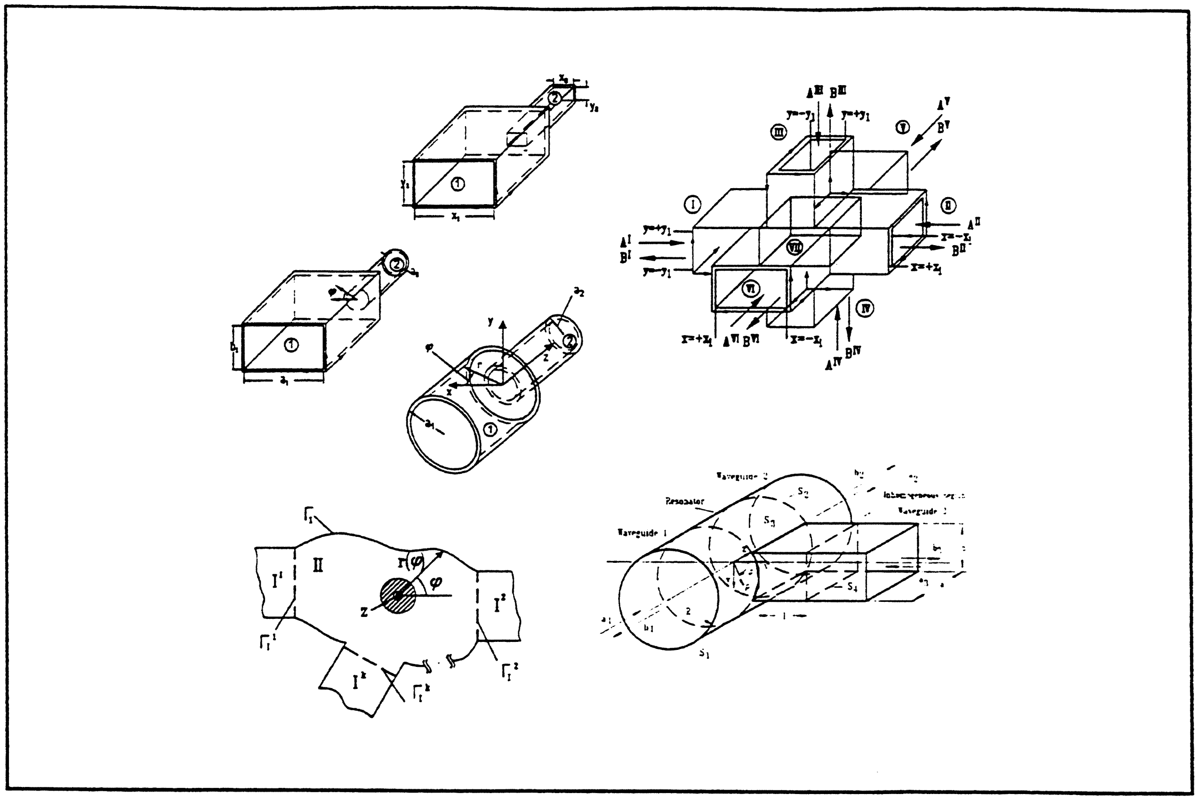

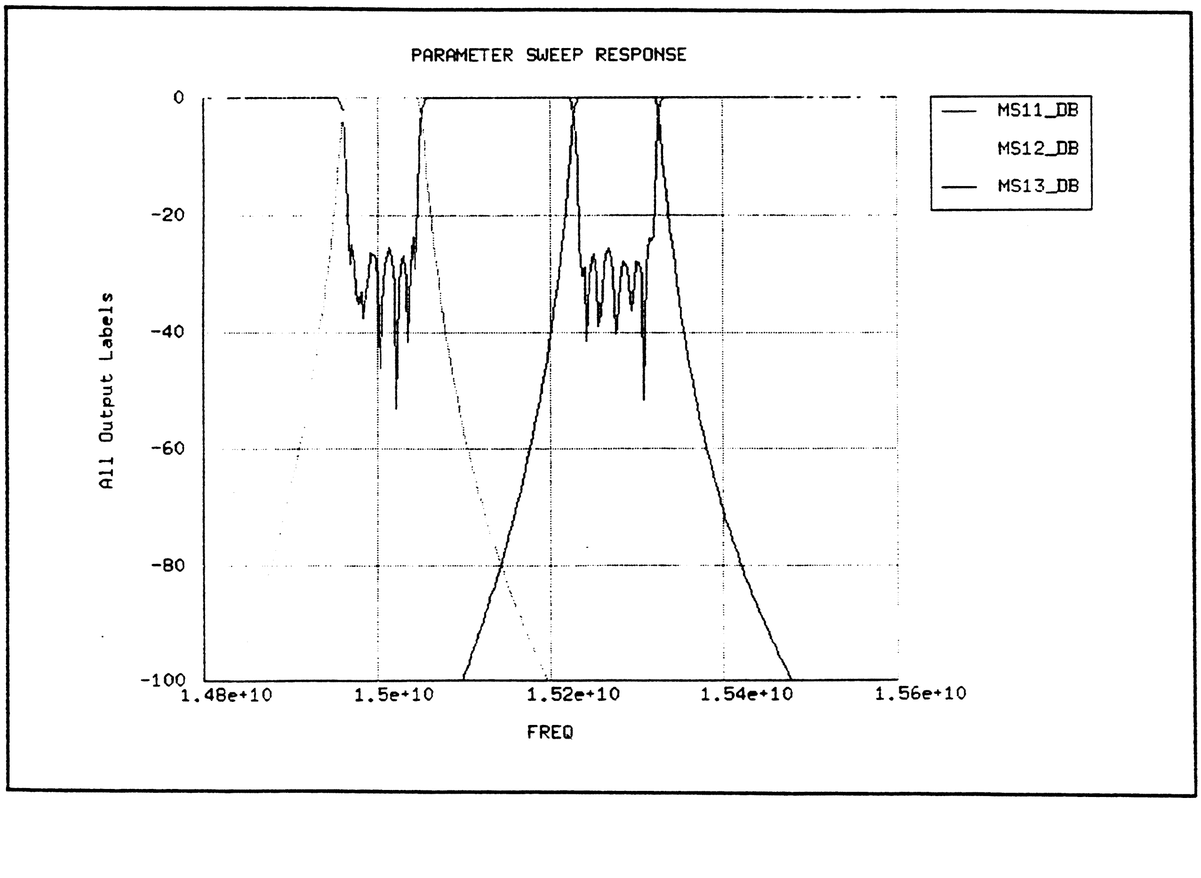
PARAMETER SWEEP RESPONSE
MS11_DB
MS12_DB
MS13_DB
All Output Labels
0
-20
-40
-60
-80
-100
1.48e+10
1.5e+10
1.52e+10
1.54e+10
1.56e+10
FREQ

Mitered H-plane corner

Ku-band (WR 62: 15.799mm × 7.899mm)

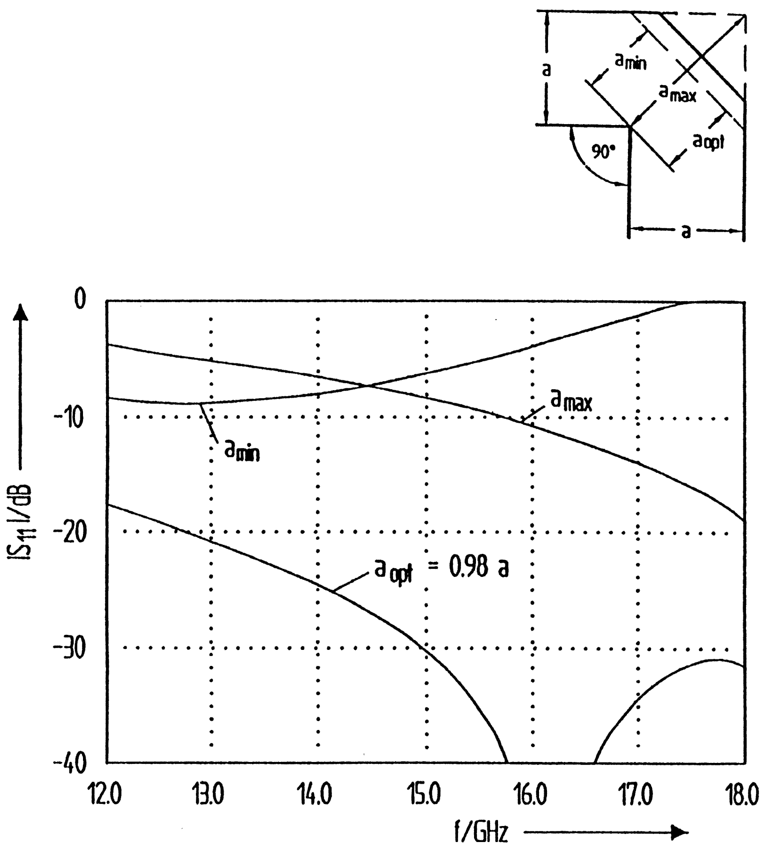

Mitered E-plane corner

Ku-band (WR 62: 15.799mm × 7.899mm)

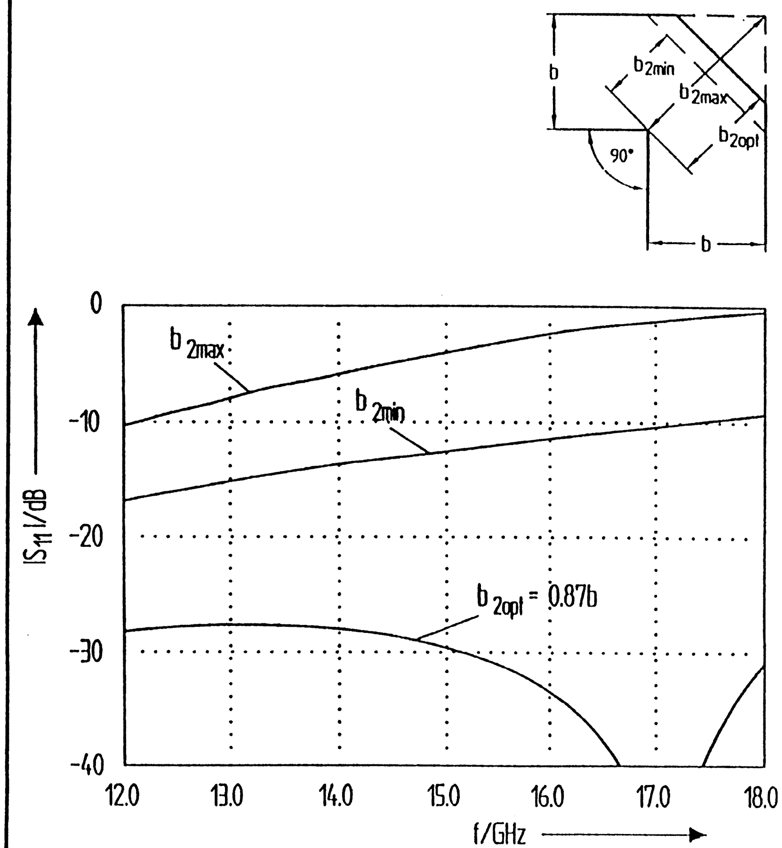

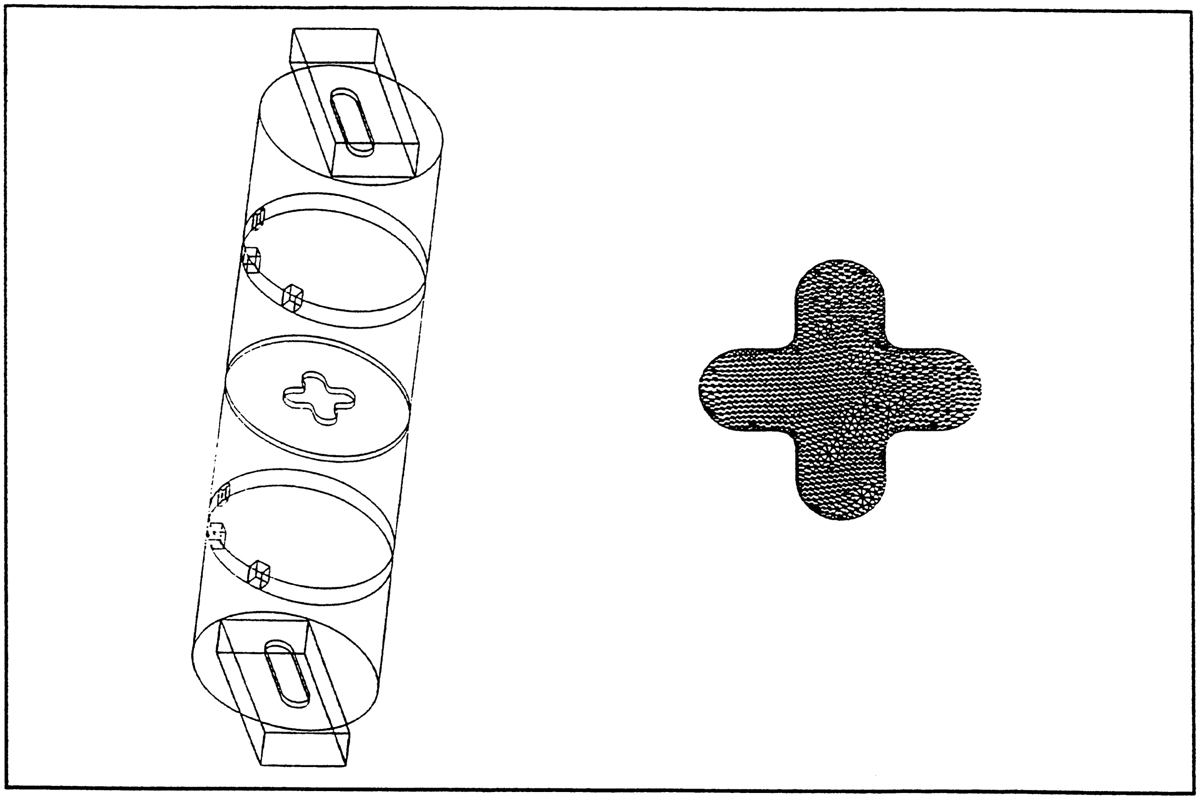

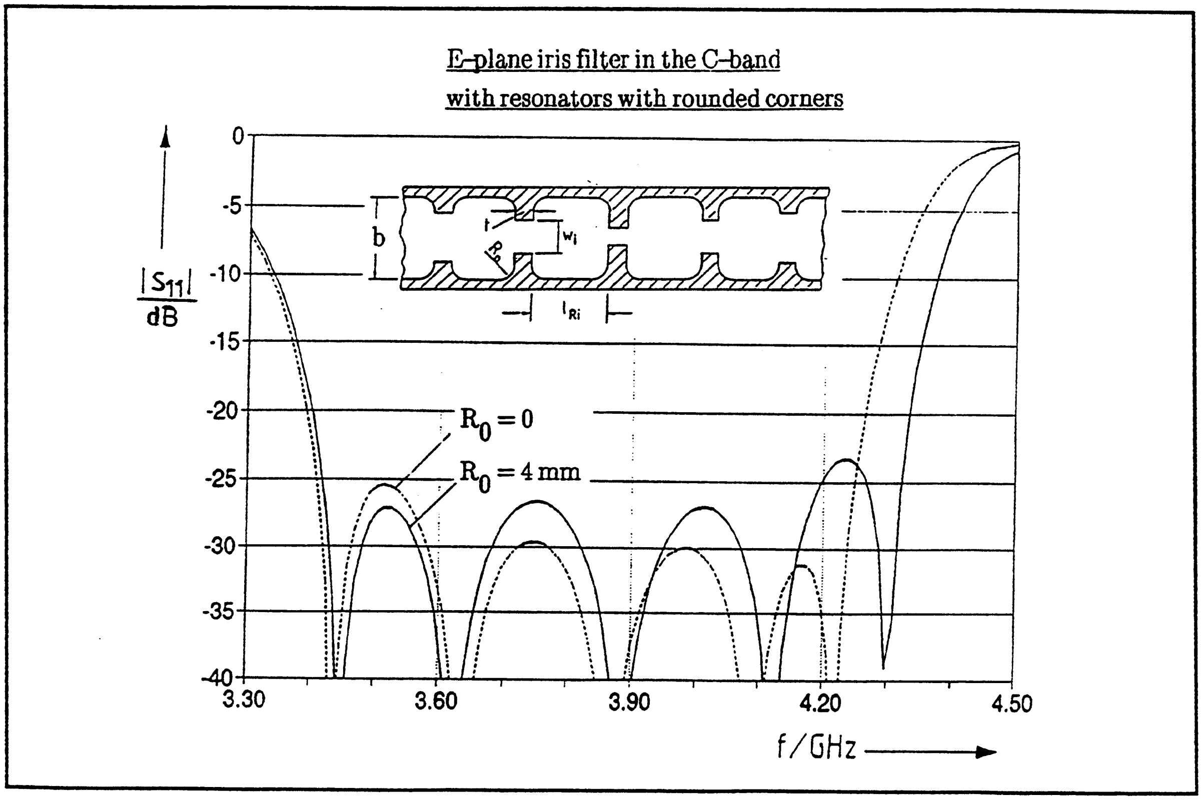

E-plane iris filter in the C-band
with resonators with rounded corners
|S11| / dB
0
-5
-10
-15
-20
-25
-30
-35
-40
3.30
3.60
3.90
4.20
4.50
f/GHz
b
r
R0
wi
lRi
R0 = 0
R0 = 4 mm

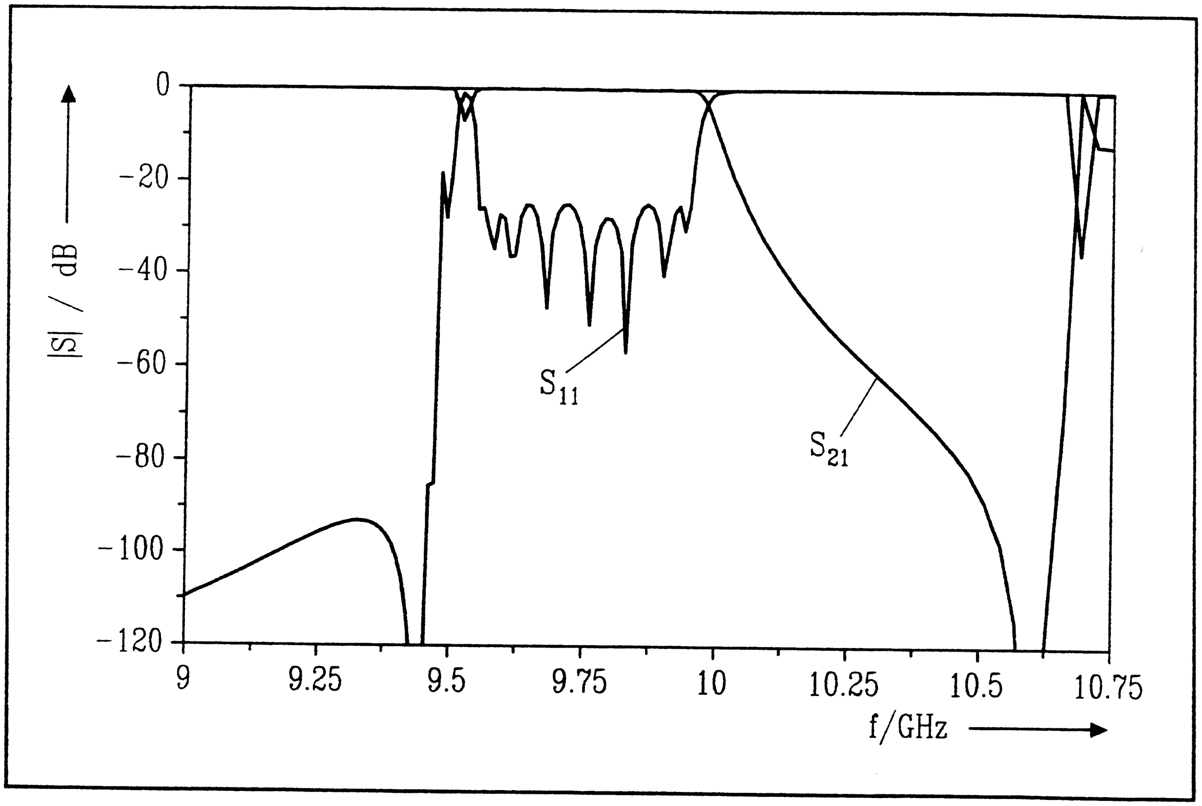

Cross-iris coupled resonator filter